APPLICATION OF DRUG DESIGN METHODS FOR INDUCING NERVE GROWTH FACTOR BIOSYNTHESIS

By

ANGELIKI KOUROUNAKIS

A DISSERTATION PRESENTED TO THE GRADUATE SCHOOL
OF THE UNIVERSITY OF FLORIDA IN PARTIAL FULFILLMENT
OF THE REQUIREMENTS FOR THE DEGREE OF
DOCTOR OF PHILOSOPHY

UNIVERSITY OF FLORIDA

1995

To my father, Dr. Panos N. Kourounakis, and mother, Dr. Lygeri P. Hadjipetrou-Kourounakis, for their dedication to science.

". . . and in the tomb of an ancient king finds a treasure of gold and precious jewels. He and his crew load down their ship almost to sinking with all this treasure, but as they sail he discovers that not only his crew, but that also he himself is now thinking of settling down, of building estates and villas on the Nile, of leading the good, comfortable, bourgeoise life. He commands, therefore, that all this treasure, even the smallest gold coin, be cast overboard, and he exclaims:

"If I could choose what gods
to carry on all my ships,
I'd choose both War and Hunger,
that fierce and fruitful pair."

For Odysseus knows well that new horizons are never gained by satisfied and comfortable men, but by those who are always at war -- with themselves; who are always hungry -- to explore new regions of thought."

(Kimon Friar, "The spiritual Odyssey of Nikos Kazantzakis")

ACKNOWLEDGMENTS

I would like to thank my advisor Dr. N. Bodor for his excellent guidance, inspiring input throughout the project, and constant encouragement, as well as for the opportunity to work on such a uniquely broad spectrum of diverse areas within the field of pharmacochemistry.

I wish to thank Dr. J. Simpkins for his advice and major contribution by providing his laboratory facilities for part of this work.

I most gratefully appreciate the valuable help and advice received by Dr. E. Wu, Dr. L. Prokai, Mrs. N. de Fiebre, Dr. S. Singh, Mrs. E. Simpson, Dr. M-J. Huang, Dr. H. Farag, and Dr. M. Badawi. I also wish to thank Dr. E. Meyer and Dr. W. Millard for the use of their labs.

I would like to extend my thanks to members of the Center: Laurie Johnston, Joan Martignago, Julie Berger, and Kathy Eberst for their helpful assistance, as well as all friends and colleagues who made this tenure pleasant.

Finally I would like to thank the members of my supervisory committee, Drs. A.R. Katritzky, M.O. James, and G. Hochhaus, for their interest in the project.

TABLE OF CONTENTS

LIST OF TABLES

LIST OF FIGURES

Abstract of Dissertation Presented to the Graduate School
of the University of Florida in Partial Fulfillment of the
Requirements for the Degree of Doctor of Philosophy

APPLICATION OF DRUG DESIGN METHODS FOR INDUCING NERVE GROWTH FACTOR BIOSYNTHESIS

By

Angeliki Kourounakis

August, 1995

Chairman: Nicholas S. Bodor
Major Department: Medicinal Chemistry

The clinical potential of nerve growth factor (NGF) as a therapeutic agent for Alzheimer's disease is undermined by its inability to cross the blood brain barrier. The alternative of up-regulating NGF in the central nervous system (CNS) by NGF-inducing compounds seems more promising, and delivery of such agents to the brain is therefore of great interest.

An integrated approach, using drug design methods (site-specific delivery, isosteric substitution, and study of quantitative structure activity relationships), was undertaken to 1) effectively stimulate NGF biosynthesis in the CNS by peripheral administration of a brain-targeted chemical delivery system (CDS) of a known inducer, 4-methylcatechol (4MC), 2) produce novel NGF-inducing

compounds, and 3) elucidate the mechanism of action of catechol derivatives as NGF-inducers.

Brain-targeted CDSs for 4MC based on the dihydropyridine <--> pyridinium redox reaction were designed and synthesised, as well as a novel brain-targeted catechol derivative. In vitro stability studies and in vivo distribution studies in rats successfully demonstrated the feasibility of sustained delivery of 4MC and derivative to the rat brain after peripheral administration of the corresponding dihydropyridine chemical delivery systems, and rapid peripheral elimination to assure minimal peripheral side effects of the bioactive compounds. Moreover, the 4MC-CDS evoked a 1.8-fold increase in NGF mRNA in the hippocampal region of the rat brain.

Bioisosters of 4MC were synthesised and evaluated for in vitro NGF-inducing activity in two cell lines. Isosteric substitution renders the molecule inactive in the L-M cell line, raising the interesting question of why the specific catechol moiety is indispensable for activity. To obtain a quantitative structure activity relationship, AM1 quantum mechanical calculations were performed on a set of 23 catechol derivatives, and the derived molecular descriptors were correlated with activity, which was shown to be associated with variables related to the oxidation of the catechols. It is therefore proposed that oxidative stress, from the autoxidation of catechols to the quinones, via perturbation in cellular homeostasis of antioxidant enzymes (e.g., glutathione peroxidase), triggers NGF biosynthesis and release.

CHAPTER 1
INTRODUCTION AND BACKGROUND

Alzheimer's Disease

In developed nations, the leading cause of senile dementia -- loss of memory and reason in the elderly -- is Alzheimer's disease (AD), which constitutes the most common neurodegenerative disease with an overall 20% likelihood of incidence over the age of 65. Although the aetiology of this progressive neurodegenerative disorder is presently unknown, it is characterised histologically by the following: (1) A decline in the number (cell death) or atrophy of neurons in the limbic system, including the hippocampus, which is central to learning, memory, and emotion. Large neurons shrink in parts of the hippocampus and the cerebral cortex while cell bodies and axons degenerate in certain acetylcholine-secreting neurons that project from the basal forebrain to the hippocampus and diverse areas of the cortex. (2) Presence of neurofibrillary tangles. The internal architecture of certain neuronic cells, for example of the hippocampus, undergoes alteration and their cytoplasm fills with bundles of helically wound protein filaments known as neurofibrillary tangles. (3) Widespread presence of senile plaques. The extracellular spaces of the hippocampus, cerebral cortex, and other

brain regions accumulate aggregates of beta-amyloid protein which constitutes the deposits of amyloid plaques, that are dramatically increased in AD.

Factors that are implemented in the development and progress of AD, apart from the age-linked changes in the brain, are head trauma, thyroid dysfunction, or immune system dysfunctions. Many theories exist on the aetiology of the diverse structural alterations that occur in the aging brain. One, for example, could be that defects slowly accrue in the DNA (gene dysfunction), proteins, or lipids of the neuronic cells, while the genetic and environmental factors contributing to this are closely intertwined; for example, damage to DNA lowers the quantity and quality of critical cell proteins such as enzymes involved in the machinery designed to excise and repair faulty nuclear DNA, or enzymes that protect from the initial damage (e.g., free radical scavengers). On the other hand, chemical modification (e.g., free radical oxidation) of cellular proteins may in turn alter cellular functions, while substantial decline with age in enzymes that inactivate free radicals, such as superoxide dismutase (SOD) and catalase, potentiate the oxidative damage on proteins. Thus, whether the damage accrued in DNA is resulting in increased oxidation of enzymes or whether the oxidation of enzymes occurs first and leads to accumulation of DNA deficits is an interesting question, although probably both sequences occur (Selkoe, 1992).

There is now increasing evidence indicating that probably most diseases at some point during their course involve free radical reactions and tissue injury. Both acute and chronic degenerative diseases are thought to involve free radical reactions in tissue injury which may be involved in multiple sites and at different

stages of the disease (Packer, 1992). The brain, and nervous system, is especially prone to radical damage. Cells of the central and peripheral nervous system, which are relatively unique in the body being postmitotic and irreplaceable, are relatively vulnerable to oxidative stress (denoted as a disturbance in the prooxidant-antioxidant balance in favor of the former), since (1) the brain consumes approximately 20% of total body oxygen, (2) the membrane lipids are very rich in polyunsaturated fatty acid side chains (susceptible to lipid peroxidation), (3) the brain is poor in catalase activity and has only moderate amounts of SOD and glutathione peroxidase (GSH-Px), and (4) some areas in the brain (e.g., substantia nigra) are rich in iron and iron ions can stimulate free radical reactions) (Halliwell, 1992).

Consequences of oxidative stress in the molecular level include lipid peroxidation, DNA and protein damage, rises in intracellular free Ca^{2+} (particularly damaging to neurons and thought to be the primary causative event in mediating necrotic neuronal death), and depletion of glutathione (GSH). Oxidation of free fatty acids produces free radicals that may contribute to neuronal damage via inflammatory reactions or may act as mediators of excitotoxicity and further enhance glutamate release. Excessive concentrations of excitatory amino acids (EAAs) kill neurons and elevated concentrations of EAA are found in many models of neurological disorders such as stroke, epilepsy, and head/spinal cord trauma (Bigge and Boxer, 1994).

The concept that oxidative stress is important in the pathogenesis of Parkinson's disease is being well substantiated in recent years (Adams and

Odunze, 1991, Jenner et al., 1992), while an increasing body of experimental data support the hypothesis that an imbalance in the regulation of oxygen-derived free radical production may result in brain damage and possibly contribute to the pathogenesis of AD neuropathology (Cohen, 1985, Halliwell and Gutteridge, 1989, Sinet and Ceballos-Picot, 1992).

Current Treatments for Alzheimer's Disease and Research Areas

The "cholinergic hypothesis" (cholinergic deficit) has led to many attempts to provide cholinergic replacement therapy. Various drugs have been developed for this purpose that show, however, only moderate effectiveness. These include cholinergic drugs (muscarinic cholinomimetics) and acetylcholinesterase inhibitors such as Tacrine (THA), Amiridin, E2020, and Velnacrine (Takeda et al., 1995, Cassidy et al., 1994, Iversen and Hargreaves, 1994).

Since cholinergic transmission can be stimulated indirectly via the γ-amino-butyric acid (GABA) system, which appears to exert inhibitory control on acetylcholine (ACh) neurons through GABA-(A) receptors, intervention with specific GABA-(A) receptor antagonists should theoretically be applicable as a therapy in AD (Krogsgaard-Larsen, 1993 and 1994, Turner, 1994).

Glutamic acid (Glu) receptor antagonists are of interest as neuroprotective drugs since hyperactivity of central Glu neurons may be one of the primary causes of degeneration of ACh neurons in AD. However, because normal function of central ACh neurons appears to be dependent on stimulation by Glu neurons and

the observed loss of Glu neurons in the progression of AD resulting in hypoactivity of EAA neuronal pathways has recently been associated with learning and memory deficits, drugs capable of both protecting and activating EAA receptors may be of therapeutic interest (Krogsgaard-Larsen, 1993 and 1994; Stone, 1994).

Nootropic agents such as idebenone and piracetame are also currently being used although their mechanism of action is not yet well elucidated (Schindler, 1994).

Another area of interest in recent years has been the "beta-amyloid theory" of AD (Cordell, 1994). For example, a compound that is a selective inhibitor of the enzyme that processes the amyloid precursor protein to yield beta-amyloid has been reported. The potential use of anti-inflammatory drugs (indomethacin has shown some promising results [Rogers, 1993]) is also of interest since the senile plaque is also a site of a local inflammatory response in the brain. Intervention by inhibiting possible processes involved in oxidative stress and the use of antioxidants like vitamin E is also under investigation (Kagan et al. 1992) (e.g., among the numerous factors involved in this aspect, aluminium ions, which have been implicated in AD, as well as calcium ions, may induce molecular structural changes and degenerative processes [Szabo and Kretzshemar, 1994]) .

A more effective strategy, however, would be to slow or stop the progression of the neurodegenerative changes that accompany the development of senile dementia rather than to try to restore function to an already damaged brain. One such approach is the administration of neurotrophic factors.

Nerve Growth Factor and the Treatment of Alzheimer's Disease

Survival, maintenance, and differentiation of neurons in the peripheral and central nervous system are affected by agents -- most of them polypeptides -- called neurotrophic factors. One of the best such characterized trophic factor is nerve growth factor (NGF) which is produced by glial and neuronal cells, both of which also express NGF receptors. Although NGF was discovered and even sequenced several decades ago, it is only in the last years that the role of this protein, and a set of closely related factors that all together constitute the neurotrophin family (including brain derived neurotrophic factor, BDNF, neurotrophin-3, NT-3, and neurotrophin-4, NT-4), is slowly being more fully understood. Nevertheless, the range of NGF actions and a mechanistic explanation for its role have not been established yet. For example, apart from its crucial role in the regulation of the developing sympathetic and sensory systems, in promoting survival of injured cholinergic neurons of the basal forebrain, and in regulating neurite outgrowth and neurotransmitter synthesizing enzymes, a possible role for NGF in the regulation of oxidant-antioxidant balance has been recently proposed (Perez-Polo et al., 1990) as part of a molecular explanation for the known effects of NGF on neuronal survival during development, after injury, and in the aged CNS. Also, recent studies indicate that NGF protects against excitotoxicity by preventing the excessive elevation of Ca^{2+} (stabilizing Ca^{2+} homeostasis) and oxidative damage via an increase in the levels of detoxifying

enzymes in the brain (Jackson et al., 1990 a and b, Cheng et al., 1991, Mattson et al., 1993 a and b, Zhang et al., 1993).

In the CNS, high expression of NGF and/or NGF receptor genes is shown in the regions containing cholinergic neurons or their fibres. Cholinergic neurons of the mammalian basal forebrain innervate the hippocampus, the neocortex, and other structures in which the produced NGF can be retrogradely transported to the basal forebrain cell bodies and exert a trophic effect, activating the expression of specific proteins like choline acetyltransferase (ChAT) -- the key enzyme for regulation of acetylcholine synthesis. NGF's activity may normally support the viability and function of these neurons (Hagg et al., 1988, Lapchack, 1993).

The cholinergic system in the human brain is important for memory and other cognitive functions. Furthermore, studies on aged rats have demonstrated the involvement of the forebrain cholinergic system in age-related learning impairments (Harbaugh, 1989).

A common feature of neurodegenerative diseases is selective dysfunction and death of specific neuronic populations in the brain. In AD, the degeneration of the basal forebrain cholinergic neurons along with their axons results in a loss of cortical and hippocampal ChAT activity which is associated with the progressive loss of cognitive function. Attempts to restore brain cholinergic function by administration of acetylcholine precursors, cholinesterase inhibitors, or cholinergic agonists are limited in success. This suggests that successful treatment may be possible only by pharmacological agents that act on some very fundamental neurochemical defect that is responsible for the observed impairments.

A strategy for therapeutic intervention might include administration of a specific trophic factor to prevent or retard neuron loss. The knowledge of sites of synthesis of NGF in the nervous system as well as distribution of NGF receptors suggests a possible future clinical use of NGF to protect and repair in the nervous system. A wealth of evidence shows that treatment with NGF (intracerebral infusion) effectively attenuates lesion-induced cholinergic deficits and cognitive impairments in animal models (Fisher et al., 1987). In addition, recent clinical study with chronic NGF treatment (infusion of NGF in the brain) in an Alzheimer's patient showed promising results such as increased blood flow, [11C]nicotine uptake, and binding in the cerebral cortex, in addition to the normalized EEG patterns and improved performance in word recognition tests (Olson, 1993).

However, as already perceived, NGF's use in CNS disorder therapy is limited not only by the difficulty of human NGF production on a large scale, but most importantly by its inability to cross the blood brain barrier (BBB). Thus several different strategies have been considered in order to increase the neurotrophic effect of NGF on its target sites. These include (1) direct intracerebral infusion of the NGF protein; (2) slow-release biodegradable implants -- instead of chronic infusion, incorporation of NGF in biodegradable polymer capsules or microspheres would provide an implantable slow release NGF source; (3) carrier-mediated transport across the BBB -- coupling of NGF, for example, to an antibody to the transferrin receptor (CNS blood vessels are rich in this receptor) would theoretically concentrate NGF in brain vs. periphery

following i.v. injection; (4) grafting NGF-producing cells -- intracerebral transplantation of cells capable of NGF synthesis , for example Schwann cells or cells that have been genetically engineered to produce and secrete large amounts of NGF; (5) direct gene transfer to the brain -- transfection of nondividing neuronal or glial cells with NGF producing genes; (6) developing NGF receptor agonists -- increasing knowledge of the tertiary structure of NGF and receptor binding and activation domains enhances the possibility of developing low molecular weight agonists with NGF-like effects capable of passing the BBB.

An interesting alternative to the previous methods, which are limited in application and efficacy, is the use of pharmacological agents that control endogenous NGF production (that enhance NGF biosynthesis and release in the CNS), an approach that has been the focus of several studies in the past few years. Delivery to the brain of such *neurotrophomodulatory* agents would not only make NGF available to neurons without brain surgery (and consequently BBB damage), but also would produce NGF in specific CNS cell populations by targeting selected transmitter receptor subtypes, and thus this strategy would have the related advantage that the needed extra supply of NGF would be produced at naturally occurring NGF-dependent sites in the brain. Although at present the mechanisms that regulate NGF biosynthesis are still unknown, the inducibility of NGF has been demonstrated in a number of in vitro and in vivo systems by a variety of agents. Compounds with structural and functional diversity are known to induce NGF, such as cytokines (e.g., interleukin-1, -4, and -5) (Friedmann et al., 1990 and 1992, Yoshida et al., 1992, Steiner et al., 1991, Vige et al., 1991,

Awatsuji et al., 1993), 1,25-dihydroxyvitamin D3 (Wion et al., 1991, Saporito et al., 1993 b), neurotransmitters (e.g., epinephrine, dopamine) (De Bernardi et al., 1991), and steroids (e.g., dexamethasone, 17-b-estradiol) (Mocchetti, 1991).

Regulation of NGF Biosynthesis

NGF Biosynthesis

Usually NGF refers to the β-NGF which is a protein dimer consisting of two identical monomers, held together by noncovalent bonds, each consisting of a 118-amino-acid residue. The biologically active protein is generated by cleavage from a larger precursor that is encoded by a specific mRNA. Changes in the biosynthesis of NGF can be estimated by determining the content of the specific mRNA encoding for the precursor and combining it with the amount of the biologically active peptide. (If NGF content increases without a change in NGF mRNA, it can be presumed that NGF accumulates because utilization, catabolism, or axonal transport are decreased and not because of increased biosynthesis). It should also be noted that the increase in NGF mRNA elicited by the variety of agents that will be mentioned below is not due to non-specific change in total mRNA synthesis in the cells, since the mRNA for the stable structural protein cyclophilin, or for other proteins like proenkephalin and calmodulin, is unchanged.

Neurotransmitter Receptor Regulation of NGF Biosynthesis

BAR activation

In the rat C-6 glioma cell line (a CNS-derived glial tumour) (Schwartz et al., 1977, Schwartz and Costa, 1988, Dal Toso et al., 1987 and 1988, Follessa and Mocchetti, 1992), as well as in pure cultures of type-1 astrocytes from rat cerebral cortex (that express high levels of BARs) (Schwartz et al. 1990) and also in fibroblast cultures, it has been shown that β-adrenergic receptor (BAR) activation increases NGF mRNA and protein, which leads to increased secretion of NGF from these cells into the culture medium. The BAR-agonist isoproterenol (ISO) leads to an increase in NGF mRNA and NGF content within 2-3 hs. This effect is blocked by the β-blocker propranolol but not by the α-blocker phentolamine. The α-agonist phenylephrin has no effect on NGF mRNA level.

There has been some controversy about whether or not this stimulatory effect of ISO (and of other catecholamines such as norepinephrin, NE, and dopamine, DA) is due to its chemical structure (catechol part) and, thus, not mediated by adrenergic receptors. It was suggested that the catechol ring of catecholamines is essential and the aliphatic side chain enhances their effect while the terminal amino-residue is not essential.

A series of synthetic analogues of catecholamines, such as 4-alkylcatechols (Furukawa et al. 1990), increases the content of NGF mRNA and protein in mouse fibroblast cells, while salbutamol (a β-agonist with no catechol ring) does not. This suggests that the stimulatory effect of catecholamines on NGF biosynthesis is

not mediated by catecholaminergic receptors, and that the possibility exists of developing a variety of synthetic molecules able to enhance endogenous NGF production. However, another BAR agonist that does not possess the catecholamine typical structure, clenbuterol, elicits an increase of NGF biosynthesis in C6 glioma cells similar to that elicited by ISO. This effect is blocked by the β-2 antagonist ICI 118,551, suggesting that BAR-2 subtypes may be more involved in NGF-biosynthesis regulation (Mocchetti, 1991).

Molecular mechanisms (involved in regulation of NGF synthesis)

BAR stimulation activates adenylate cyclase which increases the intracellular c-AMP level. Thus NGF gene expression can be mediated via the activation of c-AMP-dependent protein kinase A. This hypothesis was confirmed by the increase in NGF mRNA content elicited by addition to glioma cells of dibutyryl-c-AMP (a lipophilic c-AMP analogue), by addition of forskolin which directly activates the catalytic subunit of adenylate cyclase, and by addition of PGE_1 to stimulate prostaglandin E receptors that also lead to c-AMP accumulation. (Moreover, PGE_1's effect, in increasing NGF, is potentiated by 3-isobutyl-1-methylxanthine, IBMX, a phosphodiesterase inhibitor [Dal Toso et al., 1988].)

On the other hand, an involvement of protein kinase C in the regulation of NGF mRNA content has also been suggested since the phorbol ester 12-O-tetradecanoyl phorbol-13-acetate (TPA), an activator of protein kinase C, induces NGF gene expression in mouse fibroblast cells (Wion et al. 1990, D'Mello et al. 1990).

Furthermore, NGF gene expression by activation of protein kinase A or C may involve an intermediate process: the catalytic subunit of the protein kinase phosphorylates a protein (cytosolic or nuclear) which binds to a specific promoter region of the NGF gene. Nevertheless, studies have shown that another intermediate step may be involved: NGF gene expression may be regulated by nuclear proteins ("third messengers") that are encoded by early-response genes like that of c-fos (Mocchetti et al. 1989, Heumann et al. 1991), since it has been shown that BAR stimulation and phorbol esters increase c-fos mRNA and c-fos protein preceding the increase in NGF mRNA.

Other neurotransmitters

Since BAR-stimulation induces NGF biosynthesis, it can be assumed that noradrenaline might be the physiologic regulatory stimulus in the normal brain. However, recent findings also suggest that other neurotransmitters could play a role in NGF regulation. GABAergic and glutamatergic activity seem to provide an inhibitory and excitatory input in NGF mRNA expression (Zafra et al. 1990, 1991, and 1992). Kainic acid, a glutamatergic receptor agonist, enhances NGF mRNA content in neurons of the hippocampus. So do experimental seizures (by electrical stimulation or bicuculline injection) in which it is presumed that excitatory amino-acid transmission overtakes inhibitory GABAergic transmission.

An antagonist of the N-methyl-D-aspartate -- NMDA -- sensitive glutamate receptor, MK 801, did not block NGF mRNA increase while 6-cyano-7-nitroquinoxaline-2,3-dione, CNQX (a non NMDA receptor antagonist), prevented the increase elicited by electrical stimulation suggesting that stimulation of non

NMDA receptors are involved in NGF mRNA expression. In addition, kainic acid's and bicuculline's induction of NGF mRNA is blocked by diazepam (Zafra et al. 1990).

Other neurotransmitters such as cholinergic agonists (methacholine, carbamylcholine and nicotinic acid), serotonin, and histamine fail to change NGF content.

Steroid Regulation of NGF Biosynthesis in the CNS

Adrenal steroids released during stress increase the content of NGF mRNA and protein in specific brain structures. In adrenalectomized rats, hippocampal NGF decreases. Dexamethasone (a synthetic glucocorticoid) and reserpine (which increases blood corticosterone) both elicit an increase in the amount of cortical NGF mRNA (Saporito et al., 1993 a, Fabrazzo et al., 1990). In addition, the previously mentioned bicuculline-seizure-mediated increase in NGF expression could also be due to the concomitant increased plasma corticosteroids, suggesting that adrenal steroids could be the common mechanism for induction of NGF by drugs that elicit a stressful situation.

Other hormones that are capable of inducing NGF expression include thyroxin and 17-β-estradiol. In the C-6 glioma cell culture, 17-β-estradiol enhances the *de novo* synthesis of NGF protein and increases the amount of NGF secreted by these cells into the surrounding medium (Perez-Polo et al. 1977).

Mechanism(s) of NGF induction

It has become clear that diverse mechanisms exist by which a variety of agents enhance NGF biosynthesis and secretion, both in vitro and in vivo. Presently however, there is only preliminary knowledge on *how* specific compounds upregulate NGF biosynthesis.

The structural diversity of NGF-inducing compounds but most importantly the variety of cell cultures used to demonstrate activity in vitro (Table 1) or in vivo systems (Table 2) provide additional complications since direct comparisons of unrelated systems is usually not possible. Furthermore, specific compounds have been shown to have differing NGF-inducing profiles in various cell types.

Catecholamines are potent in stimulating NGF synthesis and secretion in the C6 glioma cell line and the fibroblastic L-M cell line. In C6 cells their activity seems to be associated with β-adrenergic receptor stimulation (as discussed previously) since β-adrenergic antagonists block their effect while other structurally diverse β-agonists also appear to be effective.

In the L-M cell line however, the effect of catecholamines seems not to be mediated by β-adrenergic receptor activation. Evidence indicates that their effect is due to the catechol part of their molecule and not mediated by adrenergic receptors that are present in this cell line, since alpha or beta adrenergic antagonists do not block their effect. In addition, m- or p-dehydroxy precursors of catecholamines (4- or 3- aminoalkyl phenols), m-O-methylated metabolites (2-methoxy-4-aminoalkyl phenols), or non-catechol adrenergic agonists show no

Table 1. Compounds that induce NGF in cell culture.

Compound	Cell type
Steroids	
Dexamethasone	Primary hippocampal neurons
Aldosterone	Primary hippocampal neurons
1,25-Dihydroxyvitamin D3	Mouse fibroblast L929 cells
Catechols	
Dopamine and epinephrine	Mouse fibroblast L-M cells
	Quiescent primary astrocytes
Dopa and norepinephrine	Mouse fibroblast L-M cells
	Primary Schwann cells
Isoproterenol	Mouse fibroblast L-M cells
	Quiescent primary astrocytes
	C6-2B rat glioma cells
	Primary rat Schwann cells
	Primary cortical astrocytes
4-methylcatechol	Mouse fibroblast L-M cells
	Quiescent primary astrocytes
	Mouse fibroblast L929 cells
4-alkylcatechols and diacetylated derivatives	Mouse fibroblast L-M cells
	Quiescent primary astrocytes
Benzoquinone derivatives	
1,4-benzoquinone	Primary mouse astroglial cells
Idebenone	Primary mouse astroglial cells
Vitamin K3	Primary mouse astroglial cells
Pyrroloquinoline quinone	Primary mouse astroglial cells
Growth factors and cytokines	
IL-1β	Cultured explants of adult rat sciatic nerve
	Primary rat mesangial cells
	Primary rat astrocytes
	Hippocampal cultures
IL-4 and 5	Mouse astrocytes
Acidic fibroblast growth factor (aFGF)	Primary rat astrocytes
Basic fibroblast growth factor (bFGF)	Primary rat fibroblasts and astrocytes
Tumor necrosis factor-α (TNF-α)	Primary rat astrocytes
Epidermal growth factor	Primary rat astrocytes
TGF-β1	Primary rat astrocytes
Miscellaneous compounds	
Retinoic acid	Mouse fibroblast L929 cells
Prostaglandin E1	C6-2B rat glioma cells
Prostaglandin E2	Primary rat hippocampal cultures
Lipopolysaccharide	Primary rat hippocampal cultures
Phorbol 12-myristate 13-acetate (PMA/TPA)	Mouse fibroblast L929 cells
HTLV tax protein	NIH 3T3 cells
fos gene product	Transgenic mice
Serum factor	Mouse fibroblast L929 cells
Mixed gangliosides	Primary rat Schwann cells
Hericenones C, D, and E	Primary mouse astroglial cells
Fellutamide A	Mouse fibroblast L-M cells
Propentophylline	Primary mouse astroglial cells
Dibutyryl cAMP	C6-2B rat glioma cells
Forskolin and cAMP analogs	C6-2B rat glioma cells
	Primary Schwann cells
Kainic acid	Primary rat hippocampal neurons

Table 2. Compounds that induce NGF in vivo.

Compound	Site of induction
Interleukin-1β (IL-1β)	Adult rat hippocampus and cortex
	Astrocytes of adult rat basal forebrain and hippocampus
Transforming growth factor-β1 (TGF-β1)	Adult rat hippocampus
Thyroid hormone	Female mouse salivary gland
	Aged rat hippocampus
Colchicine	Multiple adult rat brain regions, including hippocampus, cortex, and basal forebrain
Kainic acid	Adult rat hippocampus and cortex
	Multiple adult rat brain regions, including hippocampus, cortex, and basal forebrain
NMDA	Adult rat hippocampus
Clenbuterol	Adult rat cortex
Isoproterenol	Adult rat cortex and hippocampus
1.25-Dihydroxyvitamin D3	Adult rat cortex and hippocampus
4-Methylcatechol	Adult rat cortex and hippocampus
Dexamethasone	Adrenalectomized adult rat cortex and hippocampus
	Adult rat hippocampus
Reserpine	Adrenalectomized adult rat cortex
Testosterone	Mouse submaxillary gland
Corticosterone	Mouse submaxillary gland
Yohimbine	Adult rat hippocampus
Idebenone	Aged rat frontal and parietal cortex and hippocampus
Acetyl-L-carnitine	Adult rat hippocampus

stimulatory effect on NGF content (Furukawa et al., 1986 a and b, 1987 and 1989). On the other hand, non-amine catechols like 4-alkylcatechols (1, 2 dihydroxy-4-alkylbenzenes) demonstrated high activity. A simple catechol derivative such as 4-methylcatechol (4MC) is one of the most potent stimulators of NGF synthesis and secretion in L-M cells, demonstrating therefore that the only structural requirement for activity lies within the catechol functional moiety of the molecule, although the specific mechanism by which catechol or catecholamine analogues stimulate NGF synthesis in this cell line is still under investigation.

Potential for Treating Neurodegenerative Diseases with NGF-Inducing Compounds

There is substantial evidence demonstrating the feasibility of developing an NGF-inducing therapeutic. The significant correlation between in vivo and in vitro results of several compounds is encouraging. It would be important to understand the, as yet ill-defined, multiple mechanisms of NGF induction for the development of an NGF-inducing therapeutic, by eliminating compounds that act via non-specific ways, and by developing a drug with the appropriate specificity and efficacy by rational (mechanism-based) design.

Potential complications, such as inability of these compounds to penetrate the BBB after peripheral administration or toxicity/side effects due to up-regulation of NGF in the periphery, may successfully be overcome by delivering the compounds that enhance NGF selectively into the brain by the use of an

appropriate brain-targeted chemical-delivery system such as the one based on the dihydropyridine <--> pyridinium redox reaction.

BBB and the Redox-Based Chemical Delivery System of Drugs to the Brain

The major obstacle in drug delivery to the brain is the BBB, a complex of morphological and enzymatic components that retard the passage of both large and small molecules that are not essential for cerebral function while housing specific transport systems for essential molecules. The tight junctions of the cerebral capillary endothelial cells exclude hydrophilic compounds and high molecular weight substances from entering the brain while lipophilic compounds, utilizing transcellular transport, can readily pass through the phospholipoidal membranes and enter the brain.

A general method that has proven useful in selectively enhancing drug delivery to the CNS is the chemical delivery system (CDS) that exploits the distinct properties of the BBB. This CDS is based upon the dihydropyridine <--> pyridinium salt redox reaction. In this redox-delivery system, the lipoidal dihydropyridine moiety (Figure 1) is covalently attached to the drug, thus increasing its lipophilicity and its BBB permeability. Upon systemic administration, and after extensive distribution, the dihydropyridine is oxidized to the charged pyridinium ion in the brain and in systemic tissues by the same means as the ubiquitous NADPH <--> NADP redox system. The charged pyridinium-drug moiety is thus retained, or "locked", in the brain since the BBB prevents

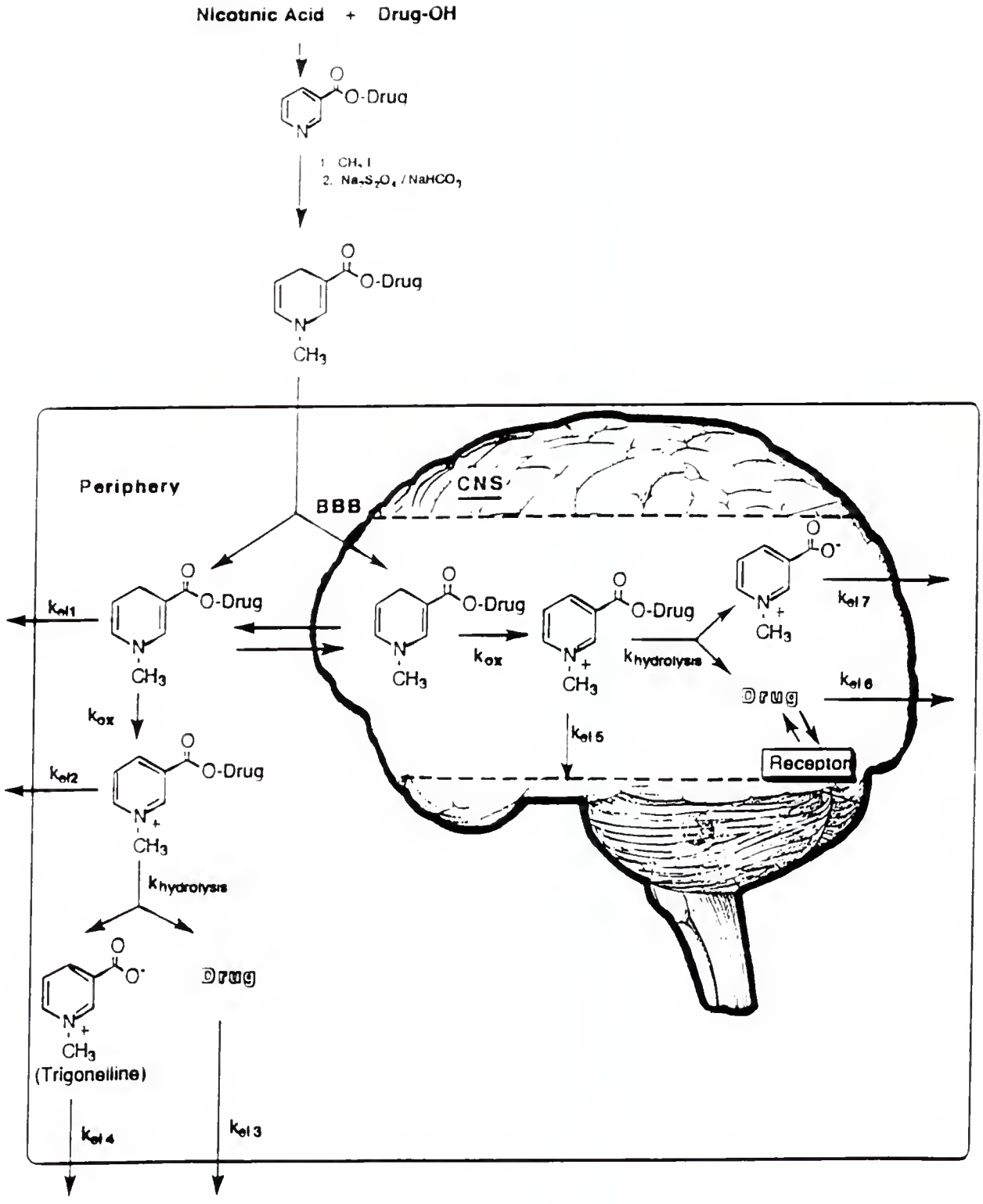

Figure 1. Representation of the drug-targetor complex that promotes CNS retention and accelerated peripheral elimination.

rapid reequilibration of polar species, and enzymatic hydrolysis of the drug-carrier complex results in a sustained release of active drug. Meanwhile, in the periphery, the ionized pyridinium-drug moiety can be rapidly cleared by renal or biliary excretion due to its increased hydrophilicity (Figure 1). The overall result is that peripheral (side) effects or toxicity should be reduced by preventing significant accumulation of the parent active agent while it is specifically delivered to its site of action (bioreceptors in the CNS). Consequently, apart from improvement of its therapeutic index, central toxicity is also attenuated since the majority of the active species is present in the form of an inactive carrier complex. Since it was first proposed in 1978 by N. S. Bodor, the brain-targeted CDS has been extensively applied to various pharmacologically active agents (Bodor et al., 1981a and b, and 1983).

Drug Design Based on Isosteric Replacement or QSAR

The Therapeutic Index (T.I.), defined as the ratio of the toxic dose by the effective dose, is the most important characteristic of a drug. Among the principal goals of Drug Design is the improvement (increase) of the T.I. of a drug either by increasing the toxic dose, or in other words reducing the toxicity of the active substance (an approach which is accomplished with, for e.g., the development of Site Specific Chemical Delivery Systems, such as the one described previously), or else by reducing the effective dose of a drug which is the effort to increase activity or potency of the active substance. One of the approaches towards the

latter is by molecular manipulations of the active compound of known chemical structure (the "lead"). Lead finding includes the identification of novel compounds displaying an interesting biological activity and compounds with a newly discovered biological activity. Among the various methods for lead optimisation, but also for (further) elucidation of the mechanism of action of a bioactive substance, are bioisosteric replacement and Quantitative Structure Activity Relationship (QSAR) methods.

Bioisosterism

"Every physiologically active compound of known structure is a challenge to the medicinal chemist - a challenge either to better it, or merely to equal it. There are numerous ways of attacking such a problem. One of the methods which has been used frequently, very often with success, is that of isosteric replacement" (H.L. Friedman).

The concept of isosterism was first introduced by Langmuir (1919) who expanded the principle of similarity in properties of the elements in the same group of the periodic table (due to the same electronic configuration) to molecules or groups of atoms which possess the same number and arrangement of electrons. Isosters have similar stereochemical and electronic properties. Isoelectronic groups have similar electronic structure for e.g. same total charge and charge distribution, while isosymmetric have similar stereochemistry. In related bioactive compounds chemically more-or-less equivalent groups (isosteric) can be

distinguished in which the equivalence may include, apart from steric or electronic properties, properties such as lipo or hydrophility. A more biological approach in this field was given by Friedman who extended Langmuir's older concept of isosterism by introducing the principal of bioisosterism. Bioisosteric groups are chemical groups which are considered to be equivalent and therefore interchangeable as far as their contribution to biological activity is concerned. Thus, compounds are termed "bioisosteric" if they fit the broadest definition for isosters and have the same type of biological activity.

A rational approach of lead optimisation by molecular modifications is the replacement of components/substituents on the active molecule with others of similar electronic configuration and/or stereochemistry by applying Friedman's rules of bioisosterism.

Several bioisosteric groups of the catechol moiety are known as shown in Figure 2. Since this moiety, contained in several β-adrenergic compounds (catecholamines), is sensitive to metabolism by COMT (catechol-O-methyltransferase) (Guldberg et al 1975), analogues were sought that would not be substrates for this enzyme. Thus, structures that would substitute for the catechol function were developed, basically in order to discover drugs with higher β-adrenergic activity/selectivity and longer duration of action.

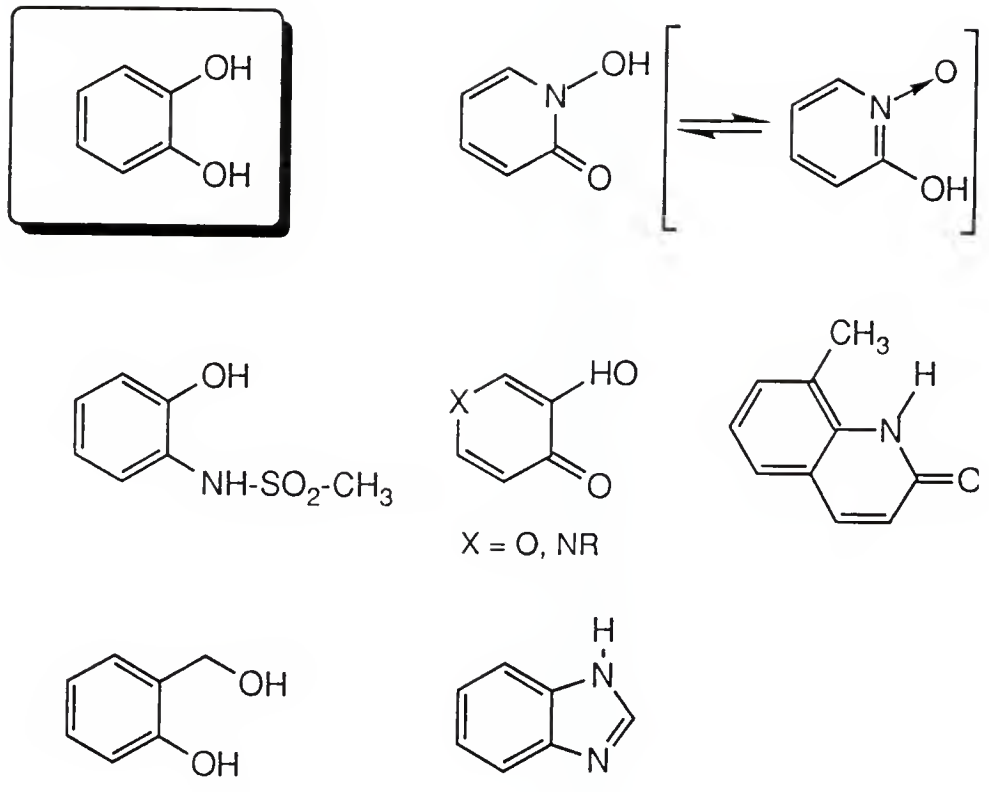

Figure 2. Catechol and bioisosteric groups.

Quantitative Structure Activity Relationships

Based on the simple yet fundamental reasoning that some form of chemical interaction, between the molecules of a drug and part of the molecules composing the biological object, is responsible for the biological effect of a compound, one can expect that chemical properties of the drug are decisive for its biological potentialities, and thus, that structure activity relationships (SAR) are inherent in drug action.

The study of the relationship between molecular structure and activity could be considered to have started with Mendeleev and the periodic classification of the elements and has continued on to quantum chemistry and the wide development of computers.

Assuming that the chemical structure is determinant of a drug's action, then certain quantitative properties of the molecule should be correlated with the quantitative expression of the biological activity. The idea that chemical structure of drugs could be correlated mathematically with their biological effect, was first expressed in the late 19th century by Crum-Brown and Fazer. The semiempirical approach to SAR by Meyer and Overton, the development of Hammett's σ constants for the electronic effect of substituents on rates and equilibria of organic reactions, the definition by Taft of the steric parameter Es, and the development of hydrophobic parameters, π and f, by Hansch and Rekker, using the partition coefficients from the octanol/water model system were the sources that gave the tools for handling the problem of SAR on a quantitative basis (Hansch, 1971).

Further progress in Quantitative Structure Activity Relationships (QSAR), has been indispensably connected with the use of the rapidly developed computers and computational chemistry.

QSAR is more than a means for optimizing activity: it is based on the assumption that the relative importance of physicochemical properties for the biological activity of compounds can be described in numerical terms, thus objectively rationalising the interaction of drugs with macromolecular systems. The most important physicochemical parameters related to activity of compounds are electronic (e.g. dipole moments, quantum chemical parameters), hydrophobic (e.g. log P), and steric parameters derived from linear free energy relationships or from geometric considerations. Estimation of such molecular properties on a theoretical basis has been facilitated by the development and advancement of computational chemistry.

Computer Aided Drug Design and Computational Chemistry

Progress during the past few years in the field of Computer Aided Drug Design has rendered techniques that can extend QSAR by representing electronic and steric molecular properties graphically in 3D and quantifying them. Among the various methods for evaluation of molecular properties on a theoretical basis are force-field or empirical potential energy methods (molecular mechanics) and molecular orbital calculations (quantum mechanics).

Molecular Mechanics (M.M.) is a method to calculate energies based on the assumption that the total energy of a molecule is the sum of the individual contributions of the electrical and mechanical energy. The internal energy of a molecule can be expressed as a potential function , which has a minimum corresponding to the equilibrium geometry, and is a sum of a number of potential functions related to bond stretching, valence angle bending, torsional angle changes, non-bonded (van der Waals) interactions, electrostatic (coulombic) interactions and hydrogen bonding. Thus, M.M. uses a "classical elastic force-field" to make predictions about the equilibrium structure of a molecule (stable conformations). Force-fields used most frequently are MM2, AMBER and CHARMM, although no method can guarantee finding the absolute lowest energy --the global minimum-- since energy minimization will stop at the first local minima encountered without realising that more stable minima may be accessible.

In Quantum Mechanical Calculations, molecular energies are calculated by using the Schroedinger equation with the Molecular Orbital (M.O.) formalism, which can provide greater accuracy along with the ability to model electronic effects not treated by molecular mechanics. The Schroedinger equation of a given molecular system can be solved either with no approximations at all (ab initio) or with the introduction of some approximations (semiempirical). The GAUSSIAN and HONDO series are typical ab initio programs. Semiempirical methods use several approximations including CNDO, INDO and NDDO. Dewar has used these approximations to develop a number of semiempirical methods. In the approximations used, various terms were parameterized using experimental data,

in order to generate molecular orbital methods that provided "chemical accuracy". Thus, MNDO and AM1 (Austin Model 1) were developed based on the NDDO approximation. They have several advantages over the other models, and, AM1, which is also faster, is considered to represent , in its present form, the best that can be achieved using the NDDO approximation as a basis.

Quantum chemical calculations can provide detailed insight into the electronic nature of the molecular structures. Properties reproduced by this method are for e.g. charge distribution, dipole moments, electronic density, HOMO (highest occupied molecular orbital) energy, LUMO (lowest unoccupied molecular orbital) energy, transition energy, π electron energy, resonance or delocalization energy, electron density, net charge, heat of formation, molecular geometries. Furthermore, predictive models for partition coefficients (LogP) have been developed in recent years based on M.O. calculations. Most of these parameters along with others have shown at times to correlate with the activity of drugs, rendering quantum chemical calculations to be of great value in QSAR studies.

CHAPTER 2
CURRENT STUDY AND ITS OBJECTIVES

Brain-Enhanced Delivery of Potential Neurotrophomodulators

4-methylcatechol (4MC) is a potent NGF stimulator both in vitro (mouse fibroblast L929 cells and L-M cells) (Carswell et al., 1992, Furukawa et al., 1991) and in vivo, in the rat peripheral nervous system (Kaechi et al., 1993, Hanaoka et al., 1994) and in the rat brain after intracerebroventricular injection (Saporito et al., 1993). Peripheral administration of 4MC, as in the case of most pharmacologically active or not agents, excludes it from entering the brain, since the morphological and enzymatic components of the BBB not only prohibit large molecules such as peptides (e.g. NGF) from entering the brain but also small molecules that lack adequate lipophilicity. Efficient and sustained delivery of 4MC to the brain could be achieved by means of an appropriate brain-targeted chemical delivery system (CDS) such as the one based on the dihydropyridine <--> pyridinium salt redox reaction described previously.

Several CDSs were designed as potential brain selective targetry forms for 4-methylcatechol (Figure 3, A), in which one of the catecholic hydroxyl groups is esterified with the dihydropyridine targetor while the other is usually masked with an other lipophilic moiety or esterified with a second targetor.

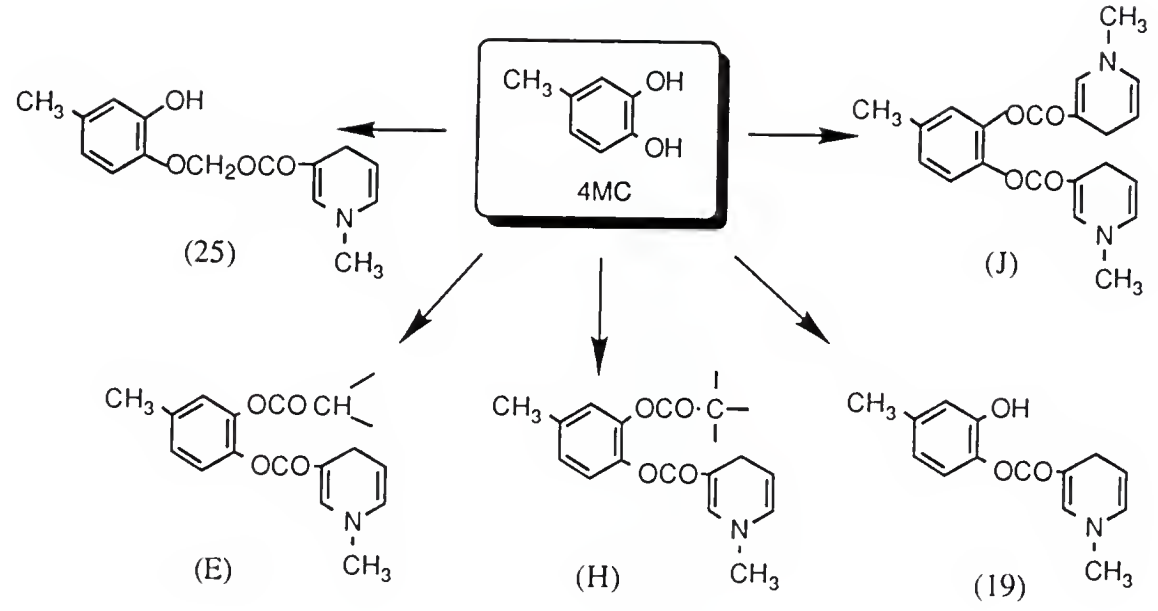

A.

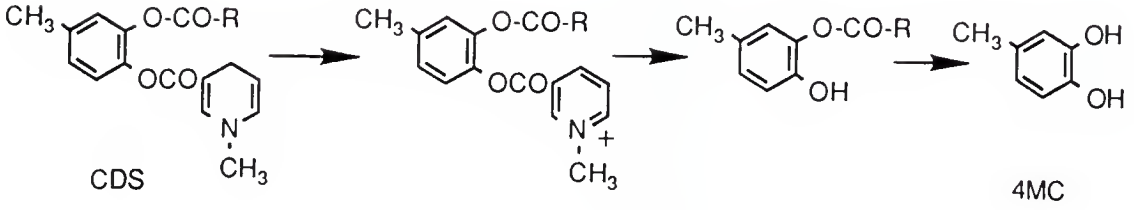

B.

Figure 3. A) Scheme of 4MC CDSs. B) Metabolism of the CDSs.

Furthermore, a redox analogue (4) of dopamine was designed, in which the amino group of dopamine is derivatized in the dihydropyridine ring, in order for the analogue to function as a CDS for the 4-alkyl-catechol moiety (Figure 4, A). The hydroxyl groups are protected in this case with lipophilic functions while the targetor is placed on the side alkyl chain of the molecule. The derivative is designed in a way that in vivo metabolism (in the brain) will liberate the 4-substituted catechol moiety which is expected not only to have NGF stimulatory activity due to its catechol part but also to "lock" in its site of action, the brain.

Specific objectives are:

1) Synthesis of the above mentioned CDSs.

2) Development of a suitable analytical system to evaluate the stability of the CDSs and metabolites in various buffer systems and biological media in order to determine the feasibility of delivery of 4MC and its derivative by this method. pH-profiles of representative CDS's and their quaternary metabolites as well as half-lives in rat blood, brain and liver homogenate are determined.

3) Evaluation of the in vivo distribution of the CDSs and their metabolites in order to determine whether the CDS is accomplishing its purpose, the selective and sustained delivery of the compounds of interest to the brain. In all cases, the dihydro moiety is expected to be oxidized (in vivo) after entering the brain and subsequent hydrolysis of the esters will liberate 4-MC (Figure 3, B) or the pyridinium catechol derivative (Figure 4, A). In vivo studies (in rat) of CDS J and 4 are performed to demonstrate oxidation of the CDSs, rapid peripheral

elimination of the pyridinium salt, and sustained central delivery of final compounds (metabolites) of interest.

4) Determination of the in vivo NGF-stimulatory activity of the 4MC-CDS J by pharmacological testing in suitable animal models. NGF stimulatory activity in the rat hippocampus and cerebral cortex, brain regions where NGF is predominantly expressed, is estimated by measuring the NGF mRNA content in these regions after treating rats with a single iv injection of the compound; the dose is based on the brain concentration observed in the distribution studies as well as the concentrations of 4-methylcatechol that stimulate NGF secretion in vitro/in vivo.

Synthesis and In Vitro Evaluation of Catechol Isosters and Derivative as NGF-Inducers

In order to produce novel NGF-stimulating compounds, while also attempting to elucidate the mechanism of action of the catechol derivatives on NGF induction, two isosters of 4MC were designed, synthesized and evaluated for in vitro activity. The functional catechol moiety of 4MC was substituted by two isosteric/isoelectronic moieties, chemical groups that are considered to be equivalent and therefore interchangeable as far as their contribution to biological activity is concerned. Since the only functional moiety that can be responsible for activity in the molecule of 4MC is the catechol moiety, biologically active

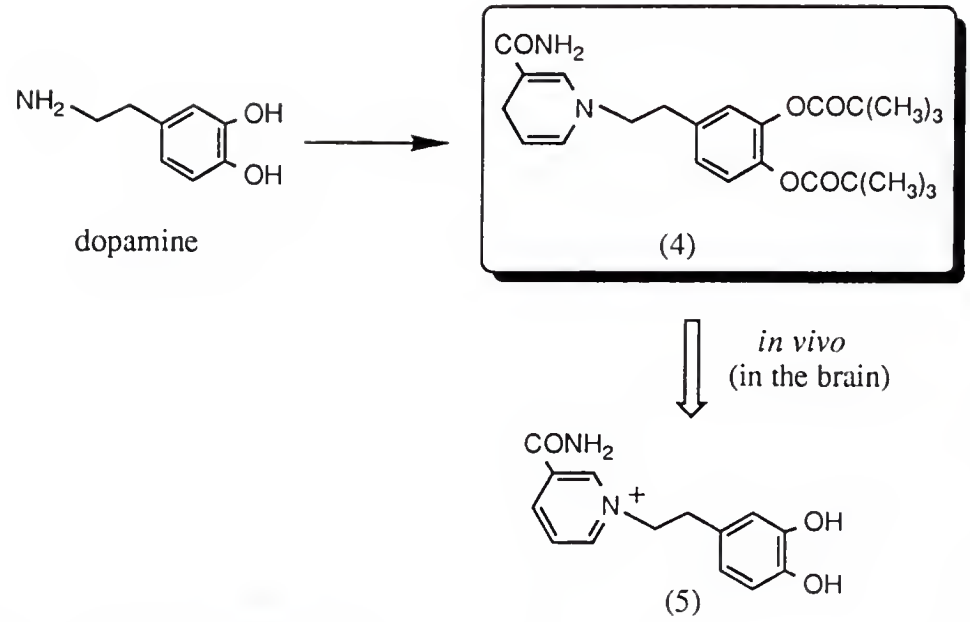

A.

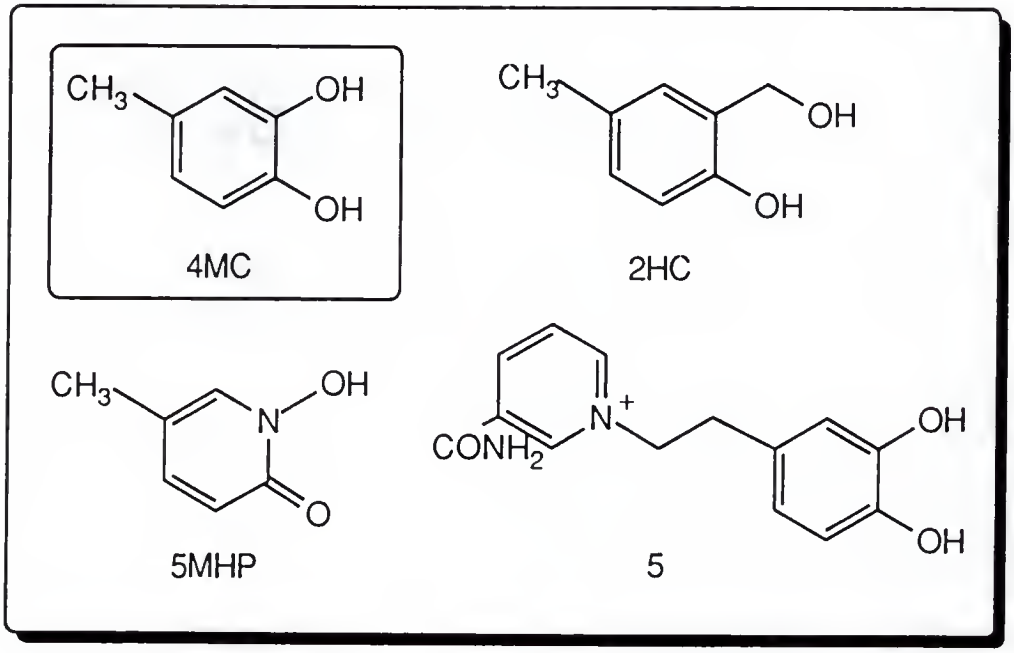

B.

Figure 4. A) Redox analogue of dopamine and its metabolite. B) 4MC, isosters and derivative.

compounds are expected to be derived by substituting it with the aforementioned functions.

Thus, two compounds are synthesized, 5-methyl-1-hydroxy-2-pyridone (5MHP) and 2-hydroxymethyl-p-cresol (2HC) (Figure 4, B), and their biological activity as NGF-stimulators was evaluated in vitro in two cell lines. Furthermore, in the case that the isosters prove to be active in vitro, appropriate CDSs are intended to be prepared.

In addition, the pyridinium catechol derivative 5, being the final metabolite of 4, is separately synthesised and also evaluated for in vitro NGF stimulatory activity, in order to establish that this novel catechol derivative is indeed active as other catechols and therefore to establish the usefulness of 4 as a CDS for the NGF-inducing catechol moiety.

Quantitative Structure Activity Relationships of Catechol Derivatives on NGF Secretion in L-M Cells

Some preliminary structure activity relationships of the catechol analogues suggested that the catechol ring is essential for the stimulatory effect on NGF synthesis. From the structure-effect of the aliphatic side chain it was deduced that β-hydroxylation decreased, N-substitution (non-bulky) enhanced, while α-carboxylation decreased the stimulation effect on NGF synthesis (Furukawa et al. 1991). Also, shortening of the chain length progressively reduced activity except in the case of alkyl side chains without any substituents, where the opposite was

observed. The question, therefore, that arises is why the catechol moiety is responsible for activity and, furthermore, what specific characteristics of that moiety, as modified by varying substitution on the ring, influence that activity.

In order to study the effects of the side chain on the catechol moiety of the molecules and to correlate characteristics of the molecular structure with activity, a set of 23 substituted catechols, with activities indicated in literature data, are characterized by various electronic, steric, and thermodynamic factors derived from the semi-empirical AM1 method. By correlating activity with the calculated descriptors, using simple or multiple regression analysis, a quantitative structure-activity relationship of catechol derivatives on NGF secretion in L-M cells could be obtained.

CHAPTER 3
EXPERIMENTAL AND RESULTS

Synthesis

All chemicals used were reagent grade obtained from Aldrich Company and solvents from Fisher Scientific. All melting points were recorded using Fisher-Johns melting point apparatus and are uncorrected. NMR data were recorded with Varian T-90, QE-300, or Varian Unity-300 spectrometer and are reported in parts per million (δ) relative to tetramethylsilane. The Elemental analyses were carried out either at Atlantic Microlab. Inc., Atlanta, Ga, or at the Analytical Services of the Department of Chemistry of the University of Florida. FAB or Electron Ionization mass spectrometry was performed with Kratos MFC 500. Ultra Violet spectra were obtained with a Perkin Elmer UV/VIS spectrometer Lambda II. Thin Layer Chromatography was carried out using Merck DC-aluminium foil Plates coated to a thickness of 0.2 mm with silica gel 60 containing Florescent (254) indicator, or aluminum oxide 60 F neutral (Type E). The High Performance Liquid Chromatography (HPLC) system consisted of a SP 8810 precision isocratic pump, SP4290 injector, Waters RCM C-18 column, SP 8450 UV/visible detector and SP4290 integrator. The mobile phase consisted of acetonitrile-water or methanol-water in different proportions.

Synthesis of 4-Methylcatechol Chemical Delivery Systems

The synthetic scheme followed for the preparation of the 4-methylcatechol CDSs is represented in figure 5. Synthesis of the respective intermediates and final compounds is described below.

Synthesis of 3-hydroxy-4-nicotinoyloxytoluene (A) and 3,4-nicotinoyloxytoluene (B) :

4-Methylcatechol (34.7 mmols) was dissolved in 90 ml pyridine and 52.1 mmols of nicotinoyl chloride hydrochloride was added. After heating under reflux for 48 h, the pyridine was distilled under vacuum at 60 °C, and methylene chloride added. The mixture was washed with ice-cold water and dried over Na_2SO_4. The products (A) and (B) were separated by flash chromatography (silica gel, 2% methanol in chloroform). Yield: 12.6 mmols (2.88 g) of (A) and 8.9 mmols (2.97 g) of (B).

(A): White solid, m.p.: 176-178 °C.

^{1}H-NMR (DMSO-d6) δ (ppm) (Figures 6 and 7) : 9.61 (bs, 1H, for Ph-OH) 9.21 (t, 1H, for pyrid. H-2, $J_{2,4\text{-}6}$=1.2-0.8 Hz) 8.87 (dt, 1H, for pyrid. H-6, $J_{6,5}$=4.5 Hz, $J_{6,4\text{-}2}$=2.1, 0.8 Hz) 8.43 (dt, 1H, for pyrid. H-4 $J_{4,5}$=8.1 Hz, $J_{4,6\text{-}2}$=2.1, 1.5 Hz) 7.63 (dd, 1H, for pyrid. H-5, $J_{5,6}$=4.8 Hz, $J_{5,4}$=7.5 Hz) 7.02 (d, for Ph-H-5 - *para* esterified molecule - $J_{5,6}$=8.1 Hz) 6.97 (s, for Ph-H-2' - *meta* esterified isomer) 6.925 (d, for Ph-H-5', $J_{5',6'}$=9 Hz) 6.85 (d for Ph-H-6', $J_{6',5'}$=8.1 Hz) 6.77 (s, for Ph-H-2) 6.64 (dd for Ph-H-6, $J_{6,5}$=8.1 Hz, $J_{6,2}$=1.2 Hz) (Total integration for all phenylic protons, range 7.02-6.64 ppm, is 3 H. The integration ratio of the

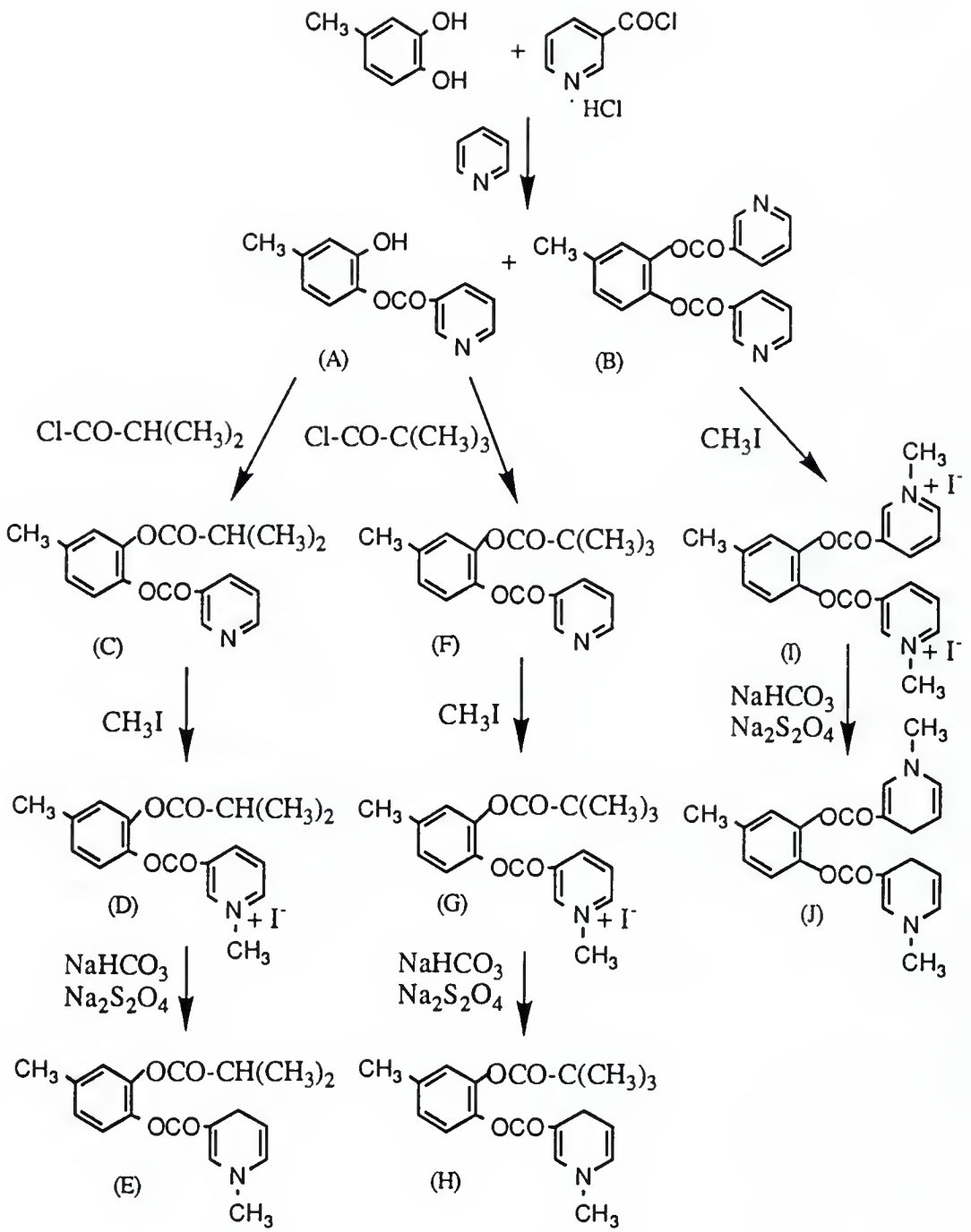

Figure 5. Synthetic scheme for the preparation of the 4-methylcatechol CDSs.

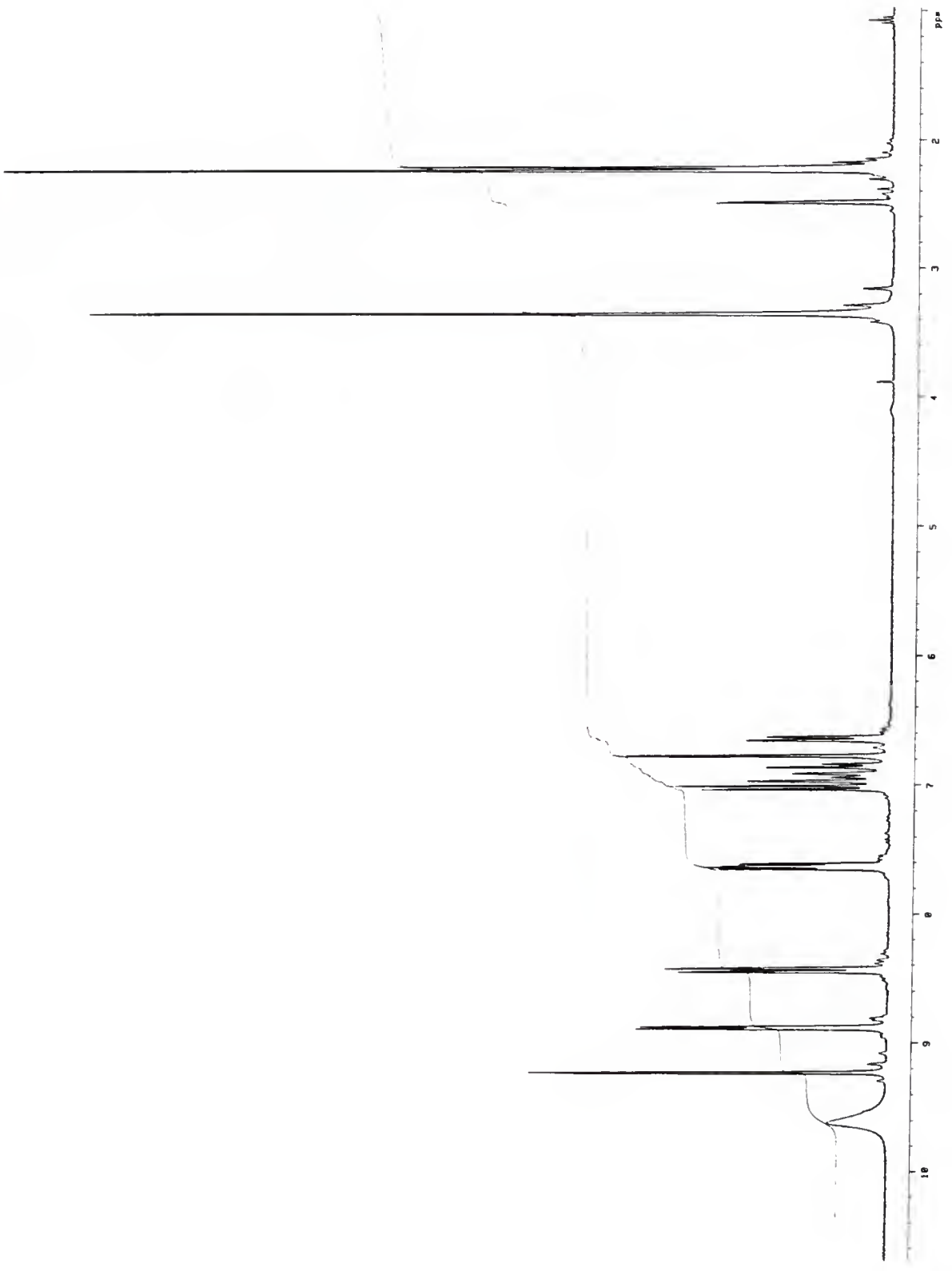

Figure 6. ^{1}H NMR spectrum of 3-hydroxy-4-nicotinoyloxytoluene (A).

(A)

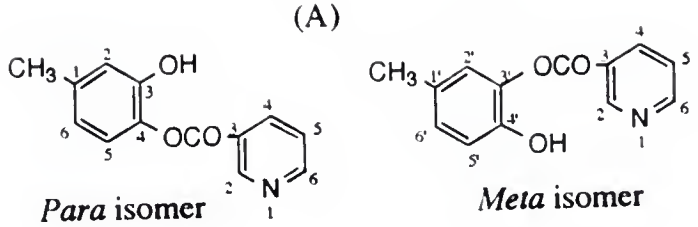

Para isomer *Meta* isomer

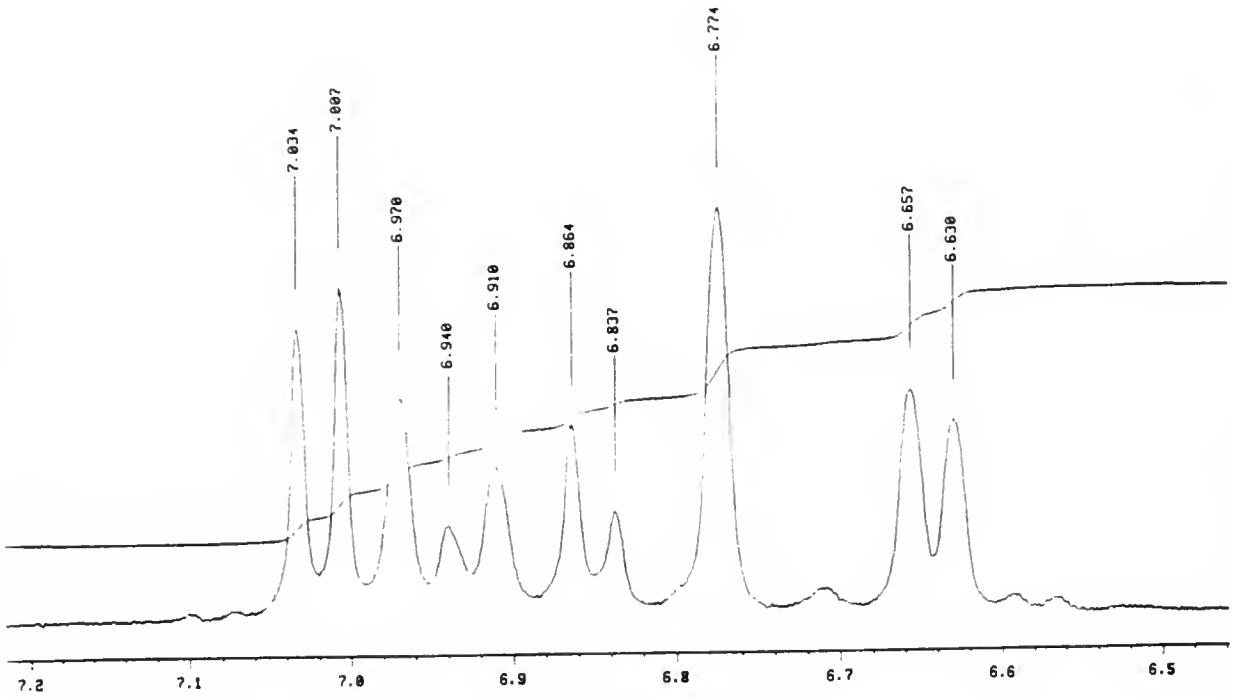

Figure 7. Expansion of the aromatic region of the ^{1}H-NMR spectrum of 3-hydroxy-4-nicotinoyloxytoluene (A).

specific H peaks of the phenyl ring are: H2-H2'= 6:4, H6-H6' = 6:4, and H5-H5'= 6:4.) 2.23 (d, total 3H, for Ph-CH_3, ratio of two isomers -ratio of the 2 peaks- 6:4).

Elemental analysis for $C_{13}H_{11}O_3N$: Theory: C 68.12, H 4.80, N 6.11. Found: C 68.02, H 4.82, N 6.03.

(MW=229) EI (Electron Ionization) Mass 230$[M+H]^+$,100. HPLC: Single peak of retention time 1.77 min (60% acetonitrile in water) and 1.76 min (80% methanol in water).

(B): White solid, m.p.: 91-92 ^oC

^{1}H-NMR ($CDCl_3$) δ (ppm): 9.2 (t, 2H, for 2 pyrid. H-2, $J_{2,4-6}$=1.8 Hz) 8.72 (dt, 2H, for 2 pyrid. H-6, $J_{6,5}$=5.1 Hz, $J_{6,4-2}$=1.8, 1.2 Hz) 8.25 (dt, 2H, for 2 pyrid. H-4, $J_{4,5}$=8.1 Hz, $J_{4,2-6}$=1.8 Hz) 7.3 (dd, 2H, for 2 pyrid. H-5, $J_{5,6}$=5.1 Hz, $J_{5,4}$=7.8 Hz) 7.29 (s, 1H, for Ph-H-2) 7.2 (d, for Ph-H-5, $J_{5,6}$=7.5 Hz) 7.12 (d, for Ph-H-6, $J_{6,5}$=8.7 Hz) 2.38 (s, 3H, for Ph-CH_3).

Elemental analysis for $C_{19}H_{14}O_4N_2$: Theory: C 68.26, H 4.19, N 8.38 Found: C 68.35, H 4.19, N 8.34. (MW= 334) EI Mass 335 $[M+H]^+$,98, 357 $[M+Na]^+$,100.

Synthesis of 3-isobutyryloxy-4-nicotinoyloxytoluene (C) :

In a suspension of 9 mmols (2 g) of monoester (A) in $CHCl_3$, 2 ml (18 mmols) of isobutyryl chloride in $CHCl_3$ was added dropwise (1:2) and small amount of pyridine. The mixture was refluxed for 48 hs. After evaporating the solvents, the product (viscous liquid) was purified by column chromatography (silica gel, 10% methanol in chloroform). Yield: 60%.

^{1}H-NMR ($CDCl_3$) δ (ppm): 9.36 (d, 1H, for pyrid. H-2, $J_{2,4}$=1.7 Hz) 8.85 (dt, 1H, for pyrid. H-6, $J_{6,5}$=4.8 Hz, $J_{6,4}$=1.3 Hz) 8.42 (dt, 1H, for pyrid. H-4, $J_{4,5}$=8 Hz, $J_{4,2}$=1.95 Hz) 7.46 (qt, 1H, for pyrid. H-5, $J_{5,4}$=7.9 Hz, $J_{5,6}$=4.86 Hz, $J_{5,2}$=1 Hz) 7.19-7.04 (m, 3H, for 3 Ph-H) 2.68 (septet of d, 1H, J=7 Hz, J=2.58 Hz) 2.38 (s, 3H, for 3 Ph-H) 1.15-1.12 (dd, 6H, for i-propyl 2 CH_3, J=1.95 Hz, J=7 Hz).

Elemental analysis for $C_{17}H_{17}O_4N$: Theory: C 68.22, H 5.68, N 4.68 Found: C 68.57, H 5.92, N 4.63.

Synthesis of 3-isobutyryloxy-4-(N-methylnicotinoyloxy)toluene iodide (D) :

In a solution of (C) in anhydrous acetone, an excess of methyl iodide was added. The mixture was heated at 50 °C for 8h. After distilling part of the solvent, ether was added and the semi solid precipitate was triturated to give a yellow crystalline mass which was filtered and washed with ether. Yield: 71%.

Bright yellow solid, m.p.: 131-133 °C.

^{1}H-NMR (DMSO-d_6) δ (ppm): 9.7 (s, 1H, for pyridinium H-2) 9.2 (d, 1H, for pyrid. H-6) 9.0 (d, 1H, for pyrid. H-4) 8.2 (t, 1H, for pyrid. H-5) 7.2 (m, 3H, for 3Ph-H) 4.4 (s, 3H, for N-CH_3) 2.8-2.6 (m, 1H, for i-propyl CH) 2.3 (s,3H, for Ph-CH_3) 1.1 (d, 6H, for i-propyl 2 CH_3).

Elemental analysis for $C_{18}H_{20}O_4NI$: Theory: C 48.97, H 4.53, N 3.17, I 28.79. Found: C 49.02, H 4.61, N 3.13, I 28.83. (MW= 441) EI Mass 314[M-I]$^+$,100.

Synthesis of 3-isobutyryloxy-4-(N-methyl-1,4-dihydronicotinoyloxy)toluene (E) :

Compound (D) (2 mmols) was dissolved in deaerated water, peroxide-free ether was added and the mixture cooled. 4 mmoles of $NaHCO_3$ was added slowly followed by 4 mmols $Na_2S_2O_4$. The reaction mixture was stirred in an ice bath, under N_2, for 2 hs. The layers were separated, washed and the combined ether solutions dried and evaporated to give a yellow viscous liquid. It reduces rapidly methanolic silver nitrate.

^{1}H-NMR ($CDCl_3$) δ (ppm): 7-6.8 (m, 3H, for Ph-H) 6.7 (dd, 1H, for dihydropyr. H-2) 5.65 (dt, 1H, dihydropyr. H-6) 4.85 (m, 1H, dihydropyr. H-5) 3.15 (bs, 1H, dihydropyr. H-4) 2.95 (s, 3H, for N-CH_3) 2.8 (m, 1H, for i-propyl CH) 2.3 (3H, for Ph-CH_3) 1.3 (m, 6H, for i-propyl 2 CH_3).

(MW=315) EI Mass 338$[M+Na]^+$,100. UV (in MeOH) λmax 270, 345 nm.

Synthesis of 3-pivaloyloxy-4-nicotinoyloxytoluene (F) :

Compound (A) (2.8 mmols) was dissolved in 15 ml $CHCl_3$ and excess (0.012 mols) of pivaloyl chloride in 10 ml $CHCl_3$ was added dropwise. After the addition of 5 ml pyridine the reaction mixture was stirred at room temperature for 10 hs. The solvents were evaporated and toluene added. The white undissolved solid was filtered off and the filtrate was condensed and purified by flash chromatography (silica gel, 2% methanol in chloroform) to yield a viscous liquid. Yield: 68.7%.

^{1}H-NMR ($CDCl_3$) δ (ppm): 9.36 (d, 1H, for pyrid. H-2, $J_{2,4}$=2) 8.86 (dt, 1H, for pyrid. H-6, $J_{6,5}$=4.5 Hz, $J_{6,4}$=2 Hz) 8.42 (dt, 1H, for pyrid. H-4, $J_{4,5}$=8 Hz,

$J_{4,2\text{-}6}$=2 Hz) 7.47 (dd, 1H, for pyrid. H-5, $J_{5,4}$=8 Hz, $J_{5,6}$=4.5 Hz) 7.2-7.0 2 (m, 3H, for 3 Ph-H) 2.4 (s, 3H, for Ph-CH_3) 1.2 (s, 9H, for t-butyl 3 CH_3).

(MW=313) EI Mass 336$[M+Na]^+$,100, 314$[M+H]^+$,75.

Synthesis of 3-pivaloyloxy-4-(N-methylnicotinoyloxy)toluene iodide (G) :

Compound (F) (1.6 mmols) was dissolved in 20 ml anhydrous acetone and 5ml iodomethane was added. The mixture was refluxed for 24 hs. Ether was added to get a yellow precipitate which was filtered off and recrystallized by acetone/ether. Yield: 50%.

Bright yellow solid, m.p.:140-142 ^oC.

^{1}H-NMR (DMSO-d_6) δ (ppm): 9.7 (s, 1H, for pyrid. H-2) 9.3 (d, 1H, for pyrid. H-6, $J_{6,5}$=4.8 Hz) 9.14 (d, 1H, for pyrid. H-4, $J_{4,5}$=6.4 Hz) 8.35 (t, 1H, for pyrid. H-5, $J_{5,4\text{-}6}$=7.6 Hz) 7.4-7.2 (m, 3H, for 3 Ph-H) 4.5 (s, 3H, for N-CH_3) 2.4 (s, 3H, for Ph-CH_3) 1.15 (s, 9H, for t-butyl 3 CH_3).

Elemental analysis for $C_{19}H_{22}O_4NI$: Theory: C 50.10, H 4.83, N 3.07, I 27.91. Found: C 50.21, H 4.86, N 3.04.

(MW=455) EI Mass 328$[M-I]^+$,100.

Synthesis of 3-pivaloyloxy-4-(N-methyl-1,4-dihydronicotinoyloxy)toluene (H) :

Compound (G) (0.13 mmols) was dissolved in 8 ml deaerated water and 5 ml peroxide-free ether was added. $NaHCO_3$ (0.52 mmols) was slowly added while stirring in an ice bath and then 0.52 mmols of $Na_2S_2O_4$. The reaction was stirred for 1 h under N_2 and then the layers were separated, and washed. The ether layers were dried over Na_2SO_4, then filtered and evaporated to yield a yellow viscous liquid. Yield: 30%. The product reduces instantly methanolic silver nitrate.

^{1}H-NMR ($CDCl_3$) δ (ppm): 7-6.8 (3H, for 3 Ph-H) 6.65 (1H, for dihydro H-2) 5.65 (d, 1H, for dihydro H-6) 4.84 (1H, for dihydro H-5, $J_{5,4}$=8 Hz) 3.15 (m, 2H, for pyrid. 2 H-4) 2.42 (s, 3H, for N-CH_3) 2.35 (s, 3H, for Ph-CH_3) 1.4 (s, 9H, for t-butyl 3 CH_3).

(MW=329) EI Mass 352$[M+Na]^+$,100. UV (MeOH) λmax 268, 345 nm.

Synthesis of 3,4-(N-methylnicotinoyloxy)toluene iodide (I) :

To 0.65g (1.9 mmols) of nicotinoyl diester of 4-methylcatechol (B) dissolved in MeOH, an excess of iodomethane was added and the mixture was heated at 40 °C for 2hs. The solvent was evaporated, acetone was added, and stirred for 1h, to give a yellow precipitate which was filtered off and recrystallized from methanol/ether to give 0.74g (61.6 % yield) of the diquaternary salt.

Yellow solid, m.p.: 204-206 °C.

^{1}H-NMR (DMSO-d_6) δ (ppm): 9.7 (2H) 9.2 (d ,2H) 9.1 (d, 2H) 8.4 (m, 2H) 7.5 (m, 3H) 4.5 (s, 6H) 2.5 (s, 3H).

Elemental analysis for $C_{21}H_{20}O_4N_2I_2$: Theory: C 40.77, H 3.23, N 4.53, I 41.10. Found: C 40.83, H 3.25, N 4.56, I 41.13. (MW=618)

Synthesis of 3,4-(N-methyl-1,4-dihydronicotinoyloxy)toluene (J) :

Compound (I) (1.2 mmols) was dissolved in deaerated water, ethyl acetate was added and the mixture cooled in an ice-bath. $NaHCO_3$ (9.6 mmols) was added very slowly followed by 9.6 mmols of $Na_2S_2O_4$. The whole procedure was conducted under N_2. The mixture was stirred for 1h 45 min. The two layers were separated, washed and the combined ethyl acetate extracts were dried over

Na_2SO_4. After filtration and evaporation it yielded a yellow liquid that reduces instantly methanolic silver nitrate.

^{1}H-NMR ($CDCl_3$) δ (ppm): 6.95-6.67 (m, 5H, for 3 Ph-H and 2 dihyropyridine H-2) 5.7 (d, 2H, for 2 dihydropyridine H-6) 4.9 (m, 2H, for 2 dihydropyridine H-5) 3.2 (bs, 4H, for 2 dihydropyridine H-4) 3.02 (s, 3H, for Ph-CH_3) 2.3 (d, 6H, for 2 N-CH_3). (MW=366) EI Mass 389$[M+Na]^+$,100. UV (MeOH) λmax 280 and 353 nm (Figure 8).

Synthesis of the Redox Analog of Dopamine

The synthetic scheme for this preparation is depicted in Figure 9 and respective synthesis of intermediates and final product described below.

Synthesis of 3-carbamoyl-1-(2,4-dinitro)phenylpyridinium chloride ('Zincke-type reagent') (1) :

Nicotinamide (0.065 mols) and 0.098 mols of 2,4-dinitro-chloro-benzene were mixed and heated in a 90 °C oil bath for 75 min. The melt was dissolved in MeOH and ether was added to precipitate a yellow solid. Using the same system the product was re-precipitated 3 times and then dissolved in water and treated with charcoal. The product, 3-carbamoyl-1-(2,4-dinitro)phenylpyridinium chloride (or 'Zincke reagent') (1), was freeze-dried to a pale foamy solid. Yield: 33%. m.p.: 141-142 °C.

^{1}H-NMR (DMSO-d_6) δ (ppm): 9.8 (bs, 1H) 9.4 (d, 1H) 9.1 (d, 1H) 8.9-8.7 (m, 3H) 8.4-8.2 (m, 2H) 8.1 (bs, 1H).

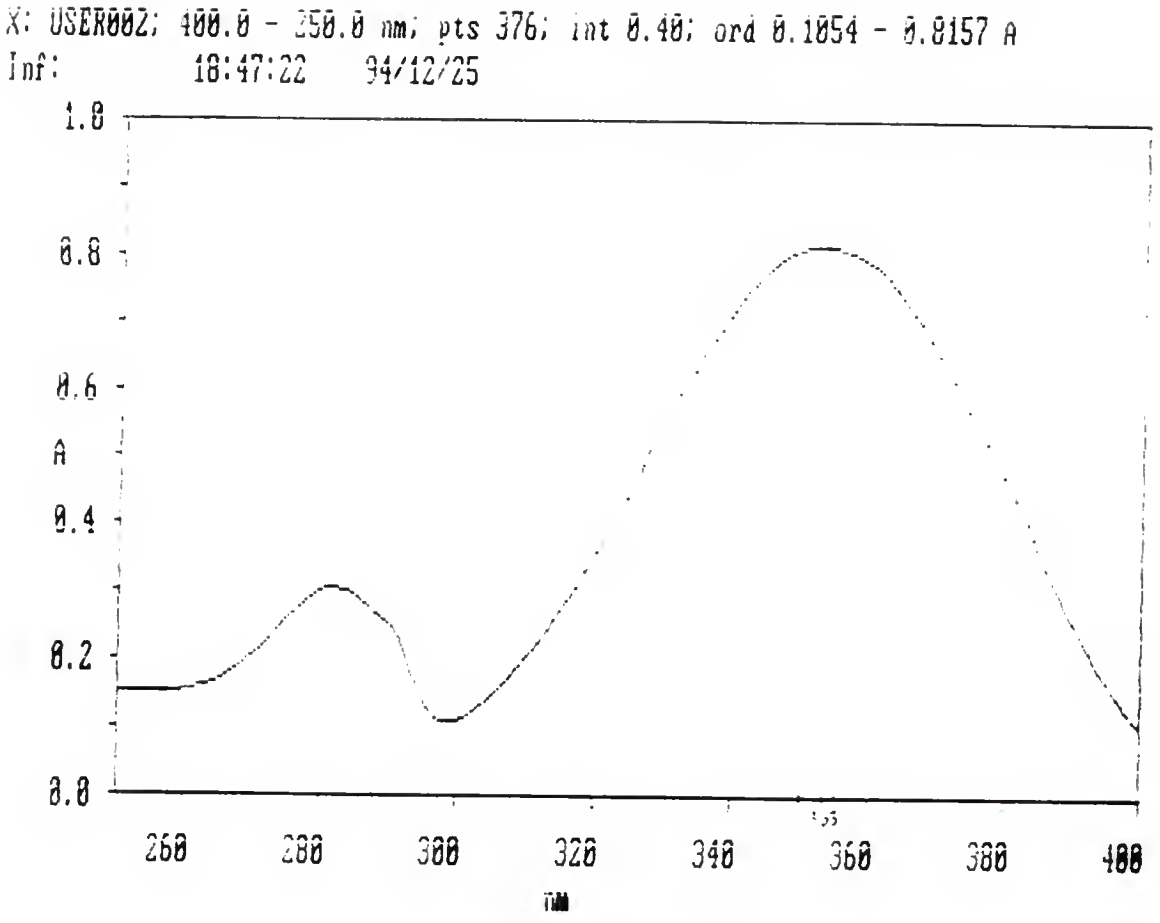

Figure 8. Ultra Violet Spectrum of Dihydro compound J. (Typical UV spectrum obtained by all dihydro compounds synthesized in this study)

Synthesis of di-O-pivaloyl dopamine (trifluoroacetate) (2) :

In a suspension of 4g of dopamine hydrochloride in 20 ml trifluoro acetic acid (TFA), 10 ml pivaloyl chloride was added dropwise. After stirring for 45 hs the TFA was distilled and the product was isolated by column chromatography (silica gel, 10 % methanol in chloroform). Yield: 92%.

Pale white solid, m.p.: 108-109 ^{o}C.

^{1}H-NMR ($CDCl_3$) δ (ppm): 7.7 (br, 2H) 7 (3H) 3 (m, 4H) 1.3(s 18H).

Elemental analysis for $C_{20}H_{28}O_6NF_3$: Theory: C 55.17, H 6.4, N 3.2. Found: C 54.85, H 6.5, N 3.12.

Synthesis of 1-(3',4'-dipivaloylphenethyl)-3-carbamoylpyridinium trifluoroacetate (3) :

To a solution of 4.62 mmols of (1) and 9.25 mmols of (2) in 10 ml anhydrous MeOH, 1.28 ml tetraethylamine (TEA) (in 6 ml MeOH) was added dropwise. The mixture was stirred for 30 min and refluxed for 30 min. Upon cooling, a yellow solid precipitated (by-product) and was removed. The filtrate was evaporated and dissolved in a small amount of MeOH and ether was added to precipitate a pale solid, which was recrystallized several times by methanol/ether. Yield: 52%.

Pale coloured solid, m.p.: 194-198 ^{o}C.

^{1}H-NMR (DMSO-d_6) δ (ppm): 9.61 (s, 1H) 9.15 (d, 1H) 8.96 (d, 1H) 8.63 (s, 1H, for 1H of $CONH_2$) 8.25 (t, 1H) 8.16 (s. 1H, for 1H of $CONH_2$) 7.2 (m, 3H) 4.9 (t. 2H) 3.15 (m, for H_2O and CH_2-Ph) 1.3 (d ,18H). (MW=540) EI Mass 427 $[M\text{-}CF_3COO^-]^+$,100.

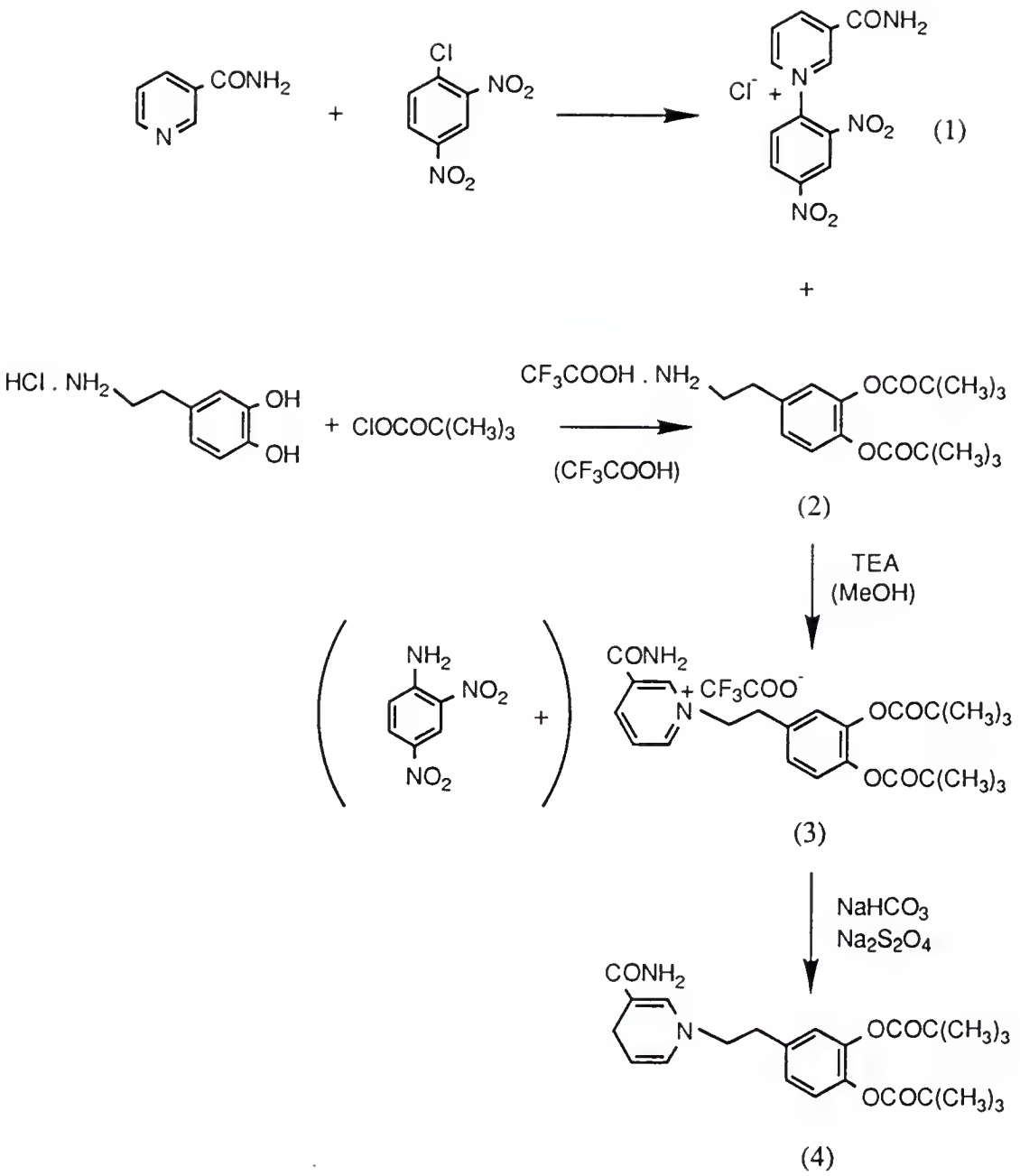

Figure 9. Synthetic scheme for the preparation of the redox analog of dopamine (4).

Elemental analysis for $C_{26}H_{31}O_7N_2F_3$: Theory: C 57.70, H 5.74, N 5.18. Found: C 57.70, H 5.73, N 5.21.

Synthesis of 1-(3',4'-dipivaloylphenethyl)-3-carbamoyl-1,4 dihydropyridine (4) :

Compound (3) (1.076 mmols) was dissolved in deaerated water, peroxide-free ether was added and the mixture cooled. $NaHCO_3$ (5 mmols) was added slowly followed by 5 mmols of $Na_2S_2O_4$ and the reaction mixture was stirred in an ice-bath, under N_2, for 3 hs. The two layers were then separated, washed, and the combined ether solutions dried and evaporated to give the product. Yield: 45.4%. The product reduces instantly methanolic silver nitrate.

Yellow solid, m.p.: 62-66 ^oC.

^1H-NMR ($CDCl_3$) δ (ppm): 7.06 (s, 2H) 6.96 (s, 1H) 6.91(s, 1H) for ArH and dihydropyridine H-2, 5.65 (d, 1H) for dihydropyridine H-6, 5.25 (bs, 2H) for $CONH_2$, 4.71 (m, 1H) for dihydropyridine H-5, 3.32 (t,2H) 3.13 (s, 2H) for dihydropyridine 2 H-4, 2.81 (t, 2H) 1.35 (d, 18H). (MW=428) EI Mass 451$[M+Na]^+$,100.

UV (in MeOH) lmax 270, 345 nm.

Elemental analysis for $C_{24}H_{32}O_5N_2$: Theory: C 67.29, H7.48, N 6.54. Found: C 67.58, H 7.65, N 6.28.

Synthesis of the Pyridinium Catechol Derivative and a Dimethoxy CDS

Synthesis of these products was conducted according to the reactions shown in Figure 10. Synthesis of the final products and intermediate is described below.

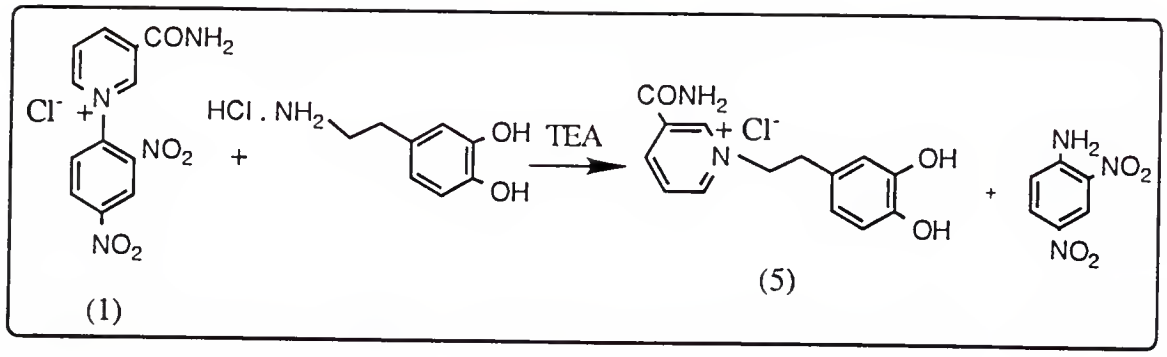

A.

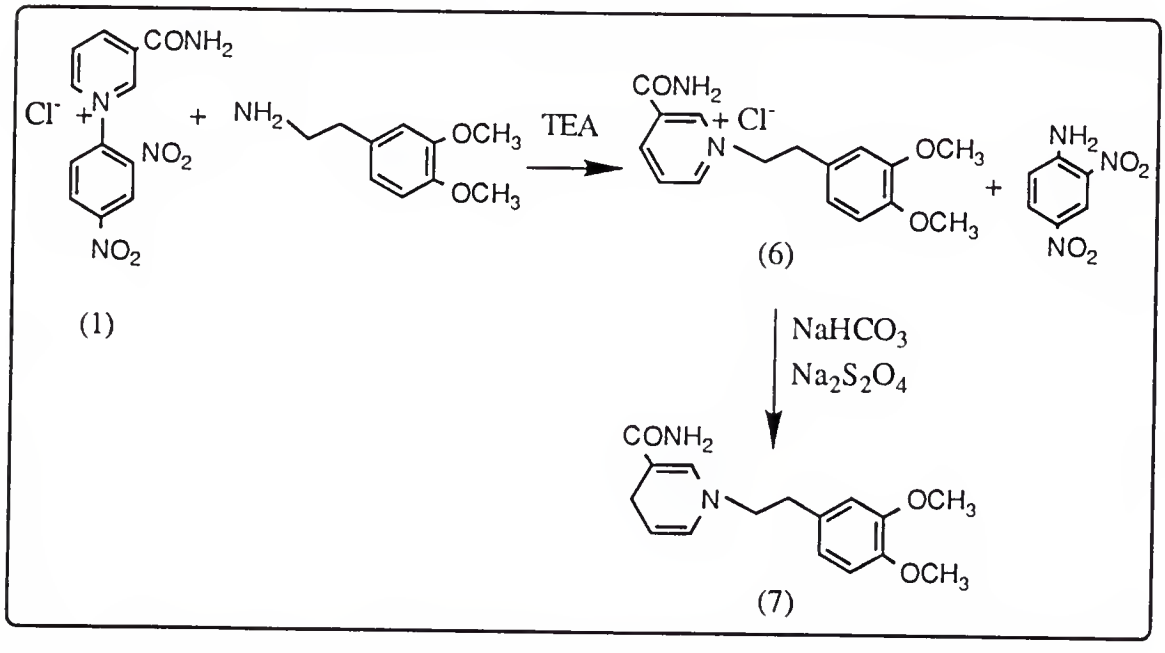

B.

Figure 10. A) Synthesis of the pyridinium catechol derivative (5). B) Synthesis of the methoxy CDS (7).

Synthesis of 1-(3',4'-dihydroxyphenethyl)-3-carbamoylpyridinium chloride (5) :

To a solution of 4.6 mmols of dopamine hydrochloride, in 10 ml methanol, 4.6 mmols of TEA was added followed by 2.3 mmols of the Zincke type reagent (1) in 3 ml methanol. The mixture was refluxed for 1 h. Upon cooling the yellow precipitate was removed and to the filtrate ether was added to precipitate a yellow solid. m.p.: 234-235 °C

^{1}H-NMR (DMSO-d_6) δ (ppm): 9.3 (s, 1H) 9.05-8.8 (m, 5H) 8.2 (m, 2H) 6.6 (m, 2H) 6.4 (d, 1H) 4.8 (t, 2H for N-CH_2) 3.1 (t, 2H for Ar-CH_2). (MW=294) EI Mass 259 $[M\text{-}Cl^-]^+$,100.

Elemental analysis for $C_{14}H_{15}O_3N_2Cl$: Theory: C 57.04, H 5.09, N 9.51 Cl 12.05. Found: C 55.40, H 5.18, N 9.19 Cl 11.59.

Synthesis of 1-(3',4'-dimethoxyphenethyl)-3-carbamoylpyridinium chloride (6) :

To a solution of 6.15 mmols of dimethoxy-phenethylamine in 8 ml dry methanol, 3.07 mmols of the Zincke type reagent (1) were added and the mixture stirred for 2 hs at room temperature. After cooling on ice, the yellow precipitate (by-product) was filtered off. Ether was then added to the solution to give an orange precipitate which was recrystallized from methanol/ether. Yield: 77%.

Orange coloured solid, m.p.: 235-239 °C

^{1}H-NMR (DMSO-d_6) δ (ppm): 9.64 (s, 1H, for pyridinium H-2) 9.07 (d, 1H, for pyrid. H-6, $J_{6,5}$=6.3 Hz) 8.97 (d, 1H, pyrid. H-4, $J_{4,5}$=8.1 Hz) 8.82 (s, 1H, for 1 of $CONH_2$) 8.19 (dd, 1H, for pyrid. H-5, $J_{5,6}$=6.3 Hz, $J_{5,4}$=8.1 Hz) 8.16 (s, 1H, for 1 of $CONH_2$) 6.92 (d, 1H, for phenylic H-2, $J_{2,6}$=1.8 Hz) 6.82 (d, 1H, for

phenylic H-5, $J_{5,6}$=8.1 Hz) 6.67 (dd, 1H, for phenylic H-6, $J_{6,5}$=8.1 Hz, $J_{6,2}$=1.8 Hz) 4.84 (t, 2H, for N-CH_2) 3.7 (d, 6H for 2 CH_3O) 3.21 (t, 2H, for Ph-CH_2).

(MW=322) EI Mass 287[M-Cl^-]$^+$,100.

Elemental analysis for $C_{16}H_{19}O_3N_2Cl$: Theory: C 59.53 H5.89, N 8.68, Cl 11.00. Found: C 59.46, H 5.90, N 8.61, Cl 10.92.

Synthesis of 1-(3',4'-dimethoxyphenethyl)-3-carbamoyl-1,4 dihydropyridine (7) :

To a solution of 0.309 mmols of (6) in deaerated water, methylene chloride was added and the mixture cooled. 5 mmols of $NaHCO_3$ were added slowly followed by 5 mmols of $Na_2S_2O_4$ and the reaction mixture was stirred in cool under N_2, for 3 hs. The two layers were then separated, washed and the combined organic layers dried over Na_2SO_4. After evaporation, a yellow semi solid was obtained. Purity checked by HPLC: single peak using two different systems (1.48 min retention time with 60% acetonitrile-water, flow rate 2ml/min, or 1.6 min with 80% methanol in water)

^{1}H-NMR ($CDCl_3$) δ (ppm): 7.02 (s, 1H) 6.8 (d, 1H) 6.7 (m, 2H) 5.65 (d, 1H) 5.48 (s, 2H) 4.7 (m, 1H) 3.86 (d, 6H) 3.3 (t, 2H) 3.14 (s, 2H) 2.76 (t, 2H). (MW=288) UV (in MeOH) λmax 280, 355 nm.

Synthesis of 2-Hydroxymethyl-p-Cresol

Synthesis of 2-hydroxymethyl-p-cresol(2HC) was performed according to Figure 11 (A) as follows:

A solution of p-cresol (32 mmols), benzene boronic acid (49 mmols), propionic acid (16 mmols), and paraformaldehyde (0.23 mols), in dry benzene (130 ml), was heated under reflux, with azeotropic removal of water using a Dean-Stark type separator, for 8 hs. The large excess of paraformaldehyde was added portionwise in intervals of 1.5-2 hs. Evaporation of the solvent, extraction with dichloromethane, washing with aqueous Na_2CO_3 and water and evaporation of the solvent after drying gave a residue which recrystallized from petroleum ether to the 2-phenyl-4H-1,3,2-dioxaborin derivative 8, Figure 11, A. In the next step, a mixture of derivative 8 (4.5 mmols), 30% hydrogen peroxide solution (5ml) and tetrahydrofuran (5ml) was stirred at 0-25 ^oC for 2.5 hs. The reaction mixture was poured into ice-water, extracted with ether several times, and the extracts were washed with sodium hydrogen sulphite solution. After drying and removing the solvent, the residue was recrystallized from ether/petroleum ether to pure 2HC.

White solid, m.p.: 104-105 ^oC.

^{1}H-NMR (DMSO-d_6) δ (ppm): 7.05 (b, 1H, for Ph-O-H) 7.01 (dd, 1H, for C_5-H, $J_{6,5}$ = 8.4 Hz, $J_{3,5}$ = 1.5 Hz) 6.86 (ds, 1H, for C_3-H, $J_{3,5}$ = 1.5 Hz) , 6.8 (d, 1H, for C_6-H, $J_{6,5}$ = 8.4 Hz) 4.83 (s, 2H, for CH_2) 2.25, (s, 3H, for CH_3) 1.65 (s, 1H, for CH_2-O<u>H</u>).

Elemental analysis for $C_8H_{10}O_2$: Theory: C, 69.56, H, 7.24. Found: C, 69.43, H, 7.28.

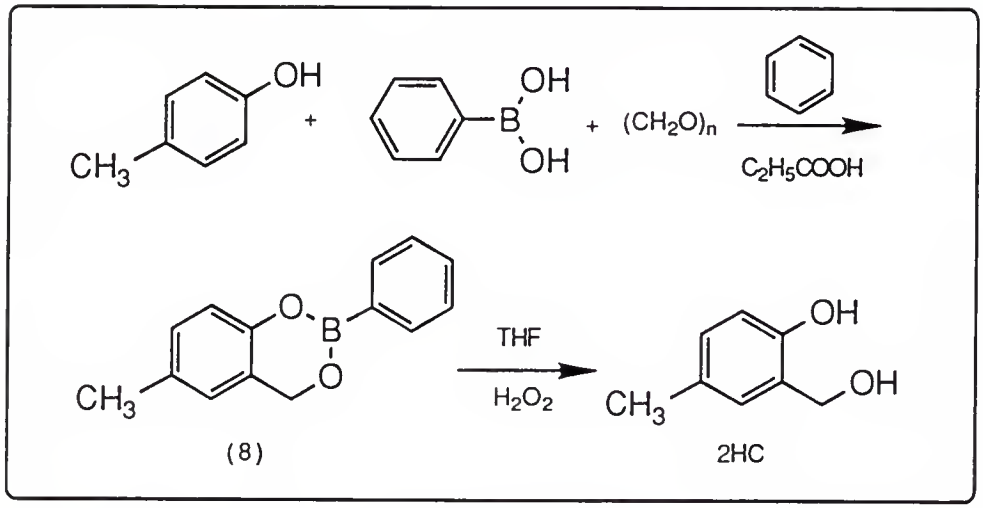

A.

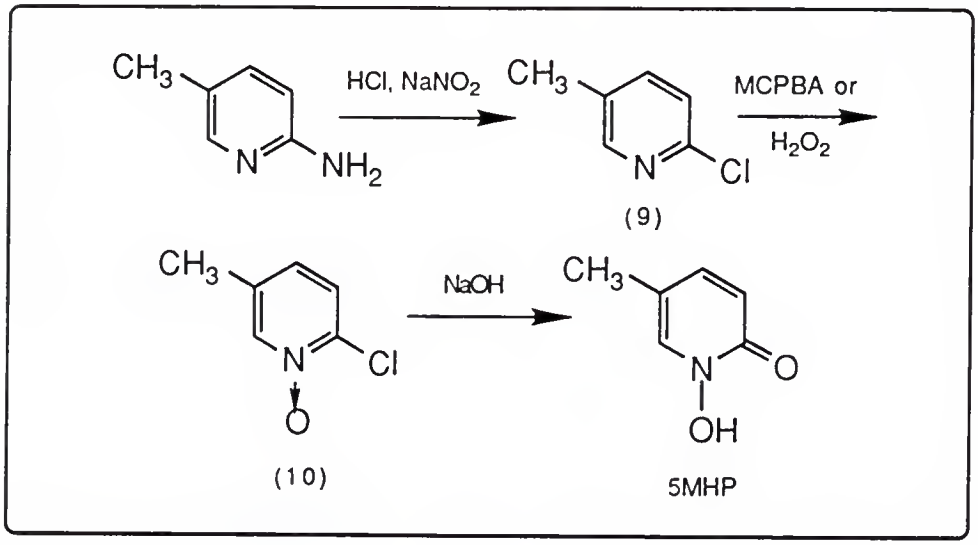

B.

Figure 11. Synthetic scheme for the preparation of A) 2-hydroxymethyl p-cresol (2HC) and B) 5-methyl-1-hydroxy-2-pyridone (5MHP).

Synthesis of 5-Methyl-1-Hydroxy-2-Pyridone

Synthesis of 5-methyl-1-hydroxy-2-pyridone (5MHP) was performed according to Figure 11 (B) as follows:

5-Methyl-2-amino pyridine was converted to the 2-chloro derivative (9), figure 11 B, according to the procedure described in Lister et al., 1968, in 60 % yield. N-Oxidation of the chloro derivative using 3-chloroperbenzoic acid, gave the N-oxide (10) which was separated from the accompanying 3-chlorobenzoic acid by vacuum liquid chromatography, using silica gel as an adsorbent. The N-oxide was obtained solely and in 70 % yield when the chloro derivative was heated with 30 % H_2O_2 in acetic acid at 76 ^oC for 40 hs and the product was crystallized from ethyl acetate (m.p. 70-72 ^oC). The final product, 5-methyl-1-hydroxy-2-pyridone was obtained directly (70 % yield) from the N-oxide on alkaline hydrolysis by boiling with 1N NaOH aqueous solution for 24 hs. The product precipitated from chloroform solution by addition of hexane in crystalline form and showed one spot on TLC plates of silica gel using several solvent systems.

White solid, m.p.: 155-156 ^oC.

^{1}H-NMR (DMSO-d_6) δ (ppm): 12 (s, 1H, for N-OH), 7.5 (s, 1H) 7.2 (dd, 1H) 6.5 (d, 1H) for three aromatic protons, 2.1 (s, 3H, for C-CH_3).

Elemental analysis for $C_6H_7NO_2$: Theory: C, 57.6, H, 5.6, N, 11.2. Found C, 57.5, H, 5.65, N, 11.11.

Synthesis of 3-{(N-Methyl-1,4-Dihydronicotinoyloxy)Methyl}-4-(N-Methyl-1,4-Dihydronicotinoyloxy)Toluene

Synthetic scheme for the preparation of 3-{(N-methyl-1,4-dihydro-nicotinoyloxy)methyl}-4-(N-methyl-1,4-dihydronicotinoyloxy)toluene (13), is shown in Figure 12.

Synthesis of 3-nicotinoyloxymethyl 4-nicotinoyloxytoluene (11) :

A mixture of 1.45 mmols 2HC and 4.35 mmols of nicotinoyl chloride hydrochloride in 10 ml pyridine were refluxed for 3 hs. After evaporating the pyridine, chloroform was added and the mixture washed twice with water and dried over $MgSO_4$. The product was purified by flash chromatography (silica gel, 1% methanol in methylene chloride).

Pale white solid, m.p.: 85-86 ^oC.

^1H-NMR ($CDCl_3$) δ (ppm): 9.27 (d, 1H, for pyrid. H-2, $J_{2,4}$=1.66 Hz) 9.04 ((d, 1H, for pyrid'.-connected to the 3 position of toluene- H-2', $J_{2',4'}$=1.66 Hz) 8.76 (dd, 1H, for pyrid. H-6, $J_{6,5}$=4.58 Hz, $J_{6,4}$=1.66 Hz) 8.67 (dd, 1H, for pyrid'. H-6', $J_{6',5'}$=4.58 Hz, $J_{6',4'}$=1.66 Hz) 8.32 (dt, 1H, for pyrid. H-4, $J_{4,5}$=8.33 Hz, $J_{4,2-6}$=1.66 Hz), 8.11 (dt, 1H, for pyrid'. H-4', $J_{4',5'}$=8.33 Hz, $J_{4',2'-6'}$=1.66 Hz) 7.36 (dd, 1H pyrid. H-5, $J_{5,6}$=4.58 Hz, $J_{5,4}$=8.33 Hz), 7.26 (dd, 1H,for pyrid'. H-5', $J_{5',6'}$=4.58 Hz, $J_{5',4'}$=8.33 Hz) 7.3 (d, 1H, for Ph-H-2, $J_{2,6}$=1.6 Hz) 7.2 (dd, 1H for Ar-H-5, $J_{5,6}$=8.5 Hz, $J_{5,2}$=1 Hz) 7.08 (d, 1H, for Ph-H-6, $J_{6,5}$=8.5 Hz) 5.32 (s, 2H, for Ph-CH_2-O) 2.35 (s, 3H, for Ph-CH_3).

(MW=348) EI Mass 371$[M+Na]^+$,100.

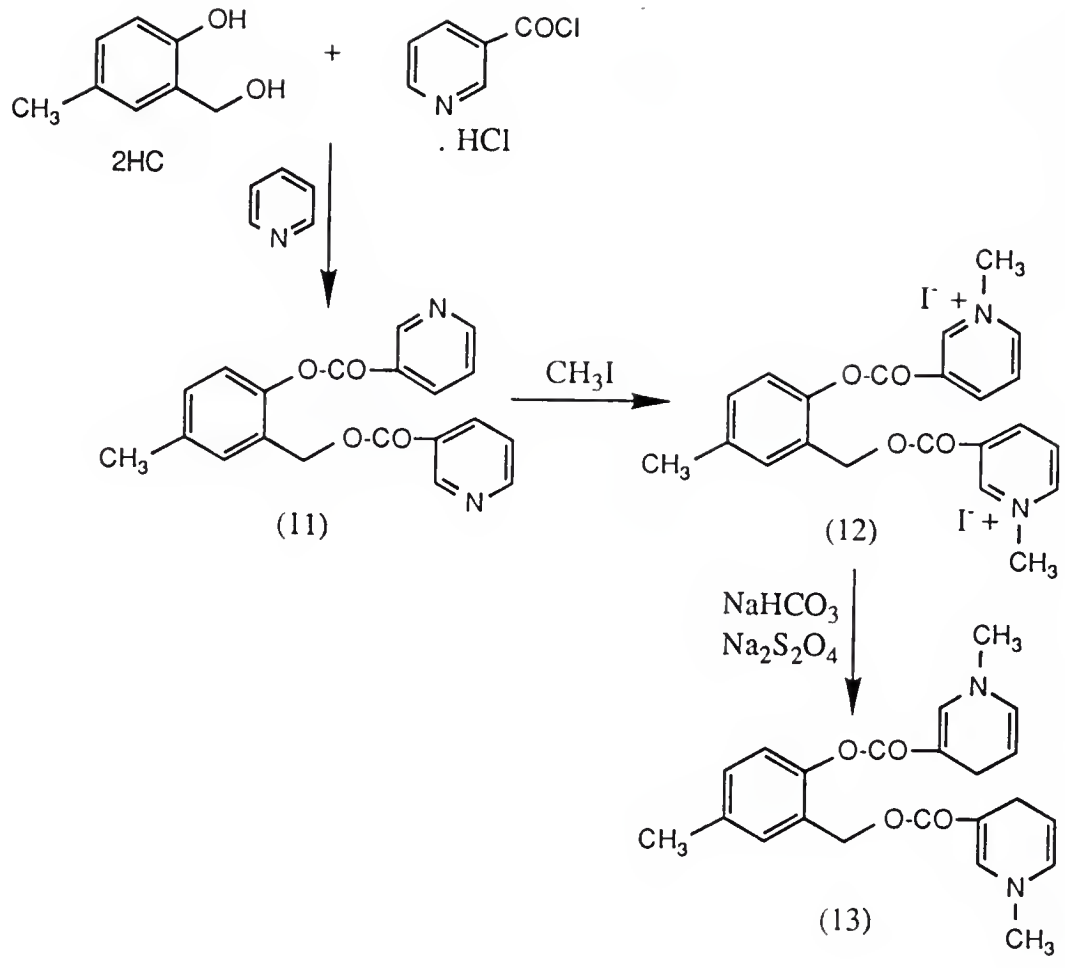

Figure 12. Synthetic scheme for the preparation of 3-{(N-methyl-1,4-dihydronicotinoyloxy)methyl}-4-(N-methyl-1,4-dihydronicotinoyloxy)toluene (13).

Elemental analysis for $C_{20}H_{16}N_2O_4$: Theory: C 68.97 H 4.6 N 8.05. Found: C 69.06 H 4.66 N 7.96.

Synthesis of 3-{(N-methylnicotinoyloxy)methyl-4-(N-methylnicotinoyloxy) toluene iodide (12) :

Excess of methyl iodide (3ml) was added to 0.55 mmols of (11) dissolved in 20 ml dry acetone. The mixture was refluxed overnight after which the yellow precipitate was filtered and washed with cold acetone. Yield 90%. (MW=632)

Yellow solid, m.p.: 160-163 °C.

^{1}H-NMR (DMSO-d_6) δ (ppm): 9.8 (bs, 1H, for pyrid. H-2) 9.47 (bs, 1H, for pyrid'.-connected to the 3 position of toluene- H-2') 9.3 (d, 1H, for pyrid. H-6, $J_{6,5}$=5.83 Hz) 9.2 (d, 1H, for pyrid'. H-6', $J_{6',5'}$=5.83 Hz) 9.15 (d, 1H, pyrid. H-4, $J_{4,5}$=8.75 Hz) 8.9 (d, 1H, pyrid'. H-4', $J_{4',5'}$=8.75 Hz) 8.35 (dd, 1H, for pyrid.H-5, $J_{5,6}$=5.83 Hz, $J_{5,4}$=8.75 Hz) 8.25 (dd, 1H, for pyrid. H-5', $J_{5',6'}$=5.83 Hz, $J_{5',4'}$=8.75 Hz) 7.56-7.33 (m, 3H, for Ph-H) 5.53 (s, 2H, for Ph-CH_2-O) 4.5 (s, 3H for N-CH_3) 4.44 (s, 3H for N'-CH_3) 2.4 (s, 3H, for Ph-CH_3).

Elemental analysis for $C_{22}H_{22}N_2O_4I_2$: Theory: C 41.77 H 3.48 N 4.43 I 40.19. Found: C 41.84 H 3.5 N 4.47 I 40.26.

Synthesis of 3-{(N-methyl-1,4-dihydronicotinoyloxy)methyl}-4-(N-methyl-1,4-dihydronicotinoyloxy)toluene (13) :

Compound (12) (0.16 mmols) was dissolved in deaerated water, methylene chloride was added and the mixture cooled in an ice-bath. $NaHCO_3$ (1.26 mmols) was added very slowly followed by 1.26 mmols of $Na_2S_2O_4$. The whole procedure was conducted under N_2. The mixture was stirred for 1h 45 min. The

two layers were separated, washed and the combined ethyl acetate extracts were dried over Na_2SO_4. After filtration and evaporation it yielded a yellow liquid that reduces instantly methanolic silver nitrate. (MW=380)

UV (CH_2Cl_2) λmax 360 nm.

Synthesis of 3-Hydroxy-4-(N-Methyl-1,4-Dihydronicotinoyloxy)Toluene

Attempted synthesis of 3-hydroxy-4-(N-methyl-1,4-dihydronicotinoyloxy) toluene (19) by various routes is shown in Figure 13.

Synthesis of nicotinic anhydride (14) :

Sodium salt of nicotinic acid (0.033 mols) (prepared by adding 0.05 mols of nicotinic acid in 50 ml aqueous solution of 0.5 mols NaOH and distilled under reduced pressure) was suspended in 200 ml warm xylene and 0.016 mols of nicotinoyl chloride hydrochloride was added and the mixture refluxed for 4h. The precipitate was filtered off and the solvent from the filtrate was evaporated. The solid product was recrystallised from benzene and stored in dessicator with P_2O_5. Yield: 50%.

White solid, m.p.: 122-126 °C

^{1}H-NMR (DMSO-d6) d (ppm): 9.1 (d, 2H, for 2 pyrid. H-2, $J_{2,4}$=2Hz) 8.82 (dd, 2H, for 2 pyrid. H-6, $J_{6,5}$=6 Hz, $J_{6,4}$=2 Hz) 8.3 (dt, 2H,for 2 pyrid. H-4, $J_{4,5}$=8 Hz, $J_{4,2\text{-}6}$=2 Hz) 7.57 (dd, 2H, for 2 pyrid. H-5, $J_{5,6}$=4.4 Hz, $J_{5,4}$=8 Hz).

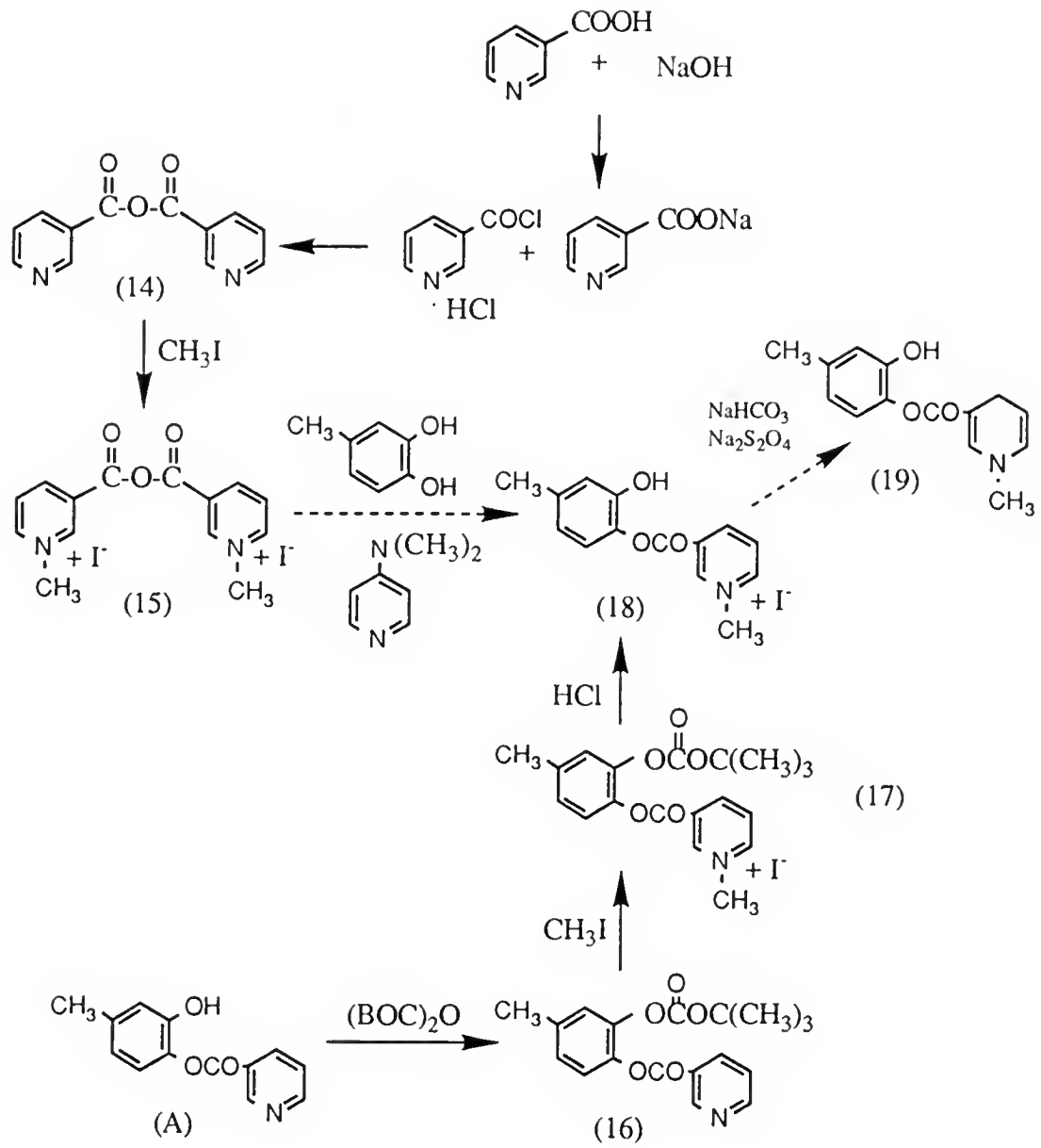

Figure 13. Synthetic schemes for the preparation of 3-hydroxy-4-(N-methyl-1,4-dihydronicotinoyloxy)toluene (19).

Synthesis of trigonelline anhydride (15) :

To 7 mmols of (14) in 75 ml acetonitrile, 20 mmols of methyl iodide (excess) were added and refluxed overnight. After cooling the precipitated solid was filtered and stored in dessicator with P_2O_5. Yield: 80%

Yellow solid, m.p.: 218-220 ^oC (MW=512)

^{1}H-NMR (DMSO-d_6) δ (ppm): 9.51 (s, 2H, for 2 pyrid. H-2) 9.2 (d, 2H, for 2 pyrid. H-6, $J_{6,5}$=4.8 Hz) 8.95 (d, 2H, for 2 pyrid. H-4, $J_{4,5}$=8.4 Hz) 8.26 (dd, 2H, for 2 pyrid. H-5, $J_{5,6}$=6 Hz, $J_{5,4}$=8.4 Hz) 4.45 (s, 6H, for 2 -N-CH_3).

Synthesis of 3-BOC-4-nicotinoyloxytoluene (16) :

To a solution of 0.43 mmols of (A) in chloroform, 1 g (excess) of di-tert-butyl-pyrocarbonate (BOC anhydride) were added and the mixture stirred at room temperature overnight. The product, white viscous liquid, was isolated by flash chromatography (silica gel, 2% methanol in methylene chloride).

Yield: 70%. (MW=329)

^{1}H-NMR d ($CDCl_3$) δ (ppm): 9.0 (bs, 1H, for pyrid. H-2), 8.8 (bd, 1H, for pyrid. H-6), .37 (dt, 1H, for pyrid. H-4), 7.39 (dd, 1H, for pyrid. H-5), 7.2-7.0 (m, 3H, for Ar-H), 2.3 (s, 3H, Ar-CH_3), 1.34 (s, 9H, for t-But)

Synthesis of 3-BOC-4-(N-methylnicotinoyloxy)toluene iodide (17) :

Excess of iodomethane (1 ml) was added to a solution of (14) (0.2 mmols), in 10 ml dry acetone. The reaction was refluxed for 2 days. The product was precipitated by addition of ether to the reaction mixture. Yield: 80%. (MW=471)

Yellow solid, m.p.: 130-133 ^oC

^{1}H-NMR (DMSO-d_6) δ (ppm): 9.78 (bs, 1H, for pyrid. H-1) 9.29 ((bd, 1H, for pyrid. H-6) 9.11 (bd, 1H, for pyrid. H-4) 8.3-8.4 (bt, 1H, for pyrid. H-5) 7.4-7.2 (m, 3H, for Ar-H) 4.5 (s, 3H, for N-CH_3) 2.38 (s, 3H, for Ar-CH_3) 1.35 (s, 9H, for t-But)

Elemental analysis for $C_{19}H_{22}NO_5I$: Theory: C 48.40 H 4.67 N 2.97 I 26.96. Found C 48.29 H 4.71 N 2.91 I 27.08.

Synthesis of 3-Hydroxy-4-(N-Methylnicotinoyloxy)Toluene Iodide (18) :

0.08 mmols of (15) were finely ground and dissolved in 1 ml of 4M HCl in Dioxane. After stirring for 2 hs, the solvents were evaporated in vacuum and the viscous liquid obtained was recrystallised by warm acetone/ether. Yield: 32%

Pale yellow solid, m.p.: 197-199 ^oC

^{1}H-NMR (DMSO-d_6) δ (ppm): 9.98, 9.83 (d, ratio of 2 peaks 7:3, total 1H, for -OH) 9.78 (bs, 1H, for pyrid. H-1) 9.3 ((bd, 1H, for pyrid. H-6) 9.14 (dt, 1H, for pyrid. H-4) 8.32 (bt, 1H, for pyrid. H-5) 7.1-6.68 (m, 3H, for Ar-H) 4.5 (s, 3H, for N-CH_3) 2.27, 2.25 (d, ratio of 2 peaks 7:3, total 3H, for Ar-CH_3).

(MW=371) EI Mass 244 $[M\text{-}I^-]^+$,100.

Synthesis of 3-hydroxy-4-{(N-methyl-1,4-dihydronicotinoyloxy)methoxy}toluene

Attempted synthesis of 3-hydroxy-4-{(N-methyl-1,4-dihydronicotinoyloxy) methoxy}toluene (25) is represented in Figure 14.

Synthesis of chloromethyl chlorosulfate (20) :

Chlorosulfonic acid (200 ml, 3 M) and bromochloromethane (100ml, 1.5M) were

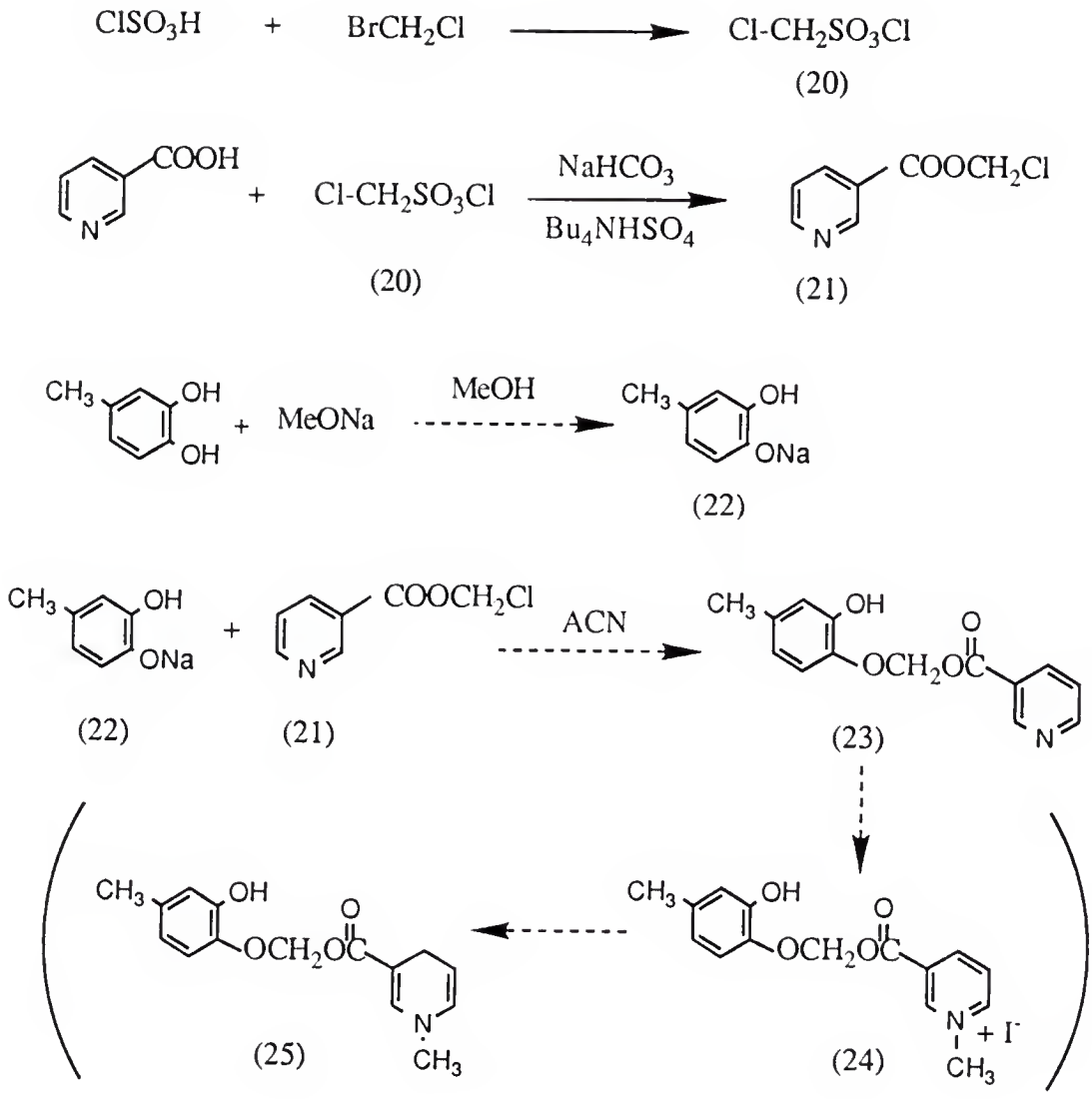

Figure 14. Synthetic scheme for the preparation of 3-hydroxy-4-{(N-methyl-1,4-dihydronicotinoyloxy)methoxy}toluene (25).

boiled for 3 hs. The mixture was poured on ice and extracted with 100ml methylene chloride, which was washed with water (100ml), dried and evaporated under vacuum. The product was distilled at 45-50 ^{o}C (9-10 mmHg). Yield: 30%.

Synthesis of chloromethyl nicotinate (21) :

To 0.04 mols of nicotinic acid in 40 ml methylene chloride and 40 ml water, 0.15 mols of $NaHCO_3$, 0.002 mols of Bu_4NHSO_4, and 0.046 mols of (20) in 10 ml methylene chloride were added. The mixture is stirred for 1 h and the layers separated. The organic layer was washed several times with water, and the product was isolated by column chromatography (neutral Al_2O_3, methylene chloride). The product was kept in solution.

^{1}H-NMR ($CDCl_3$) δ (ppm): 9.19 (bt, 1H, for H-2, $J_{2,4\text{-}6}$=2 Hz) 8.94 (dd, 1H, for H-6, $J_{6,5}$=4.5 Hz, $J_{6,2}$=2 Hz) 8.4 (dt, 1H, for H-4, $J_{4,5}$=8.5 Hz, $J_{4,2\text{-}6}$=2 Hz) 7.18 (dd, 1H, H-5, $J_{5,4}$=8.5 Hz, $J_{5,6}$=4.5 Hz) 6.2 (s, 2H, for -O-CH_2-Cl)

Synthesis of 4-methyl-2-hydroxy sodium phenoxide (22) :

To 5.82 mmols of 4-methylcatechol in 6 ml dry and deaerated methanol, 5.82 mmols of MeONa (4.37 M solution in methanol) were added and the solvent was immediately distilled under vacuum. (The product which is unstable and oxidizes in air -dark color appears rapidly- was kept under N_2.)

Attempted synthesis of 3-hydroxy-4-{(nicotinoyloxy)methoxy}toluene (23) :

Equimolar amounts of (21) and (22) were mixed in acetonitrile. The mixture was refluxed under N_2 for many days. The dark mass obtained did not contain the desired product (23). 18-crown-ether was also added during the reaction but did not alter the result.

In Vitro Stability Studies

Analytical Method

A high performance liquid chromatographic (HPLC) method was developed to assay the CDSs and their metabolites. The HPLC system consisted of an Autochrom M500 pump, Rheodyne injector, Waters RCM C-18 column, Spectroflow 757 absorbance detector and a Fisher Recordall series 5000. The mobile phase consisted of aqueous phosphate buffer solution (0.037 M, pH 6.5) and acetonitrile in different proportions. HPLC peak heights were used as a measure of the concentration of the compounds (assay detection limit 1μg/ml) and were plotted against time to evaluate the disappearance rates of the compounds. The stabilities were determined by measuring the pseudo-first order rate constant (k_{obs}, min^{-1}) or the half-life ($t_{1/2}$, min) of disappearance of the compound in the solution. k_{obs} is determined from the slope of the log of the disappearance curve (k_{obs} = slope x 2.303) and the $t_{1/2}$ of the compounds is calculated from the relation $t_{1/2} = 0.693 / k_{obs}$.

Stability in Buffers

USP standard phosphate buffer solutions (0.2M) (USP XXI, 1985) in the pH range of 4.5 to 9.5 were used in this study. Solutions of D, E, 4 and 3 in buffers were made at a concentration of 1 mg/ml. The solutions were kept at 37°C

and aliquots were taken at frequent time intervals and injected in the HPLC. The study was repeated 3 times, and the half live at each pH was calculated from the average of the values obtained. pH profiles of D and E are shown in Figure 15, while the pH profiles of 4 and 3 are represented in Figure 16.

Stability in Biological Media

A 0.3 ml aliquot of stock solution (3 mg/ml DMSO) of the CDS compounds or their quaternary metabolites were added respectively to 3 ml of biological medium (whole heparinized rat blood, 20% rat brain homogenate, or 20% rat liver homogenate, in isotonic phosphate buffer of pH 7.4), which was kept in a 37 ^{o}C water bath, to obtain a final concentration of 0.33 mg/ml biological media. Samples of 0.1 ml were taken at appropriate time intervals (0, 0.25, 0.5, 0.75, 1, 3, 5, 10, 15, 20, 30, 40, 60, 80, 100, and 120 min) and were mixed with 0.2 ml acetonitrile containing 5% DMSO. The mixtures were centrifuged and the supernatants injected in the HPLC. The experiment was repeated once more and the average half lives calculated. The stabilities (half-lives) of the 4-methyl-catechol chemical delivery systems (E, H, J) and their quaternary metabolites (D, G, I) in rat blood and brain homogenate are shown respectively in Figures 17 and 18, while the stability of 4 and 3 in rat blood, liver and brain homogenate is shown in Figure 19.

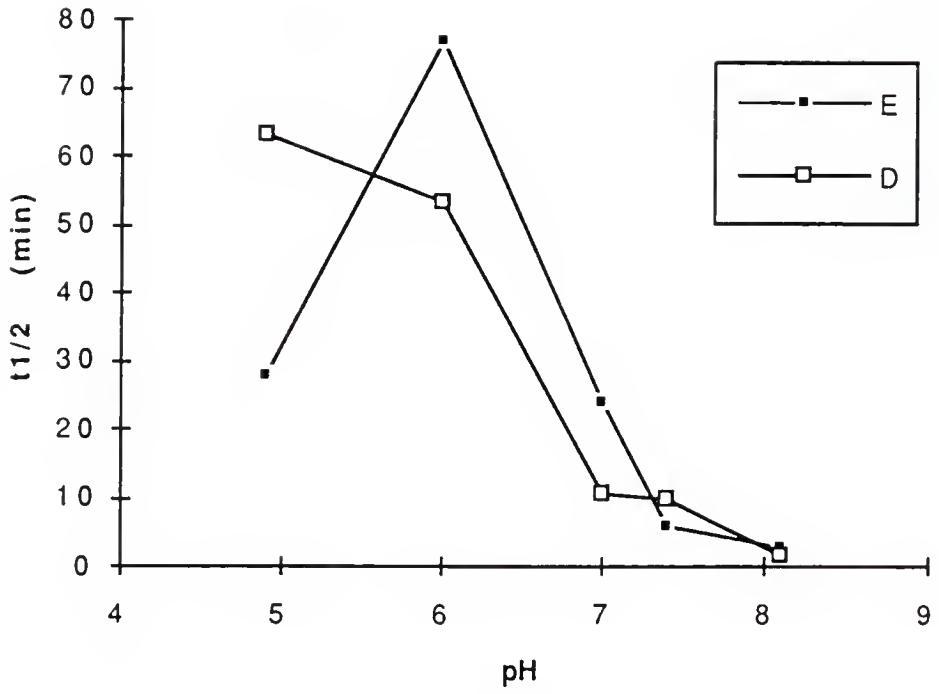

Figure 15. pH profile of 4-methyl catechol CDS (E) and its quaternary metabolite (D). Each value is the mean of three independent determinations.

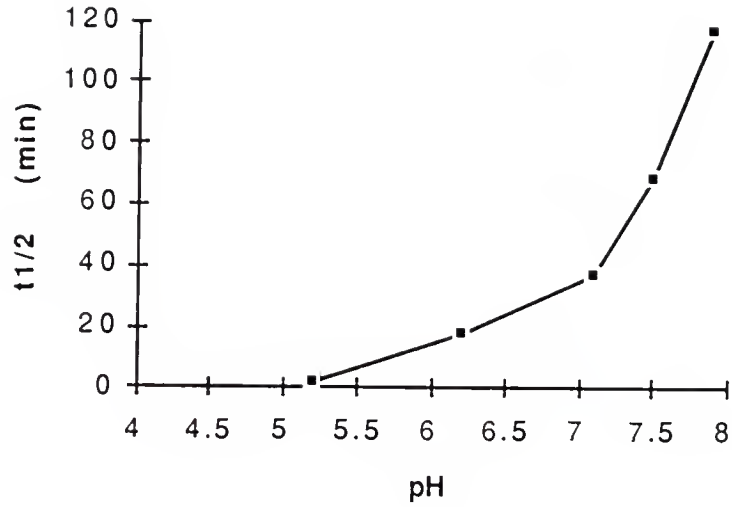

A.

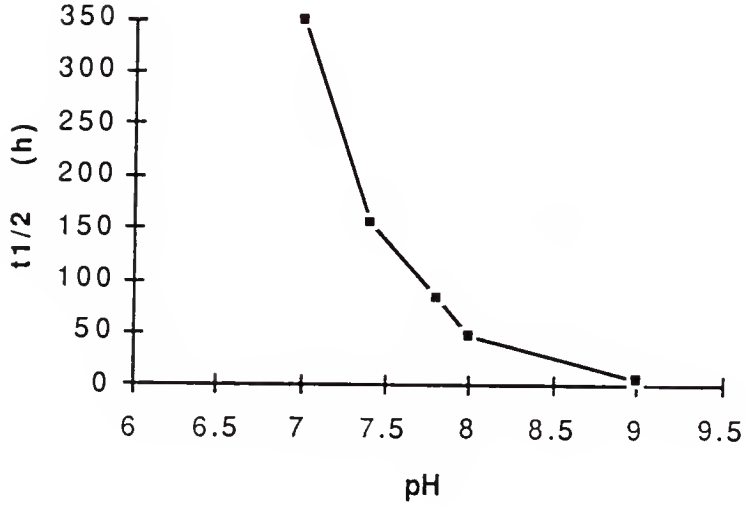

B.

Figure 16. pH profiles of CDS 4 (A) and of its quaternary metabolite 3 (B). Each value is the mean of three independent determinations.

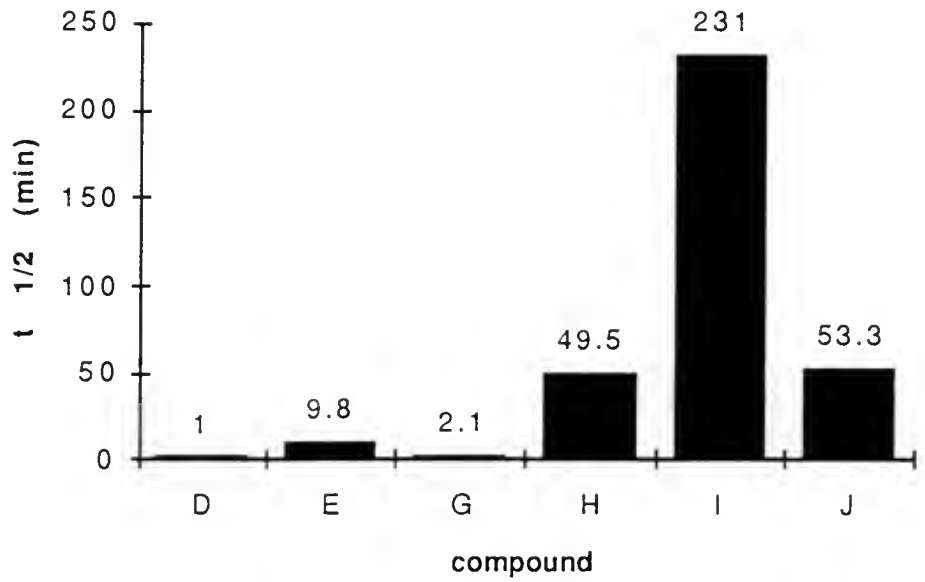

	D	E	G	H	I	J
r	0.997	0.999	0.995	0.986	0.979	0.98
k	0.666	0.071	0.326	0.014	0.003	0.013
t 1/2 (min)	1	9.8	2.1	49.5	231	53.3

Figure 17. In vitro stability in rat brain 20% homogenate of CDSs (E, H, and J) and their quaternary metabolites (D, G, and I). Each value is the mean of two independent determinations. r is the regression coefficient, k is the rate of disappearance, and $t_{1/2}$ is the half-life in minutes.

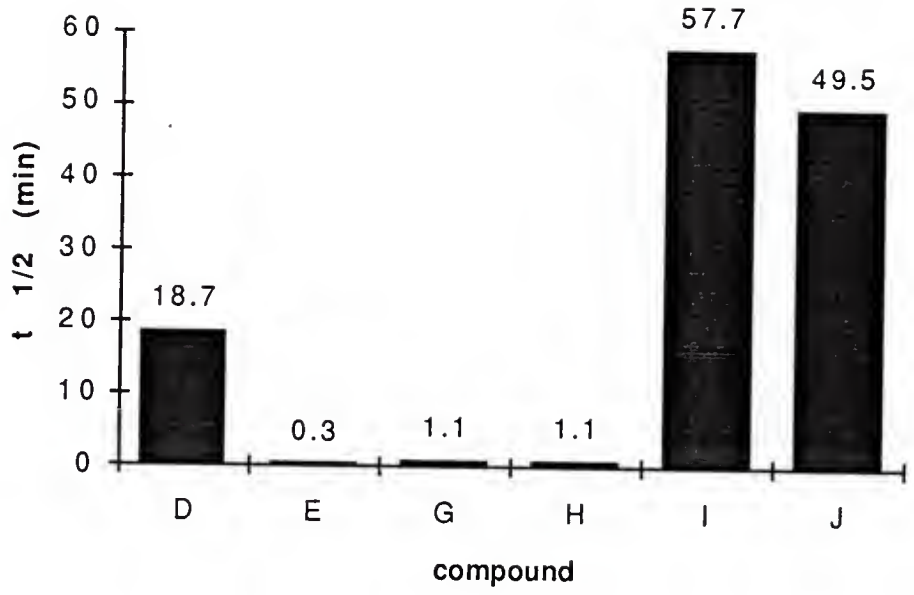

	D	E	G	H	I	J
r	0.99	0.984	0.95	0.972	0.991	0.991
k	0.037	2.23	0.642	0.633	0.012	0.014
t 1/2 (min)	18.7	0.3	1.1	1.1	57.7	49.5

Figure 18. In vitro stability in rat blood of CDSs (E, H, and J) and their quaternary metabolites (D, G, and I). Each value is the mean of two independent determinations. r is the regression coefficient, k is the rate of disappearance, and $t_{1/2}$ is the half-life in minutes.

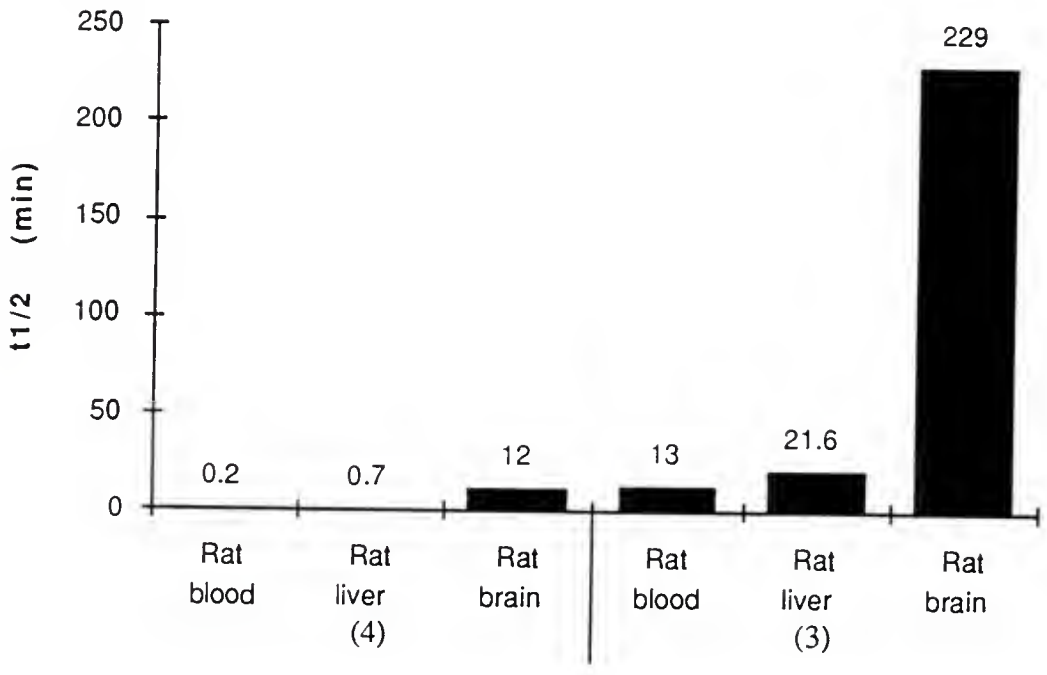

	Blood (4)	Liver (4)	Brain (4)	Blood (3)	Liver (3)	Brain (3)
r	0.986	0.99	0.991	0.995	0.989	0.612
k	3.236	1.0187	0.0574	0.053	0.032	0.003
t1/2 (min)	0.2	0.7	12	13	21.6	229

Figure 19. In vitro stability of (4) and (3) in various biological media. The first 3 columns refer to the dihydro CDS (4), while the last 3 columns refer to the quaternary (3). Each value is the mean of two independent determinations. r is the regression coefficient, k is the rate of disappearance, and $t_{1/2}$ is the half life in minutes.

In Vivo Distribution Study

Analytical Method

The HPLC system consisted of a SP 8810 precision isocratic pump, SP4290 injector, Waters RCM C-18 column, SP 8450 UV/visible detector and SP4290 integrator. The mobile phase consisted of aqueous phosphate buffer solution (0.05 M, pH 6.5) and acetonitrile in different proportions for the detection of the dihydro compounds, quaternary metabolites and final metabolites. The area under the peak was used as a measure of the concentration of the compound. Detection was made at 345 nm for the dihydro compounds and at 254 nm for metabolites.

Experimental procedure

Male Sprague Dawley rats (body weight 200-220 g) were injected intravenously (tail vein) with compounds J or 4 (50mg/Kg body weight) in 1:1 DMSO and 50% 2-hydroxypropyl-β-cyclodextrin in water. Animals were sacrificed at the appropriate time points and trunk blood, brain (and liver) collected. Samples were mixed or homogenised with 2 volumes of acetonitrile containing 5% DMSO, centrifuged, and supernatants analysed by HPLC.

Calibration curves were used to determine the concentrations of the CDSs and their metabolites in blood, brain, or liver, respectively. Results of the in vivo distribution study are represented in Figures 20-23.

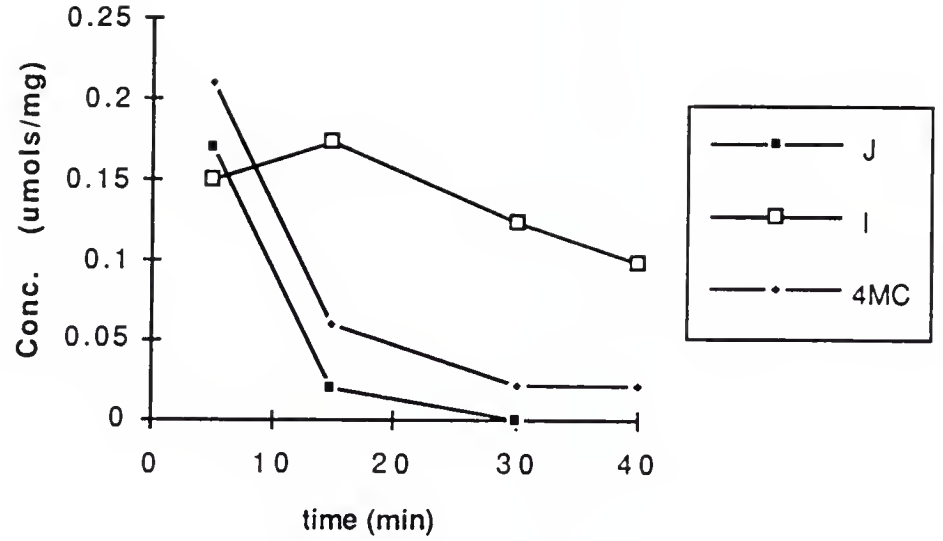

A.

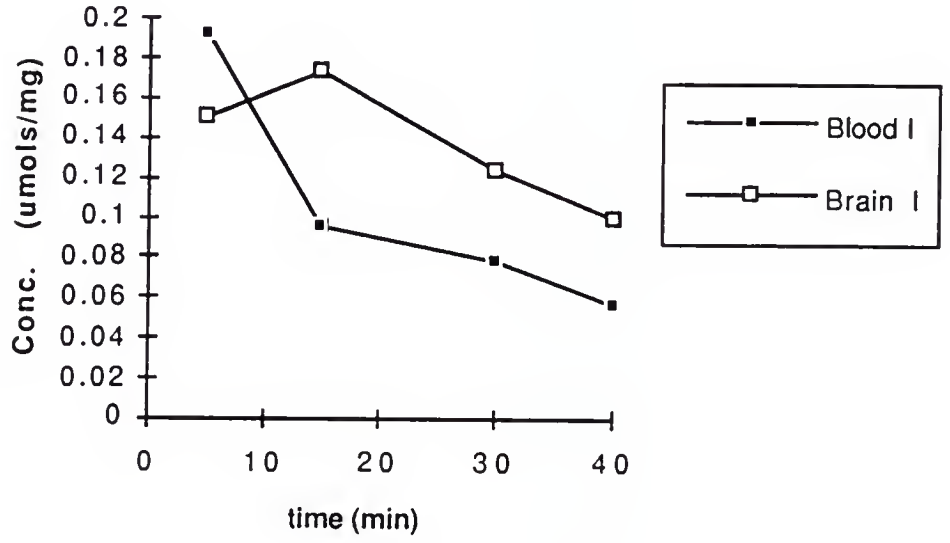

B.

Figure 20. A) In vivo brain concentration of the CDS J, its quaternary metabolite I, and final metabolite, 4-methyl catechol (4MC). B) In vivo blood/brain distribution of quaternary metabolite I. Each value is the mean of two independent determinations.

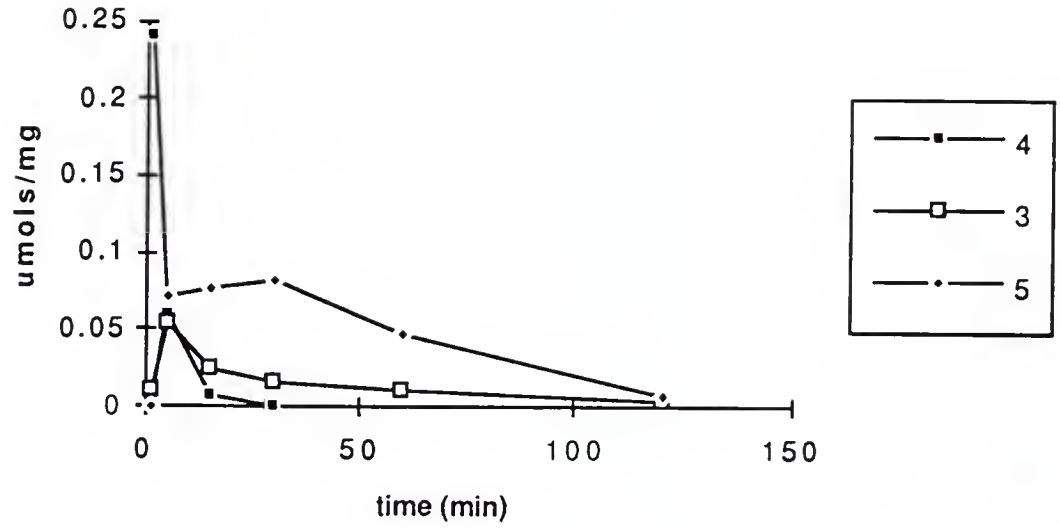

A.

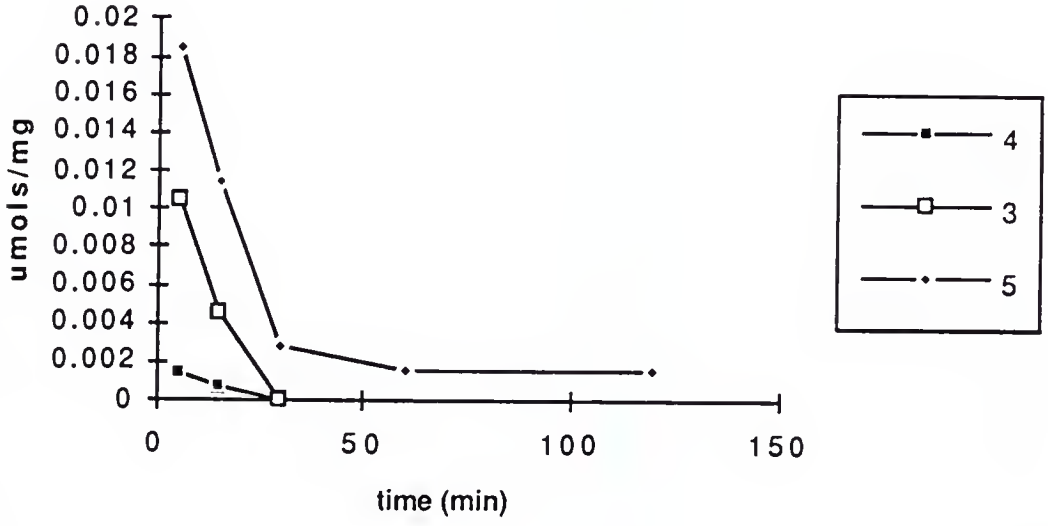

B.

Figure 21. In vivo concentrations of CDS 4, its metabolite 3, and final metabolite 5, in A) rat brain, and B) rat liver. Each value is the mean of two independent determinations.

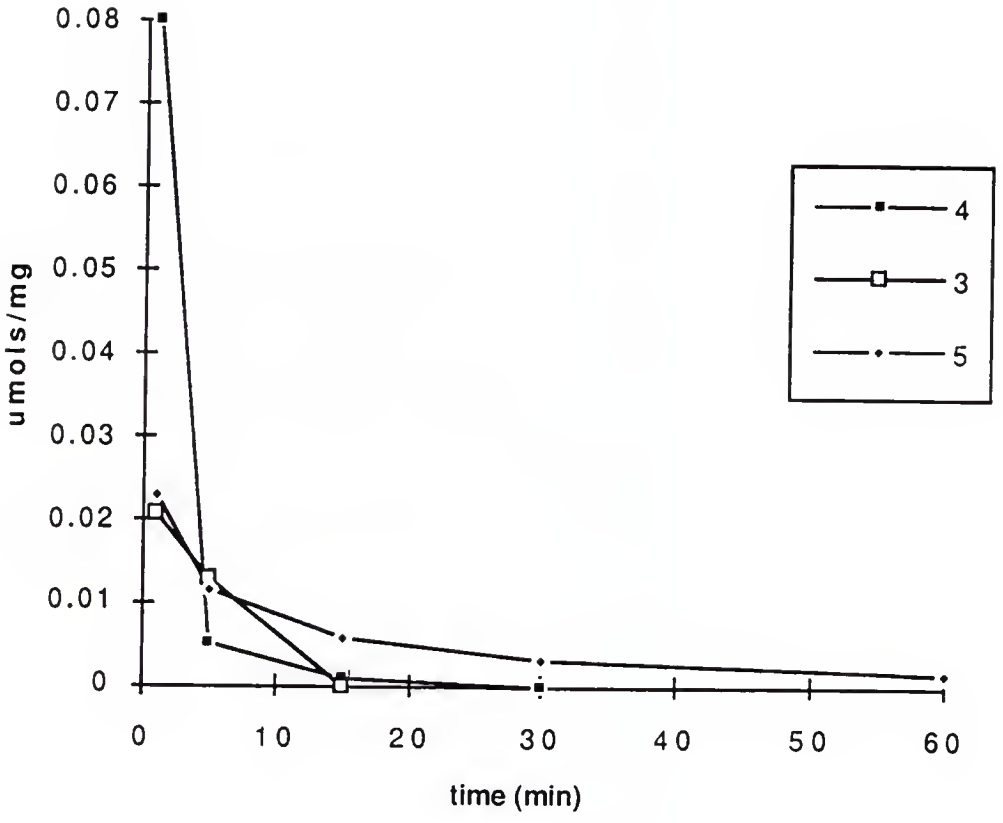

Figure 22. In vivo concentrations of CDS 4, its metabolite 3, and final metabolite 5, in rat blood. Each value is the mean of two independent determinations.

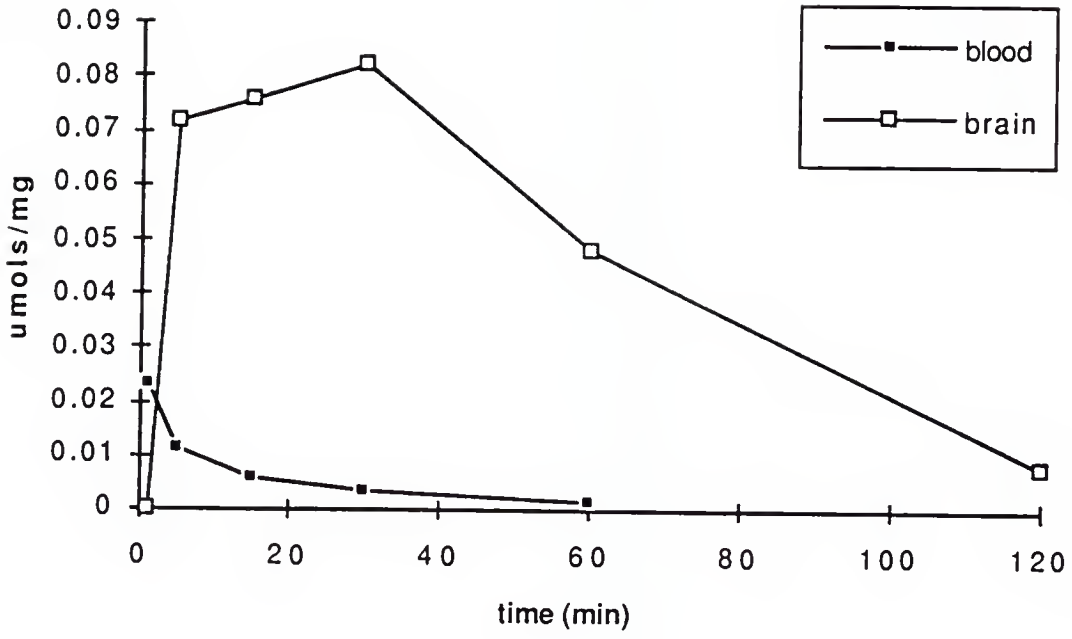

Figure 23. Blood/brain distribution of the pyridinium catechol final metabolite 5. Each value is the mean of two independent determinations.

In Vivo NGF-Stimulatory Activity

The effect of the 4-MC-CDS on the biosynthesis of NGF in the specific brain regions, hippocampus and frontal cortex, was determined by measuring the levels of NGF mRNA. Levels of NGF mRNA were quantified by the use of the dot blot technique. In summary, total RNA extracted from fresh tissue samples was blotted onto a nylon membrane and U.V. crosslinked to avoid further degradation of RNA. The nylon blot was then hybridized with a [^{32}P]-labelled NGF probe (771 bp) that recognizes the entire pre-pro sequence of the NGF mRNA. The extent of hybridization was then quantified with the use of a Betagen that measures radioactive signal of different intensity. The NGF signal was normalized by stripping the NGF probe and subsequently rehybridizing the blot with an actin probe.

For this assay, 3 groups of animals were used. Male Sprague Dawley rats (body weight 320-360 g) were injected i.v. (tail vein) with: 1) 4MC-CDS (J): 50 mg/Kg body weight (drug vehicle consisted of 1:1 DMSO-50% 2-hydroxypropyl-β-cyclodextrin in water, total injected volume: 1.8 ml/Kg), 2) drug vehicle only (1.8 ml/Kg), and 3) 4MC: dose of 4MC equimolar of the 4MC-CDS, 17 mg/Kg (in same amount of drug vehicle). After 8 hs animals were sacrificed by decapitation, and the brains removed and placed on ice-cooled surface. The hippocampus and frontal cortex were rapidly dissected out and separately placed in volume of lysis solution (4M guanidinium thiocyanate, 25 mM Na citrate, 0.5% N-lauryl

sarcosine, and 0.1 M 2-mercaptoethanol, total volume 1ml/100 mg tissue) and immediately homogenized.

RNA Isolation

Total RNA was isolated using the acid guanidinium isothiocyanate method followed by the phenol/chloroform method of purification and isopropanol precipitation (Chomczynski, 1987, and Sambrook et al., 1989). All solution used for the isolation and purification of RNA were DEPC (Diethylpyrocarbonate) treated in order to eliminate RNAses. Freshly dissected tissue (frontal cortex and hippocampus) was homogenized in lysis solution (consisting of 4M guanidinium thiocyanate, 25 mM Na citrate, 0.5 %N-lauryl sarcosine sodium salt, and 0.1M 2-mercaptoethanol) using a Polytron homogenizer. Following this lysis procedure, buffer saturated phenol (GIBCO-BRL) and chloroform/isoamyl alcohol (49:1) were utilized to purify the RNA from protein contaminants: the phenol is used in order to remove the protein contaminants while the chloroform/isoamyl purification steps help remove the residual phenol. 2M Na acetate, TRIS buffered phenol and 49:1 chloroform/isoamyl alcohol was added to the homogenate and vortexed for 1min. This suspension was subsequently centrifuged at 10,000 x g at 4 ^{o}C for 15 min. after which the aqueous top layer was aliquoted into a second tube. Phenol and chloroform/isoamyl alcohol solution were re-added to the new tube, vortexed and recentrifuged at 10,000 x g at 4 ^{o}C for 15 min. The upper phase was removed again, aliquoted into a fresh tube, and an equal volume of

isopropanol was added and vortexed. After an overnight storage at -20°C, the isopropanol containing solution was centrifuged at 10,000 x g at 4 °C, upon which a pellet was formed. The supernatant was discarded and the pellet was dissolved in a small volume of lysis solution. The isopropanol precipitation was repeated after which a wash with ice-cold 75% ethanol was performed. The ethanol was evaporated off and the remaining pellet was resuspended in 0.5% sodium dodecyl sulphate (SDS). The concentration of the RNA was evaluated spectro-photometrically at a wavelength of 260 nm. The purity of RNA was assessed by calculating the ratio of absorbance at 260/280 nm. A ratio of 2 is considered pure RNA, while samples that had ratios below 1.6 were estimated to be too contaminated by protein and thus were not used.

Blotting of Total RNA

Two concentrations (5 and 15 µg) of RNA from each sample (to ascertain linearity of hybridization versus RNA loaded) were filtered though a Nylon membrane held in a Hybri-Dot manifold (Bethesda Research Laboratories), as described below: To every 22 µg of RNA sample DEPC water was added to reach a final volume of 30 µl. Also, plasmid containing the pre-pro-NGF mRNA sequence was diluted with DEPC water to give a final concentration of 4.5 ng / 30 µl. To these samples, that were kept on ice, formamide (60 µl), formaldehyde (21 µl) and 20 x SSC (sodium chloride 30 M and sodium citrate 0.3 M) (6 µl) were added and incubated at 68 °C for >15min. After assembling and preparing the

Nylon membrane on the Hybri-Dot manifold, 243 µl of ice cold 20x SSC was added to each sample, vortexed, and placed on ice until loaded (by suction) on the Nylon membrane and U.V. crosslinked (using a U.V. Crosslinker). The dot blot was subsequently stored in a dessicator until the time of hybridization.

Preparation of the NGF Probe

The NGF probe was a gift from Dr. Scott Whittemore (Miami, Fl) and Dr. Paul Isackson (Mayo Clinic, Jacksonville). The probe was received incorporated in pBS (Bluescript). The excision of the probe from the plasmid and its purification was performed by Dr. Sonny Singh as follows: A restriction enzyme digestion was carried out using the enzymes BAMH I (4U/mg DNA) and ECOR I (5 U/mg DNA) at 37 ^{o}C for 3 hs. At this point the excised probe was separated from the plasmid by running the sample on a 1% low melting temperature agarose gel. After running the gel for 3 hs at 60 V in a cold room, the bands were photographed and the band corresponding to the NGF probe (by comparison with the DNA ladder, the separated DNA fragment had an approximate size of 800 b.p. which is very close to the actual size of the NGF probe, 771 b.p.) was cut out of the gel and placed in an eppendorf tube. The following day, the probe was extracted from the gel and purified using the phenol/chloroform/isoamyl alcohol method described previously. After the ethanol wash, the resulting pellet was resuspended in 1 x TE (pH=8) (TRIS and EDTA solution). The concentration and

purity of the DNA probe was assessed spectrophotometrically (a ratio A260/A280 nm of 1.8 is considered pure DNA).

Radiolabelling of NGF Probe and Hybridization of Nylon Membrane

The Nylon membrane was placed in a "hybridization" vial with prehybridization buffer and incubated at 42°C for approximately 2 hs. The prehybridization buffer consisted of 5 x SSPE (solution of NaCl, $NaH_2PO_4.H_2O$ and EDTA), 5 x Denhardts solution (ficoll, polyvinyl pyrrolidone, and BSA), 50% formamide, 0.5% SDS, and 100 µg/ml denatured salmon sperm DNA. During this prehybridization time period, the NGF probe (pre-pro NGF) was labelled with [a-^{32}P]-CTP (Specific activity: 3000 Ci/mM,10 µCi/µl, DuPont, New England Nuclear, Cambridge, MA) using the Random primer probe labelling kit (Gibco-BRL). After the labelling procedure was complete, the resulting labelled probe was separated from the free [^{32}P]-CTP by passing the reaction solution through a Sephadex-50 column with 1 x STE (NaCl 0.1 M, Tris.HCl 10 mM, and EDTA 10 mM). From the labelled probe fraction, 1µl was added in 4 ml of scintillation cocktail and radioactivity measured with a scintillation counter. Based on a precalculated volume of hybridization buffer to be used, the amount of labelled probe that would give a final activity of 1-2 x 10^6 cpm/ml of hybridization buffer was added to fresh prehybridization buffer producing the final hybridization solution that was maintained at 42 °C until the time of use. Following the prehybridization of the blot, the prehybridization buffer was discarded and the

nylon membrane was placed in the prepared hybridization buffer and incubated at 42 °C. Hybridization was carried out for 22 hs after which the nylon membrane was subjected to 4 washes (washes 1 and 2 with 2 x SSC/0.1% SDS at room temperature and 60 °C respectively, and washes 3 and 4 with 0.2 x SSC/0.1% SDS at 60 °C). After the washes, the membrane was placed on Whatmans filter paper, and while still damp, placed in a Betagen densitometer for overnight quantitation of NGF mRNA signal. The Dot Blot was quantitated by computer image analysis with the Betascope Blot Analyzer, Model 603 (Betagen Corp., Waltham, MA). (The data were calculated as the counts of [^{32}P]dCTP-NGF/µg RNA collected over a 16 h time period). Following this, the NGF probe was stripped from the membrane by incubation in a solution of 1mM Tris.Cl (pH 8.0), 1mM EDTA (pH8.0), and 0.1 x Denhardt's reagent, for 2 hs at 75 °C. The membrane was then rinsed with 0.1 x SSPE at room temperature and was ready for rehybridization with the actin probe. Since the amount of actin mRNA is considered an indicator of total RNA per sample, the hybridization with the actin probe was done in order to normalize the amount of NGF mRNA measured per total amount of RNA loaded for each sample. Thus, an increased NGF signal for a sample would represent, after normalizing, true stimulation of the specific mRNA synthesis and could not be attributed to variation of the total RNA loaded for that sample. The radiolabelling of the actin probe, subsequent hybridization of the membrane with it, and the quantitation of the actin mRNA signal was performed using the same procedure described previously for the NGF probe and mRNA.

Statistical Analysis and Results

Results were expressed as counts per min (cpm) for the NGF signal by cpm for the actin signal (NGF mRNA units/actin mRNA units). Analysis was performed using the ANOVA followed by Fisher PLSD test for determination of group differences.

Results showed a 1.76 fold increase in NGF mRNA compared to control in the rat hippocampus (1.3 fold increase compared to the 4-methylcatechol control) and a 1.32 fold increase in the frontal cortex (1.22 fold increase compared to 4-methylcatechol control) (Figures 24 and 25).

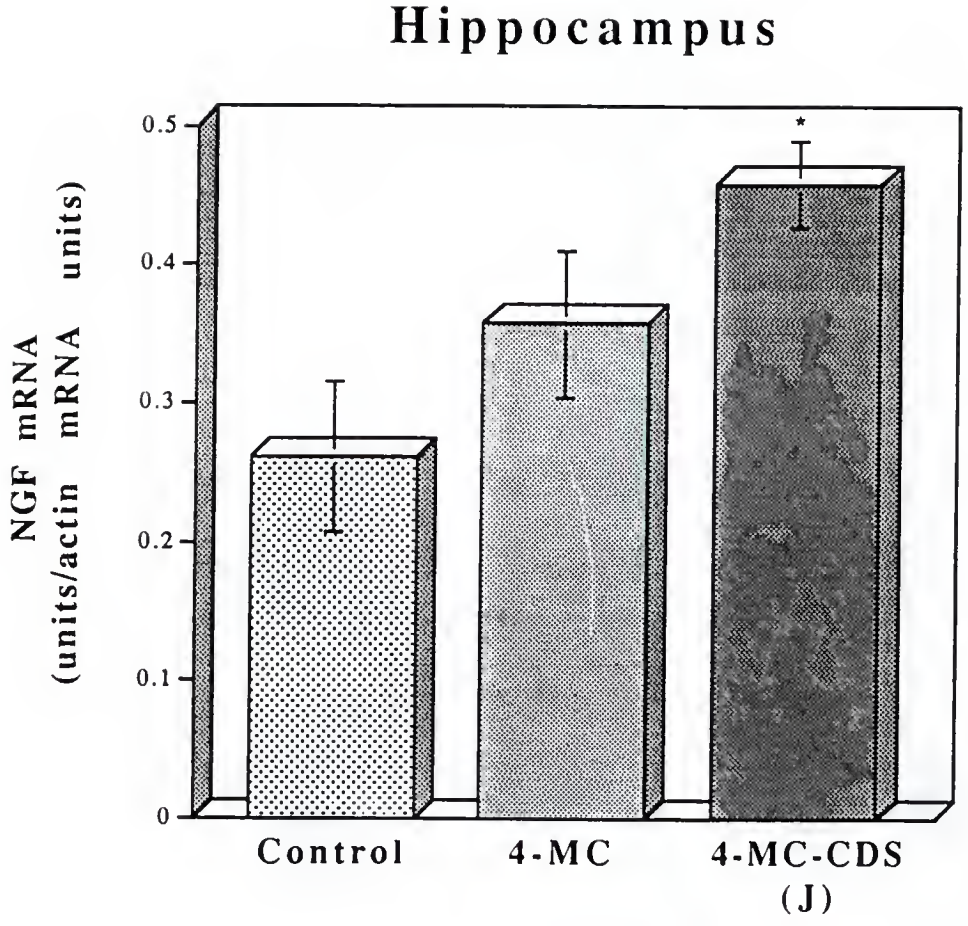

Figure 24. Effect of 4-MC-CDS (J) on *Hippocampal* NGF mRNA levels. Each value is the mean ± S.E. of 4 to 6 animals. * $P < 0.05$ relative to control according to Fisher PLSD.

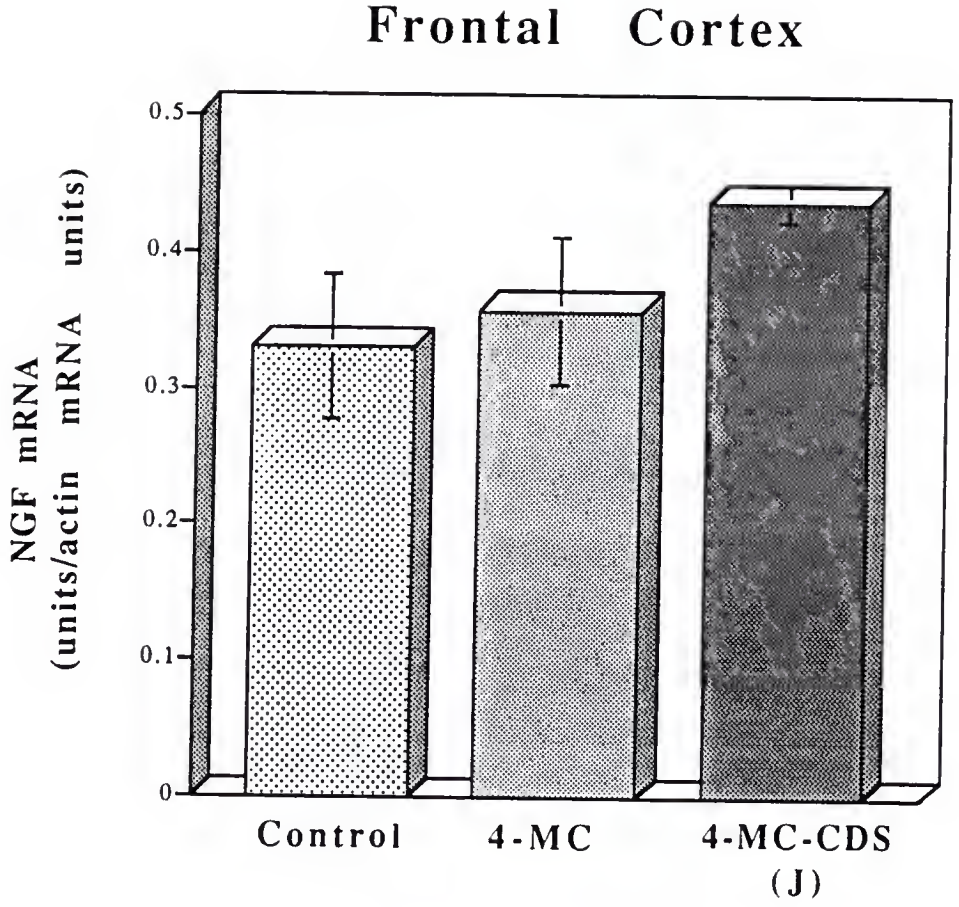

Figure 25. Effect of 4-MC-CDS (J) on *Frontal Cortical* NGF mRNA levels. Each value is the mean ± S.E. of 4 to 6 animals.

In Vitro NGF-Stimulatory Activity

Cell Cultures

Mouse L-M cells were obtained from the American Type Culture Collection (ATCC) (Rockville, MD) and maintained as monolayer cultures in medium 199 (Sigma) supplemented with 0.5% bactopeptone (Difco Laboratories, Detroit, MI), antibiotic free. Stock cultures were grown in 25 cm^2 flasks and subcultured once a week. To study the effect of the compounds, cells were inoculated in 24-well plates (well surface 2.1 cm^2) at a cell density of 4-8 x 10^4 cells/well and cultured for 3 days in peptone containing medium after which the medium was changed to medium 199 containing 0.5% bovine serum albumin (BSA) with or without any compounds, and the cells were cultured for 24 hs.

C6 glioma cell line was also obtained from the ATCC and was grown as monolayer cultures in RPMI-1640 (Sigma) serum free medium supplemented with 1% L-Glutamine and 0.5% penicillin/streptomycin in a humidified chamber with 95% air and 5% CO_2 at 37 ^oC. Incubation with compounds was performed in 25 cm^2 flasks (1-1.5 x 10^6 cells/flask) in the same serum free (SF) medium at 37 ^oC for 17 hs.

For determination of the cellular NGF mRNA levels of the C6 glioma cells, cultures were grown to confluency and subsequently incubated with or without compounds for 4 hs.

For assaying the effect of confluency on NGF biosynthesis in the C6 glioma, cells were maintained before treatments in the 25 cm^2 flasks for 1, 2, and 4 days (at which confluency levels are reached) respectively.

In all cases, the concentration of compounds used did not affect cell viability as determined by Trypan Blue dye exclusion assays.

Determination of NGF Level

L-M cells

The conditioned medium was applied directly to the double antibody enzyme-linked immunosorbent assay (ELISA).

C6 glioma cells

The NGF in the cell culture medium was quantitated using the double antibody ELISA. Also, the cell monolayers were washed with 2 ml of EDTA 0.02 % solution (Sigma) (37 ^oC) that was also immediately collected for NGF-ELISA analysis. Since neither the compounds used in this study nor the medium or EDTA solution affected the ELISA they were directly applied to the ELISA.

Intracellular NGF levels: The cell monolayers were incubated with 2 ml of EDTA 0.02 % solution for 20 min at 37 ^oC in order to remove cells from the flask wall. Cells were dislodged from the flask by shaking and pipette trituration. The cell suspension was centrifuged at 400 x g for 10 min at 4 ^oC. The supernatant was discarded, the pellet resuspended in 400 µl NGF Extraction Buffer (4 mM EDTA, 100 mM Tris HCl, 400 mM NaCl, 0.05 % Sodium Azide, and 2 % BSA)

containing Protease Inhibitors (Aprotin 20 µl of 3.5 mg/ml stock solution, and PMSF 0.174 g in 0.6 ml 95% EtOH), and transferred to siliconized microcentrifuge tubes in which the cell suspension was sonicated. The supernatant after centrifugation at 39600 x g for 15 min at 4 °C was used in the NGF ELISA.

Nerve Growth Factor ELISA

Principle and description of the sandwich NGF-b ELISA

The amount of Nerve Growth Factor (NGF) protein that is produced and excreted by the cells in the cell culture medium is measured with the double antibody ELISA. The principle involves sandwiching the NGF protein with two antibodies. (The two monoclonal antibodies against NGF were obtained from Boehringer Mannheim.) The first step is fixing adsorptively (coating) the walls of individual wells in the 96-well microliter plate with the primary anti-NGF antibody . Following washing off excess primary antibody, non-specific binding sites on the walls are saturated with blocking solution containing bovine serum albumin. Subsequently, a fixed volume of sample (culture medium) or NGF-standard (ranging from 6.25 to 800 pg/ml) is added to the wells (in triplicate) and incubated. During this step the NGF-β contained in the sample/standard is bound by the immobilised antibody. The third step involves incubating a second antibody, the anti-NGF antibody labelled with β-galactosidase (anti-NGF-β-galactosidase conjugate or else β-gal conjugate), with the NGF already bound to the primary coating antibody. The second antibody binds to a different epitope on

the NGF protein molecule thereby increasing the specificity of the assay. The amount of β-gal-conjugate bound is directly related to the NGF content of the sample, while the free β-gal-conjugate is removed by washing the wells. The amount of β-galactosidase bound in this immuncomplex is determined photometrically by adding the substrate for the enzyme, Chlorophenol red-β-galactopyranoside (CPRG), in excess quantity. The substrate is broken down into galactopyranose and chlorophenol red according to the reaction in Figure 26.

Chlorophenol red imparts a red colour to assay solution the intensity of which, after a fixed reaction time, is measured against the substrate solution at a wavelength of 574 nm. Higher concentrations of NGF correspond to a more intense colour or higher absorbency. By running a standard curve along with the samples, the amount of NGF present in a given sample is determined.

Results were expressed as concentration of NGF (pg/ml) per sample and statistical analysis of the data was performed by using ANOVA followed by the multiple comparison Fisher PLSD or Scheffe F test.

Results of treatments of C6 glioma cells and/or fibroblastic L-M cells with 4MC, 5MHP, 2HC, 5, 4, and 3 are shown in Figures 27-30 and Tables 3 and 4.

Cellular NGF mRNA Levels

The culture medium of the C6-glioma cells was removed after treatment and the monolayer cultures were surface washed with 2 ml of EDTA 0.02 % solution. After discarding this volume, the monolayers were incubated with a

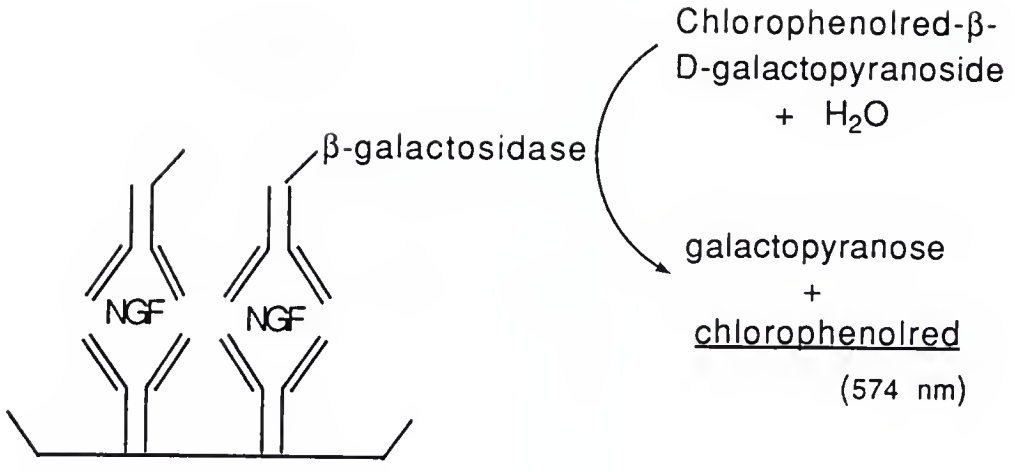

Figure 26. Schematic representation of the principle of the NGF ELISA.

fresh volume of the EDTA solution for 15 min at 37 ^{o}C. Cells were dislodged from the flask by shaking and pipette trituration. The cell suspension was centrifuged at 400 x g for 10 min at 4 ^{o}C. The supernatant was discarded, the pellet re suspended in 1 ml volume of lysis solution (4 M guanidinium thiocyanate, 25 mM Na citrate, 0.5% N-lauryl sarcosine, and 0.1 M 2-mercaptoethanol) and immediately homogenised. Total RNA isolation, blotting and hybridization was performed according to the description in the previous section. Hybridization with the NGF probe did not reveal any detectable amounts of NGF mRNA in any of the treatments, while hybridization with the actin probe resulted in a satisfactory signal, confirming that the assay (procedure) was successful and that NGF mRNA levels were just below the detection limit of the assay.

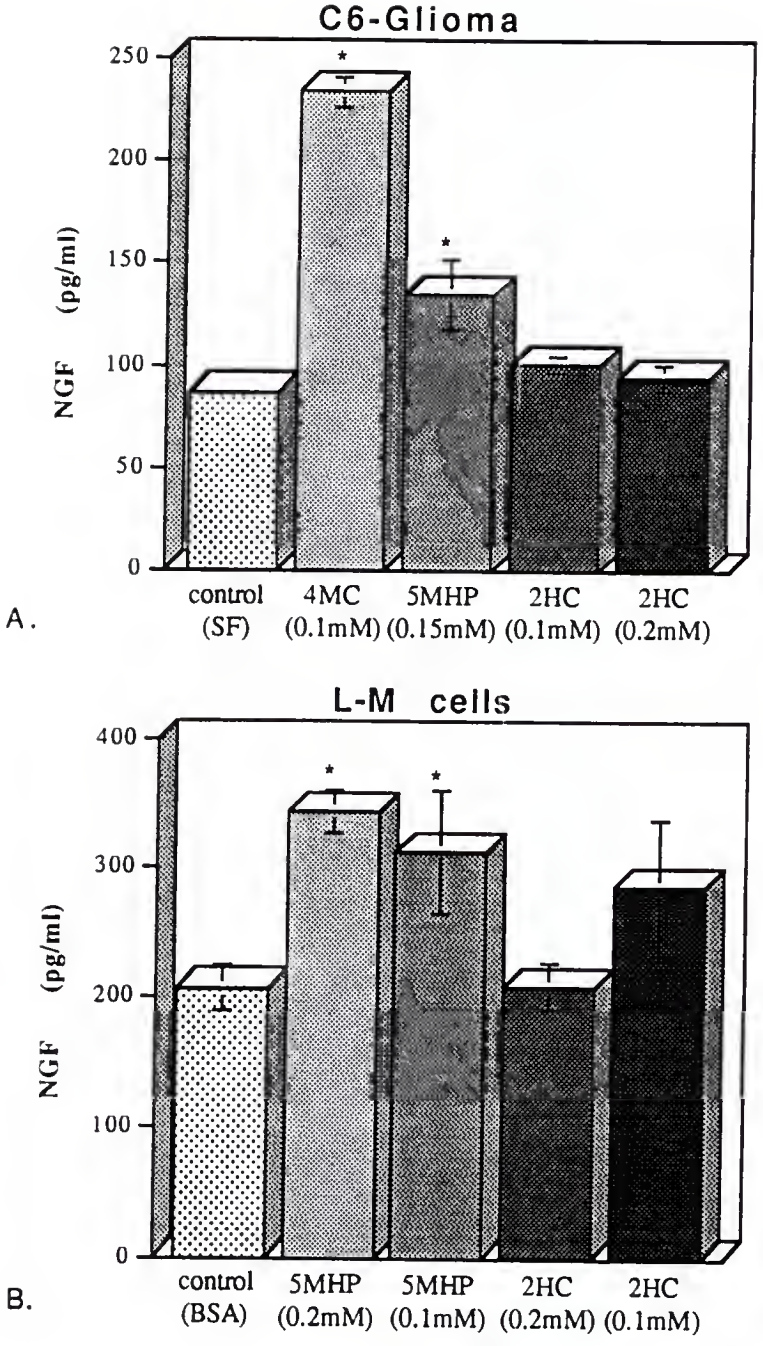

Figure 27. Effect of 4MC, 5MHP, and 2HC on NGF content in the culture medium of A) the C6 glioma and B) L-M cells. Each value is the mean ± the standard error of the mean (S.E.) of 4 to 6 independant determinations each assayed in duplicate. * $P < 0.05$ compared to control.

Table 3. Effect of treatments on the NGF content in the medium of the C6 glioma cell culture.

Treatment	NGF (fold increase ± S.E.)
Control	1 ± 0.031
4MC (0.1mM)	2.7 ± 0.078 [a]
5MHP (0.15mM)	1.55 ± 0.19 [b]
2HC (0.1mM)	1.16 ± 0.05
2HC (0.2mM)	1.09 ± 0.082

Table 4. Effect of treatments on the NGF content in the medium of the L-M cell culture.

Treatment	NGF (fold increase ±S.E.)
Control	1 ± 0.084
4MC (0.05mM)	13.84 ± 1.24 [a]
5MHP (0.1mM)	1.5 ± 0.23 [b]
5MHP (0.2mM)	1.7 ± 0.085 [b]
2HC (0.1mM)	1.4 ± 0.25
2HC (0.2mM)	1. ± 0.083

[a] $P < 0.05$ relative to control according to Scheffe F test. [b] $P < 0.05$ relative to control according to Fisher PLSD

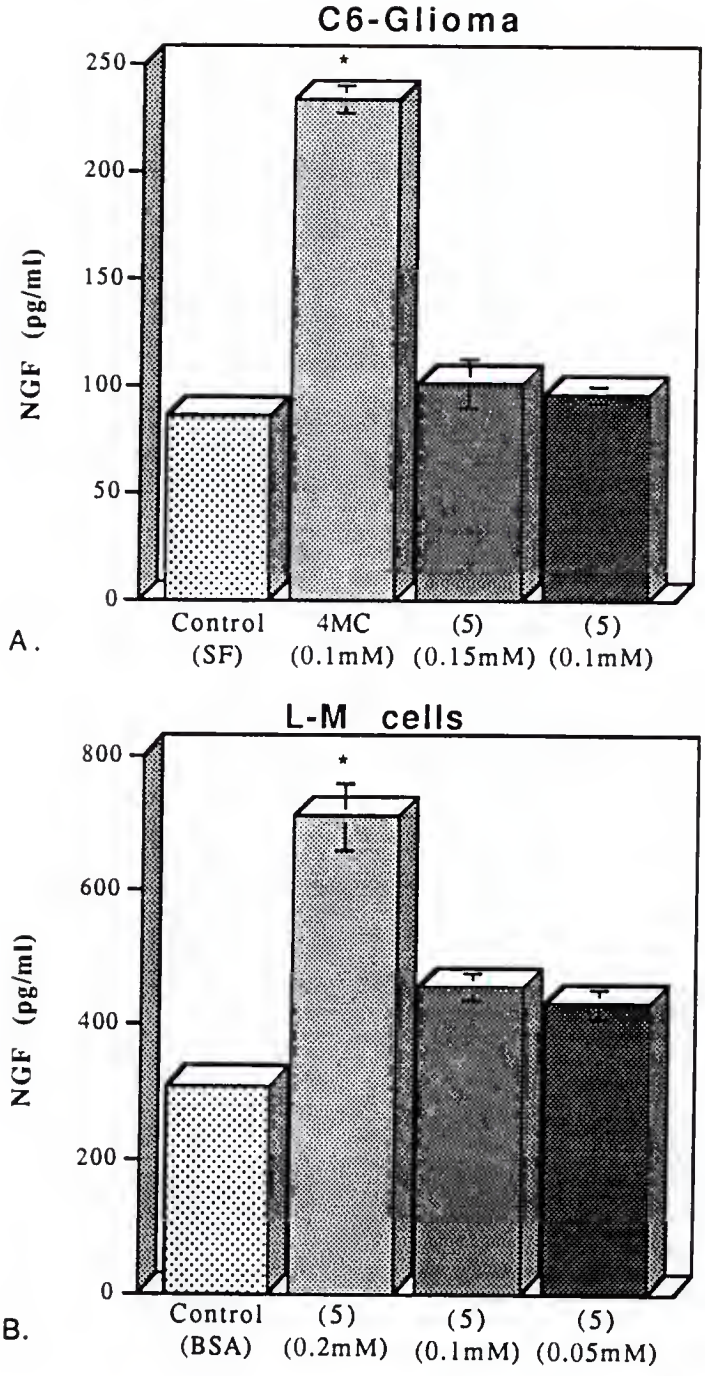

Figure 28. Effect of catechol derivative (5) on NGF content in the culture medium of the A) C6 glioma and B) L-M cells. Each value is the mean ± S.E. of 5 independent determinations each assayed in duplicate. * $P < 0.05$ relative to control according to Fisher PLSD.

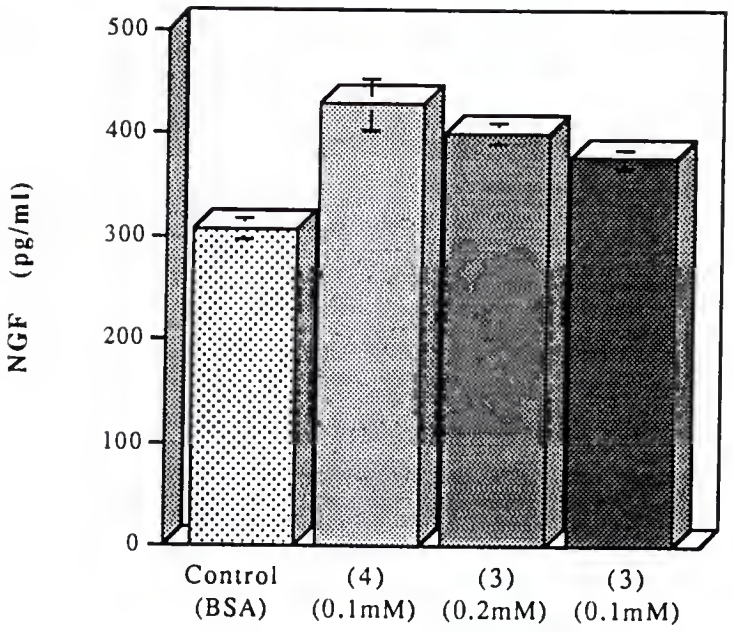

Figure 29. Effect of the redox analogue of dopamine (4) and its quaternary metabolite (3) on NGF content in the culture medium of the L-M cells. Each value is the mean ± S.E. of 5 independent determinations each assayed in duplicate.

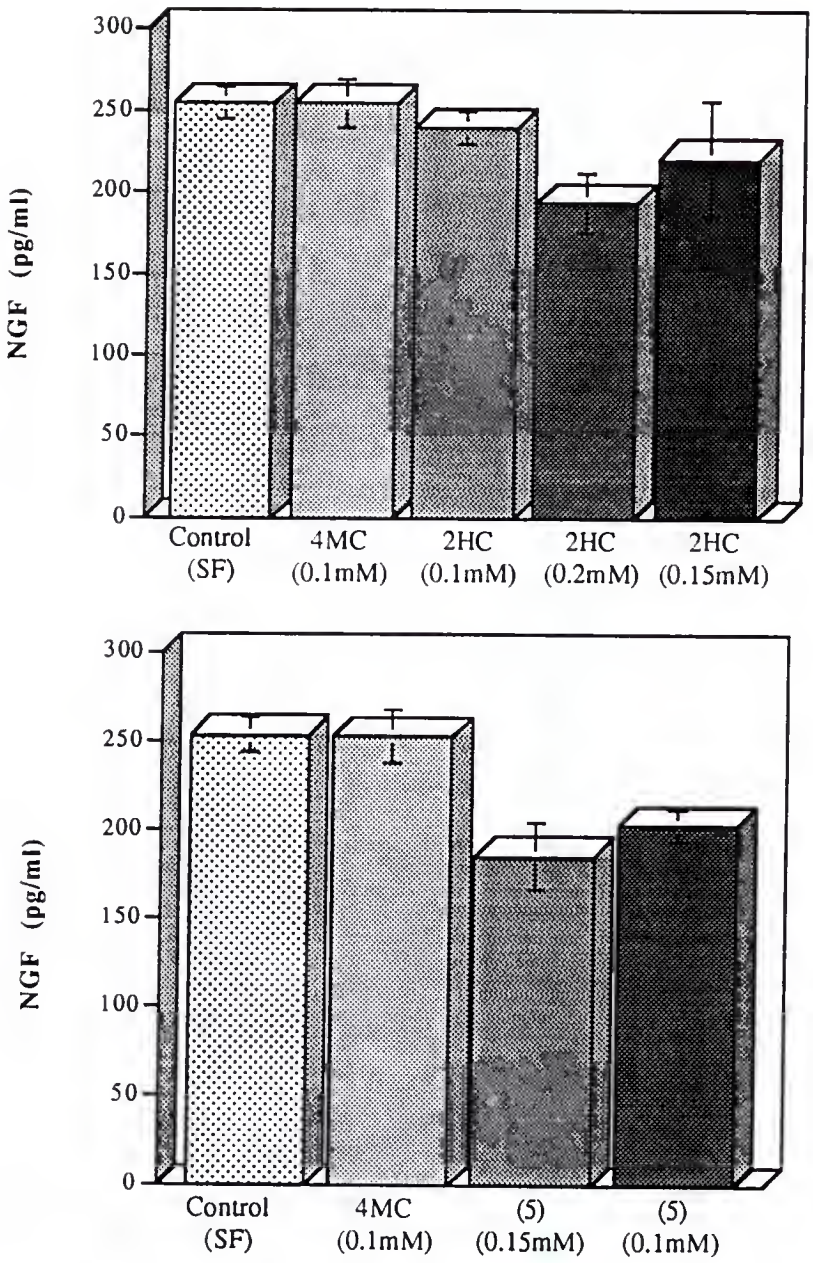

Figure 30. Effect of 4-methyl catechol, isosters 5MHP and 2HC, and catechol derivative (5) on intracellular NGF content in the C6 glioma cells. Each value is the mean ± S.E. of 5 independent determinations each assayed in duplicate.

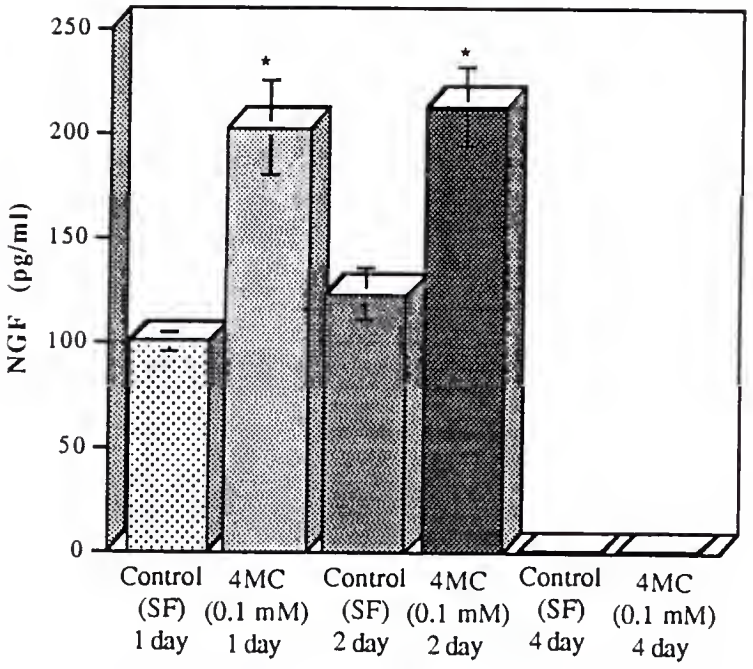

Figure 31. Effect of confluency of C6 cells on NGF biosynthesis after treatment with or without an NGF inducer (4MC). Each value is the mean ± S.E. of 5 independent determinations each assayed in duplicate. * $P < 0.05$ relative to controls according to Fisher PLSD and Scheffe F-test.

Quantitative Structure Activity Relationships of Catechol Derivatives (a Theoretical Study)

The entire set of 23 compounds (table 5) was calculated by the Tektronix CAChe (Computer Assisted Chemistry) workstation. Conformational analysis was performed by AM1 quantum mechanics. In order to reach the low energy conformation of the catechol moiety of the 4-substituted catechols, 4-methyl-catechol and isoproterenol were used as models: the relative position of the two H atoms of the two phenolic OHs was determined by interactively rotating the two O-H bonds. The dihedral angles, defined by the ring plane and the HO-C plane, were estimated respectively. As shown in Figure 32, the conformations with the lowest energy had both H atoms on the plane of the benzene ring (dihedral angles 0 or 180 degrees). In addition, the orientations of the two Hs were such that two low energy conformations were obtained (for the 4-substituted catechols) by the two possible arrangements of the apparent intramolecular H-bond between the two phenolic OH groups: the conformer 1A, with O *meta* as proton donor, and the conformer 1B, with O *para* as the proton donor (Figure 32).

1A was chosen based on the premise that catechols interact with adrenergic receptors in a similar form, and it was used as the low energy conformation in all subsequent calculations.

Parameters/descriptors of the molecules, derived from the AM1 calculated data, were: the charge at the *para*- or *meta*- O (CpO, CmO), the dipole moment in

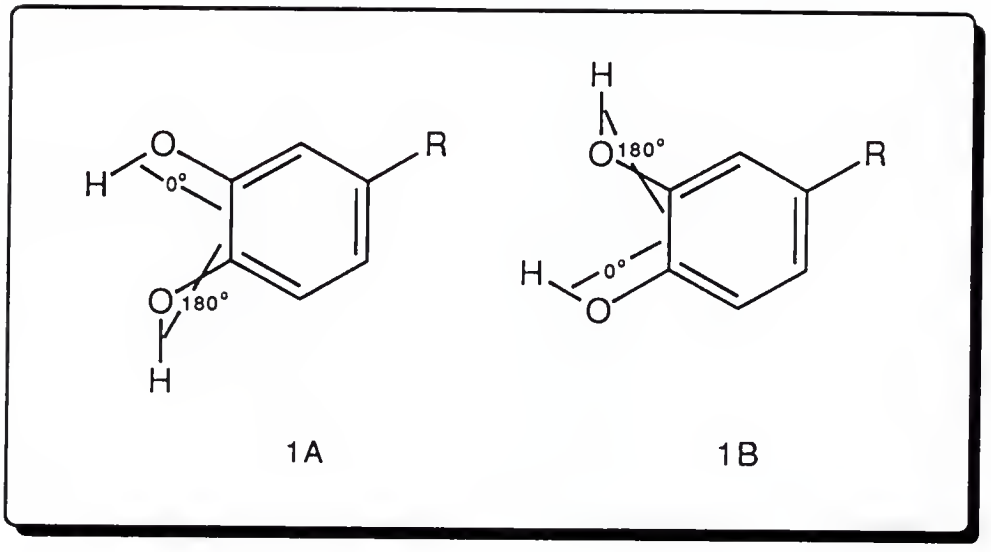

Figure 32. The two low-energy conformations of 4-alkylcatechols.

debye (DM), the vertical ionization potential (IPv) in kcal units, the contribution of the *para-* or *meta-* O to the HOMO (highest occupied molecular orbital) (HpO, HmO), and the LUMO (lowest unoccupied molecular orbital)-HOMO difference in e.V. units (HARD). Based on the AM1 optimized geometry and the van der Waals radii of each atom, the molecular volume (V), surface (S), and ovality (O), as well as the lipophilicity, expressed as log P, were obtained using the BLOGP program (Bodor et al., 1989, 1992). The ovality of the molecule (O), obtained from the calculated molecular volume and surface, is defined as the ratio of the actual surface and the minimum surface:

$$O = S / [4p(3V/4p)^{2/3}]$$

where S is the molecular surface and V is the molecular volume.

In addition, other descriptors included: 1) the adiabatic ionization potential (IPa) in kcal units, defined as the difference between the heat of formation of the radical cation of the molecule and the heat of formation of the neutral molecule. The radical cation located on the *para-* OH of the molecule was chosen as the most stable after comparison with the corresponding *meta-*. 2) the parameter "Q" (in kcal units) defined as the difference between the heat of formation of the catechols and the corresponding quinones, and, 3) the parameter "SAQ" (in kcal units) generated from the sum of the absolute values of IPa and parameter "Q".

Finally, parameters from the catechol anion, (negative charge at the *para-* O), that were used were the dipole moment (DMa) in debye units, the vertical ionization potential (IPva) in e.V. units, and the charge at the *para-* or *meta-* O (CpOa, CmOa).

Activity was expressed as concentration (mM) of the compound needed in order to increase 10 fold the NGF content in the media of the L-M cell culture after a 24h incubation. Based on literature data (Furukawa et al., 1986 a and b, 1990), this concentration was deduced after regression analysis of the initial linear part of the bell shaped curve of activity (fold increase of NGF content) vs. concentration of compound. In the presence of 0 to 0.2 mM of each compound, the increase of NGF content in the cell culture medium ranged from 1 to 16.5 fold depending on the compound. All values, extracted from the literature data, were the mean of four determinations ± SE (with SE ranging from 0.07 to 3) as indicated therein. Linear regression of the fold increase and the concentration of each compound gave excellent correlation (R = 0.92 to 0.99) and from the derived equations the concentration of each compound required for 10 fold NGF-increase was determined. For example, the activity of 4-methylcatechol (4-MC) (Furukawa et al., 1990) and epinephrine (EPINEPH) (Furukawa et al., 1986 a) were calculated as shown below:

4-MC : Fold increase in NGF ± S.E. (x)	Concentration (mM) (y)
1 (± 0)	0
7 (± 0.5)	0.02
12.5 (± 2.5)	0.04

Regression analysis gave $y = 0.003 x - 0.004$ (R=1). Thus for 10 fold increase in NGF, x=10, y (the concentration in mM) is 0.026.

EPINEPH : Fold increase in NGF ± S.E. (x)	Concentration (mM) (y)
1 (± 0)	0

6.7 (± 0.5)	0.05
11 (± 0.6)	0.1
14 (± 2)	0.15

Regression analysis gave $y = 0.011 x - 0.018$ (R=0.99). Thus for 10 fold increase in NGF, x=10, y (the concentration in mM) is 0.092.

Linear combinations of the calculated descriptors were fitted to the calculated activity by using simple or multiple regression analysis.

The set of 23 catechol derivatives (with abbreviations) included: 4-methylcatechol (4-MC), 3-methylcatechol (3-MC), 4-ethylcatechol (4-EC), 4-propylcatechol (4-PC), 4-butylcatechol (4-BC), 4-t-butylcatechol (4-tBC), 3,4-dihydroxybenzoic acid (DBA), 3,4-dihydroxybenzaldehyde (DHB), 3,4-dihydroxybenzylamine (DHBA), 3,4-dihydroxycinnamic acid (DHCA), 3,4-dihydroxyphenylpropionic acid (DHPPA), 3,4-dihydroxyphenylserine (DOPS), 3,4-dihydroxyphenylacetic acid (DOPAC), dopamine, 3,4-dihydroxyphenylglycol (DOPEG), 3,4-dihydroxymandelic acid (DOMA), 3,4-dihydroxyphenylalanine (DOPA), epinephrine (EPINEPH), isoproterenol (ISO), norepinephrine (NOREPIN), epinine, pyrocatechol (PYROCAT), and 2,3-dihydroxypyridine (DHP).

Structures of the compounds and values of the parameters calculated for each compound are shown in Table 5.

The correlation matrix is represented in Table 6, where absolute values are the correlation coefficients (multiple R).

Table 5. The set of 23 catechol derivatives and values of their descriptors.

	compound	structure	CpO	CmO	DM (debye)	log P	V (Å^3)	S (Å^2)	O	IPa (kcal)	IPv (kcal)
		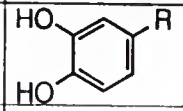									
1	4-MC	R= $-CH_3$	0.271	0.249	2.074	1.351	116.297	151.134	1.312	190.016	202.055102
2	3-MC	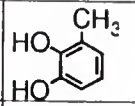	0.273	0.249	2.41	1.336	116.065	149.386	1.298	191.38	204.384201
3	4-EC	R= $-CH_2-CH_3$	0.271	0.25	2.109	1.766	132.95	171.399	1.361	189.672	201.847559
4	4-PC	R= 	0.272	0.249	2.11	2.192	149.755	192.885	1.414	189.422	201.847559
5	4-BC	R= 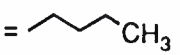	0.271	0.249	2.115	2.624	166.617	214.692	1.466	189.347	201.824498
6	4-tBC	R= $-C(CH_3)_3$	0.271	0.25	2.071	2.498	166.021	207.795	1.422	188.982	202.078163
7	DBA	R= $-COOH$	0.264	0.241	4.154	0.925	126.523	162.332	1.332	200.896	214.48465
8	DHB	R= $-CHO$	0.266	0.246	2.802	0.991	118.79	153.006	1.309	199.431	212.755121
9	DHBA	R= 	0.272	0.25	0.975	0.465	128.192	166.525	1.354	189.219	203.231182
10	DHCA	R= 	0.266	0.245	4.031	1.689	154.314	197.189	1.417	197.134	208.788735
11	DHPPA	R= 	0.269	0.246	3.411	1.863	160.39	207.619	1.454	193.846	206.943904

Table 5. --continued

	compound	structure	CpO	CmO	DM (debye)	log P	V (Å^3)	S (Å^2)	O	IPa (kcal)	IPv (kcal)
12	DOPS	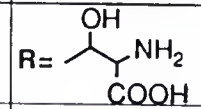	0.268	0.245	3.896	0.37	180.161	227.329	1.474	191.922	208.834856
13	DOPAC	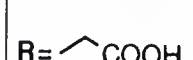	0.269	0.247	1.063	1.525	143.315	183.143	1.383	193.689	207.220629
14	DOPAMINE	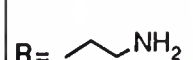	0.271	0.249	1.413	0.894	144.959	188.955	1.416	191.0597	203.300363
15	DOPEG	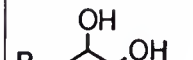	0.27	0.246	3.626	1.507	149.392	191.539	1.407	191.372	204.130537
16	DOMA	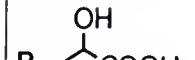	0.267	0.244	2.625	1.152	151.703	194.096	1.411	195.9671	212.017189
17	DOPA	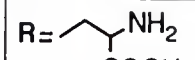	0.268	0.247	3.968	0.693	172.02	220.772	1.476	190.3469	209.226882
18	EPINEPH	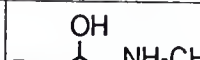	0.271	0.251	1.153	1.068	170.43	219.122	1.474	190.264	202.977518
19	ISO	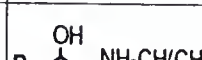	0.271	0.246	2.775	1.673	204.377	261.95	1.561	190.7759	203.046699
20	NOREPIN	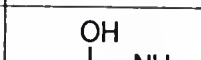	0.271	0.246	3.288	0.623	152.819	194.649	1.408	189.728	203.346484
21	EPININE		0.271	0.249	1.416	1.209	162.382	211.484	1.469	190.853	203.300363
22	PYROCAT		0.271	0.248	2.128	0.933	99.632	129.864	1.25	193.101	204.89153
23	DHP	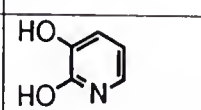	0.2669	0.2412	0.6577	-0.572	95.456	125.369	1.241	198.1156	209.987875

Table 5. --continued

	compound	HpO	HmO	HARD (e.V.)	Q (kcal)	DMa (debye)	IPva (e.V.)	CpOa	CmOa	SAQ (kcal)	activity (mM)
1	4-MC	0.3185	0.3255	9.0563	-42.801	4.12	2.758	0.5435	0.3061	232.817	0.026
2	3-MC	0.367	0.2963	9.1244	-43.265	3.965	2.763	0.5502	0.3054	234.645	0.057
3	4-EC	0.3182	0.3226	9.0596	-42.458	5.708	2.789	0.5423	0.306	232.13	0.055
4	4-PC	0.3181	0.3232	9.0585	-42.449	7.729	2.8136	0.5408	0.306	231.871	0.05
5	4-BC	0.3183	0.3218	9.0589	-42.4233	9.779	2.824	0.5405	0.3056	231.7703	0.096
6	4-tBC	0.3155	0.3347	9.0984	-42.5808	8.009	2.84	0.5407	0.3057	231.5628	0.129
7	DBA	0.2953	0.389	9.9007	-46.278	3.377	3.616	0.4914	0.2946	247.174	1.307
8	DHB	0.2994	0.3744	8.6578	-46.3551	1.9555	3.562	0.495	0.2991	245.7861	1.33
9	DHBA	0.3097	0.3448	9.0525	-43.5929	5.383	2.7148	0.3201	0.3407	232.8119	0.531
10	DHCA	0.3072	0.2945	8.96799	-45.09288	4.01599	3.69199	0.474	0.2928	242.226	0.314
11	DHPPA	0.3156	0.3456	9.04258	-43.7481	9.5547	3.0782	0.5302	0.3028	237.594	0.121

Table 5. --continued

	compound	HpO	HmO	HARD (e.V.)	Q (kcal)	DMa (debye)	IPva (e.V.)	CpOa	CmOa	SAQ (kcal)	activity (mM)
12	DOPS	0.307	0.3628	9.03835	-43.0147	10.7069	3.2725	0.5192	0.2998	234.9367	0.122
13	DOPAC	0.3117	0.35068	9.18863	-45.179	7.0784	3.1526	0.5232	0.3017	238.868	0.572
14	DOPAMINE	0.3152	0.3351	9.0557	-43.453	7.0397	2.9024	0.5374	0.3058	234.5127	0.087
15	DOPEG	0.31203	0.35045	9.06639	-43.5755	8.60485	2.9914	0.5319	0.3029	234.9475	0.161
16	DOMA	0.3097	0.3694	8.9861	-49.7407	6.5288	3.386	0.5136	0.2997	245.7078	0.825
17	DOPA	0.3148	0.336	8.97999	-44.381	8.91158	3.2455	0.5234	0.03012	234.7279	0.159
18	EPINEPH	0.3083	0.3385	9.02145	-44.7795	10.4316	2.9618	0.5336	0.3055	235.0435	0.092
19	ISO	0.311	0.3471	9.0745	-43.1239	13.555	2.9837	0.5321	0.303	233.8998	0.148
20	NOR	0.3111	0.3465	9.0957	-42.0931	8.3238	2.9735	0.5332	0.3025	231.8211	0.151
21	EPININE	0.3152	0.3362	9.05548	-43.4935	9.09112	2.9068	0.5371	0.3052	234.3465	0.075
22	PYROCAT	0.366	0.3085	9.18215	-43.6833	2.6293	2.7459	0.5486	0.3072	236.7843	0.984
23	DHP	0.3692	0.31015	9.1339	-46.8859	3.6432	3.1327	0.515	0.299	245.0015	1.33

Table 6. The correlation matrix

	CpO	CmO	DM	log P	V	S	O	IPa	IPv
CpO	1								
CmO	0.82308054	1							
DM	-0.47828417	-0.45151477	1						
log P	0.32167374	0.45550544	0.10324916	1					
V	0.10315528	0.14715862	0.30927386	0.38661558	1				
S	0.11493417	0.15608032	0.29085196	0.38122848	0.99856073	1			
O	0.1373125	0.18977752	0.25723836	0.38488327	0.98632353	0.99297205	1		
IPa	-0.88139881	-0.80271569	0.26799565	-0.35156284	-0.39700784	-0.40243585	-0.41880759	1	
IPv	-0.92839064	-0.81138702	0.42897824	-0.44860345	-0.2082015	-0.21969371	-0.24447794	0.89336367	1
HpO	0.30362141	0.01068673	-0.36418956	-0.25548451	-0.56656427	-0.56133185	-0.57864382	-0.02079504	-0.14550899
HmO	-0.46136385	-0.36979923	0.29024817	-0.15087781	0.24293972	0.23368817	0.22539149	0.32217372	0.49074782
HARD	-0.23032845	-0.37615973	0.14867017	-0.0735475	-0.17106706	-0.1769704	-0.18827304	0.26671823	0.20609073
Q	0.72334518	0.61734051	-0.01303477	0.38377965	0.24996831	0.25132984	0.25496573	-0.77306685	-0.80679466
DMa	0.32084544	0.21113017	0.08887351	0.28421185	0.90954703	0.91643557	0.9145203	-0.5542862	-0.39019812
IPva	-0.94018895	-0.73502334	0.56726236	-0.22194061	0.07655588	0.06303964	0.03965546	0.8179199	0.88326788
CpOa	0.1551935	0.0595794	0.09833698	0.32152063	0.14436251	0.14192812	0.12480961	-0.13879249	-0.19258064
CmOa	0.23487097	0.09184277	-0.3795467	0.15425195	-0.22706184	-0.22882941	-0.22686821	0.04917732	-0.26233762
SAQ	-0.87322686	-0.78036231	0.1910469	-0.38258746	-0.3660305	-0.37029503	-0.38298814	0.97359316	0.91157978
activity	-0.67487574	-0.65009661	-0.04059223	-0.49120002	-0.58872098	-0.59454285	-0.61882941	0.83464166	0.74984145

Table 6. --continued

	HpO	HmO	HARD	Q	DMa	IPva	CpOa	CmOa	SAQ
CpO									
CmO									
DM									
log P									
V									
S									
O									
IPa									
IPv									
HpO	1								
HmO	-0.68296226	1							
HARD	0.02223243	0.21988677	1						
Q	0.04379929	-0.36572569	-0.06164368	1					
DMa	-0.35239762	0.17914371	-0.13846659	0.36582553	1				
VIPa	-0.42175428	0.44424534	0.09659002	-0.67464469	-0.21073112	1			
CpOa	0.25987024	-0.19864606	-0.00455894	0.19731187	0.23128407	-0.15121407	1		
CmOa	0.05061128	0.00192074	0.0903044	0.08015063	-0.13732847	-0.23845176	-0.12417794	1	
SAQ	-0.03022322	0.35565252	0.20765366	-0.8974626	-0.51709398	0.81155857	-0.16752389	0.00535065	1
activity	0.15612011	0.33114639	0.265348	-0.72481032	-0.63853898	0.52136066	-0.29099345	0.07933196	0.84124131

Initially, the parameter that gave the best simple correlation with activity was the adiabatic ionization potential (IPa) (equation 1), followed by the vertical ionization potential (IPv) (equation 2) and the Q (equation 3).

$$\text{Activity [mM]} = -20.2391 + 0.10713\ \text{IPa} \quad (1)$$

$n = 23,\ R = 0.8346,\ \text{s.e.} = 0.2543,\ F = 48.2216$

$$\text{Activity [mM]} = -17.4749 - 0.0867\ \text{IPv} \quad (2)$$

$n = 23,\ R = 0.7498,\ \text{s.e.} = 0.3055,\ F = 26.9739$

$$\text{Activity [mM]} = -7.5492 - 0.1798\ Q \quad (3)$$

$n = 23,\ R = 0.7248,\ \text{s.e.} = 0.3181,\ F = 23.2431$

where n is the number of compounds submitted to the regression, R is the correlation coefficient, s.e. is the standard error, and F is the overall statistical significance of the equation.

Poor correlation was observed with all other parameters, for example with log P (equation 4) or HARD (e.V.) (equation 5).

$$\text{Activity [mM]} = 0.7649 - 0.3083\ \log P \quad (4)$$

$n = 23,\ R = 0.4912,\ \text{s.e.} = 0.4022,\ F = 6.6781$

$$\text{Activity [mM]} = -4.9364 + 0.5851\ \text{HARD} \quad (5)$$

$n = 23,\ R = 0.2653,\ \text{s.e.} = 0.4452,\ F = 1.5906$

where HARD, twice the absolute hardness of the molecule (as expressed by the calculated energy difference between the LUMO and HOMO), is an electronic descriptor of the polarizability of molecules (Pearson, 1986).

The best simple correlation compared to all other parameters (Table 6) relates the sum of the absolute values of IPa and parameter Q, (expressed as SAQ), with activity.

The correlation of activity with the descriptor SAQ (e.V.) is shown in equation 6:

$$\text{Activity [mM]} = -17.3832 + 0.07508\ \text{SAQ} \qquad (6)$$

$$n = 23,\ R = 0.8412,\ \text{s.e.} = 0.2496,\ F = 50.8407$$

The best relationship between activity and descriptors employs, in addition to SAQ, a geometrical descriptor of the catechol derivatives and is given by equation 7:

$$\text{Activity [mM]} = -11.8130 + 0.0632\ \text{SAQ} - 1.9763\ \text{O} \qquad (7)$$

$$n = 23,\ R = 0.9004,\ \text{s.e.} = 0.2058,\ F = 42.8571$$

where O is the ovality of the molecule that is dimensionless.

Both the 'calculated' and 'experimental' values of activity, from equation (7) and experimental data (literature) respectively, are shown in Figure 33.

Figure 34 shows the 'experimental' activity values plotted against the calculated values.

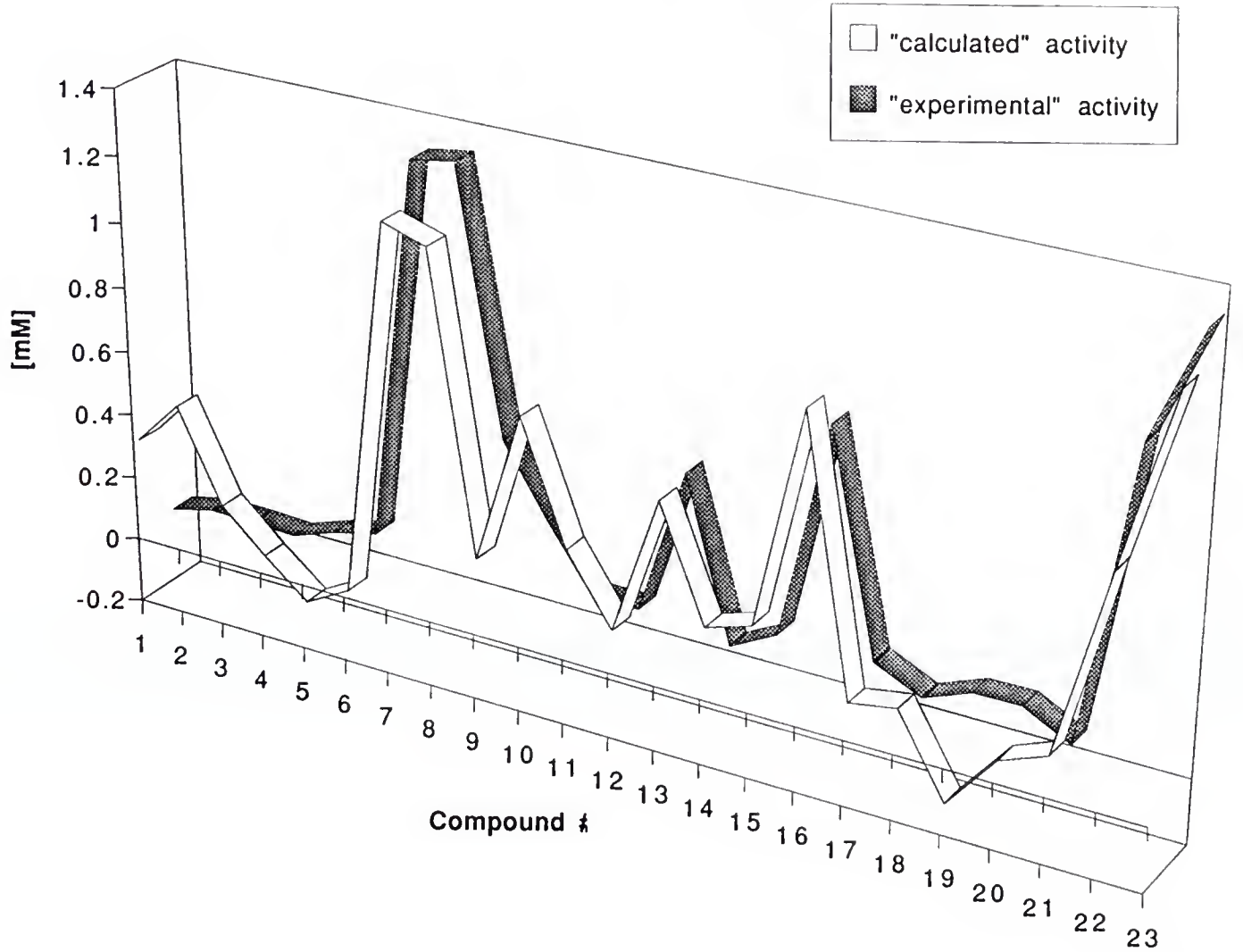

Figure 33. "Calculated" activity values derived from equation 7 fitted close to the "experimental" values.

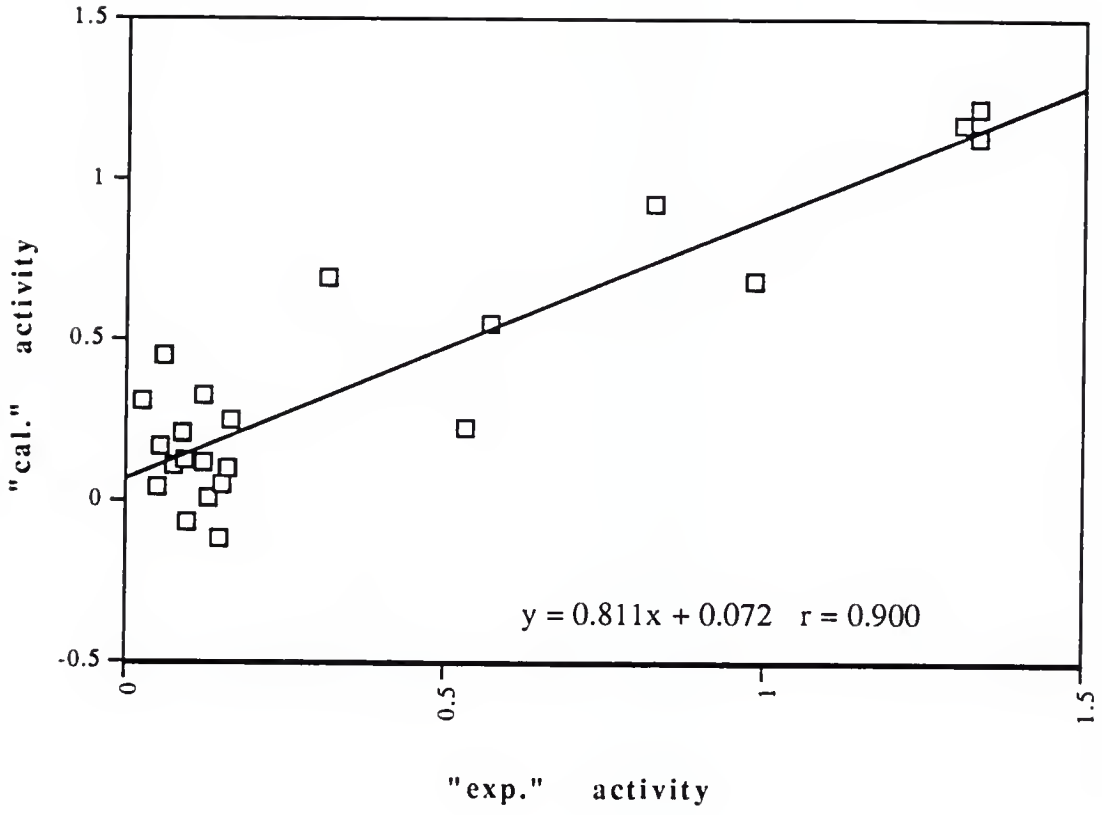

Figure 34. "Experimental" activity values of the catechol derivatives plotted against their "calculated" activity values.

CHAPTER 4
DISCUSSION

Synthesis

Mono Esterification of 4-Methylcatechol

An interesting result was obtained from the mono esterification reaction of 4-methylcatechol with nicotinoyl chloride. Compound A, as deduced from the NMR spectrum data, was a mixture of two isomers (Figure 35): the *para* esterified isomer (*para* to the methyl group of the catechol ring) appeared in slightly higher amounts (60:40) than the *meta* as derived from the proton NMR integration ratios of the phenyl hydrogen peaks or the 4-methyl hydrogen peaks (Figure 7). The two isomers were indistinguishable by all other analytical methods used. They had identical Rf values on TLC using different solvent systems, and yielded a single peak on HPLC using two different mobile phases (60% acetonitrile/water and 80% methanol/water). Thus, resolution of the two isomers could not be achieved and subsequent reactions using A as a starting material yielded non-resoluble isomeric products. The second esterification of compound A with isobutyryl chloride (or pivaloyl chloride) yielded the two

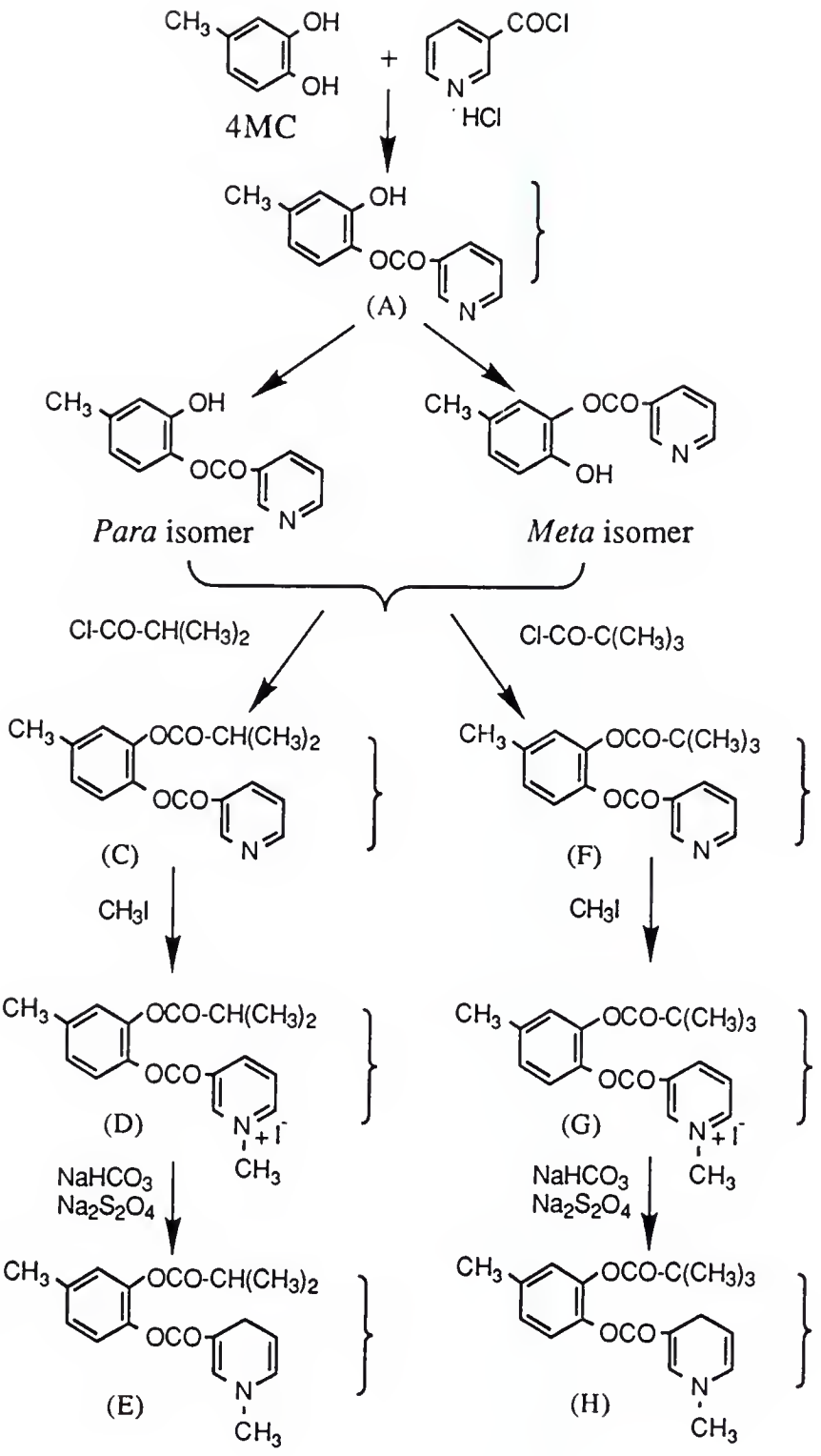

Figure 35 . Mono esterification of 4-methylcatechol leads to a mixture of the *para* and *meta* isomers.

corresponding isomers in almost equal proportions (53:47). Compounds C, D, E, F, G, and H were all approximately 1:1 mixtures of the two isomers (Figure 35), as derived from the corresponding NMR data. All gave a single peak in diverse HPLC systems, and a single spot on various TLC systems.

"Zincke" Type Reactions

The reaction used for the synthesis of the pyridinium dopamine derivatives (free, esterified or methylated catechol functions), compounds 3, 5, and 6, involves nucleophilic attack of the amine group of dopamine at the pyridinium ring of the Zincke reagent. The strong electron-withdrawing N-substituent (2,4 dinitrophenyl) of the pyridinium ring of the Zincke reagent facilitates ring opening upon reaction with the amine group of dopamine to produce the intermediate dianil of Figure 36. Subsequent recyclization renders the desired pyridinium products.

Synthesis of 2-Hydroxymethyl-p-Cresol (2HC)

The suggested mechanism of the reaction described in the previous chapter is coordination of a formaldehyde to the boron atom of a probable intermediate (substituted phenyl benzene boronate), followed by a [3,3] sigmatropic rearrangement shown in Figure 37 A.

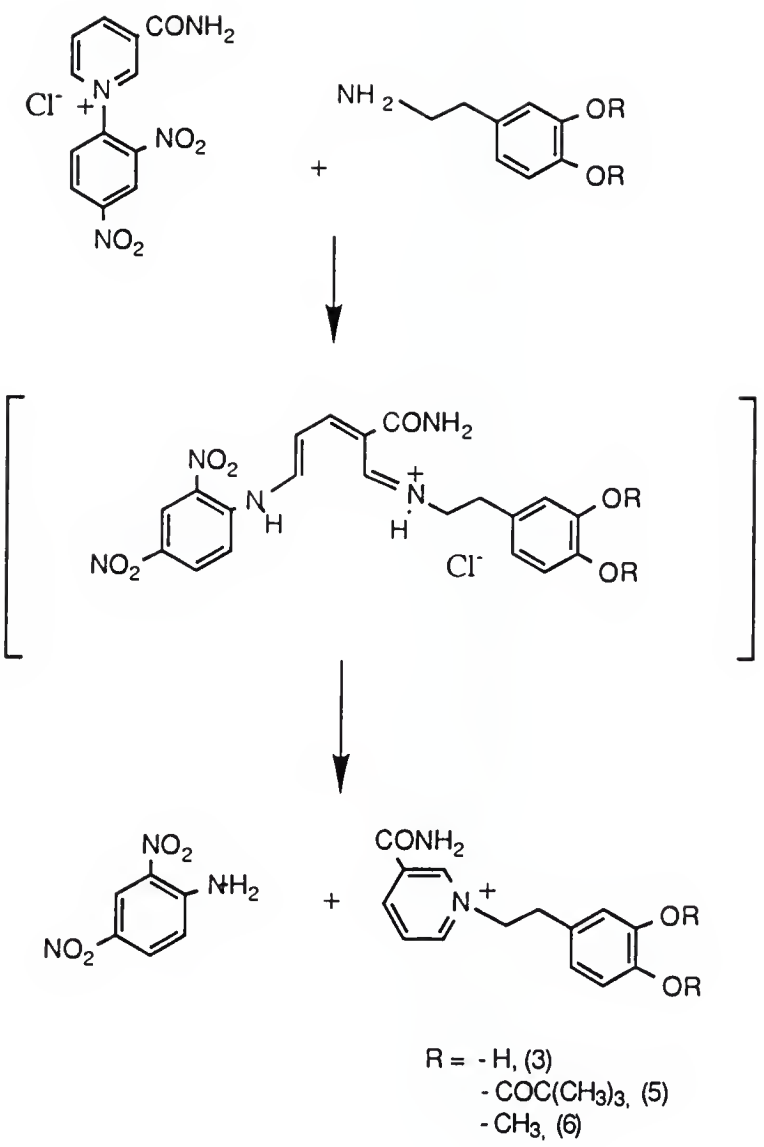

Figure 36. Reaction of the Zincke type reagent with the amine group of dopamine and related compounds is believed to go through the intermediate dianil which cyclizes to the desired pyridinium product.

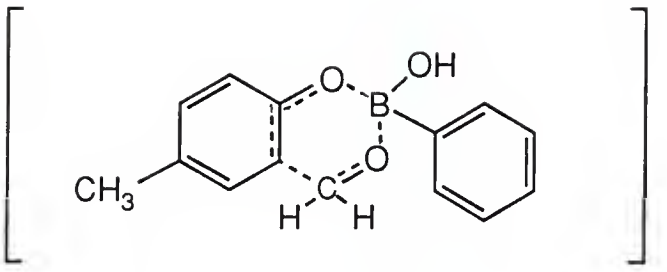

A.

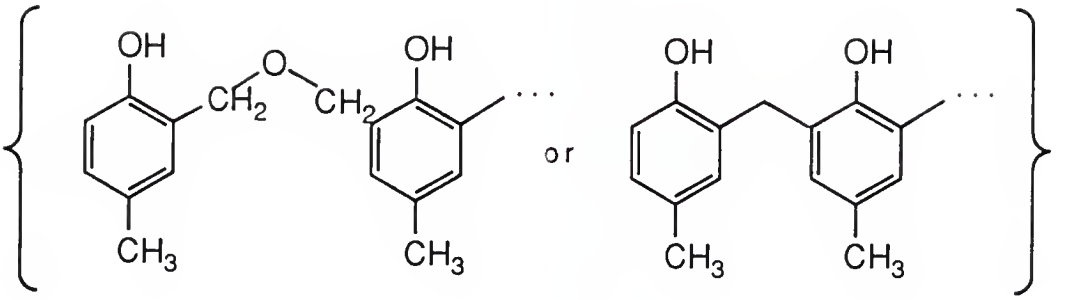

B.

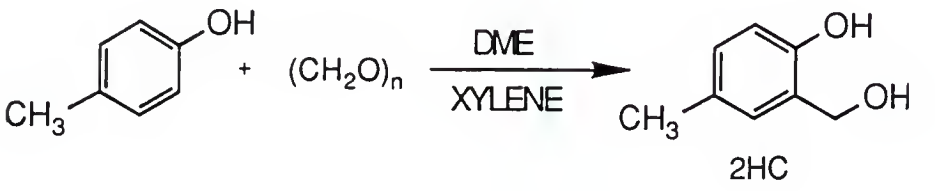

C.

Figure 37. A) Representation of the [3,3] sigmatropic RAR of the intermediate substituted phenyl benzene boronate. B) *Ortho*-bridged polyphenol derivatives. C) Uncatalysed reaction, in the presence of an ether additive (DME), for the C-*ortho* site-specific monohydroxymethylation of p-cresol with formaldehyde.

Uncatalysed reactions of formaldehyde with phenols give a variety of "phenolic resins" that have found in the past wide industrial applications, figure 37 B. However, for the synthesis of 2HC, the uncatalysed C-*ortho* site specific monohydroxymethylation of p-cresol with formaldehyde was attempted according to the procedure described in Casiraghi et al., 1981. Treatment of p-cresol with xylene with excess of paraformaldehyde (10 mol equiv.) in the presence of one mol equiv. of an ether additive such as dimethoxyethane (DME) in a closed reactor (high pressure reactor), at 135 ^{o}C for 12 hours, rendered, after purification with flash chromatography, a low yield of the desired product (Figure 37 C), and relatively large amounts of a resin substance.

Synthesis of 3-Hydroxy-4-(N-Methyl-Nicotinoyloxy) Toluene Iodide (18) and Attempted Synthesis of (25)

Since direct methylation of the pyridinium N of the monoesterified 4-methylcatechol (A) was not possible due to the free OH group, alternative synthetic pathways were attempted in order to synthesise 3-hydroxy-4-(N-methyl-nicotinoyloxy) toluene iodide.

Reaction of 4MC with the prepared trigonelline anhydride (15) (4 mmols of trigonellinate anhydrite were added to a solution of 4 mmols of 4-methyl-catechol in 65 ml anhydrous acetonitrile and to this suspension 4 mmols of DMAP was added and the mixture refluxed for several days) gave a mixture of products that could not be separated.

Another route undertaken for this synthesis was more successful: Protection of the free hydroxyl group of (A) with di-tert-butylpyrocarbonate (BOC anhydride), subsequent quaternization to the pyridinium product and elimination of the protecting group by HCl gave the desired product with good purity. Elemental analysis, however, was not successful due to mixture of the paired anion (Cl^- and I^-).

The synthesis of 3-hydroxy-4-{(N-methyl-1,4-dihydronicotinoyloxy) methoxy} toluene (25) (Figure 13) was not feasible due to rapid oxidation of 4-methyl catechol under the conditions necessary for the initial formation of the catechol sodium salt (22).

In Vitro Stability Studies

In Vitro Stability in Buffers

Theoretically, compounds with potential biological activity, apart from potency, should exhibit some stability in aqueous solution, in order to be useful for therapeutic purposes, for example in order to make stable pharmaceutical formulations. The in vitro stability study conducted herein consisted an approach to investigate these properties.

The stability of E (chosen as a representative among the three 4-methyl catechol CDSs) was studied in USP Buffers of pH range 5 to 9 at 37 ^oC, and it exhibited a bell shaped pH profile (Figure 15). The optimum stability was

observed around pH 6. Instability in more acidic conditions (in pH 5 $t_{1/2}$= 28 min) is obviously due to the hydration of the dihydro ring (Figure 38), while in alkaline conditions instability is attributed to rapid hydrolysis of the esters (in pH= 8, $t_{1/2}$=3 min).

The corresponding quaternary compound, D, appears relatively more stable in acidic conditions while it also degrades rapidly in alkaline conditions due to facilitated ester hydrolysis.

A different pH profile was obtained for dihydro compound 4 since it showed sufficient stability in more alkaline conditions (in pH=8 $t_{1/2}$= 2 hs), maintaining however the instability of the dihydros in acidic conditions due to their hydration (Figure 39).

The quaternary 3 is very stable in low pHs and rather more unstable in alkaline solutions (in pH= 8, $t_{1/2}$= 48 hs) due to eventual base-catalyzed hydrolysis of the pivaloyl esters.

Stability in Biological Media

In vitro stability studies in biological matrices may not result in absolute values but give a relative picture of the stability profile of the compounds under investigation. They also give indications of the possible metabolic profile in in vivo conditions.

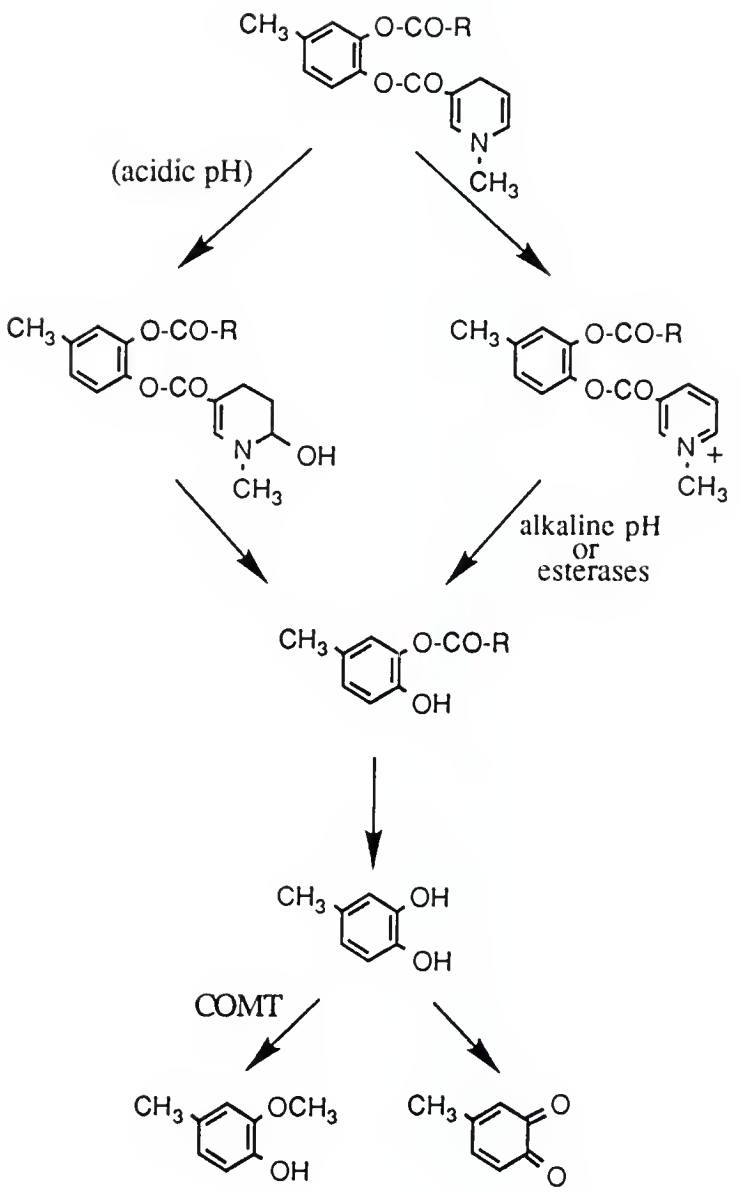

Figure 38. Degradation and metabolic pathways of 4-methylcatechol CDSs and their quaternary metabolites in vitro and/or in vivo.

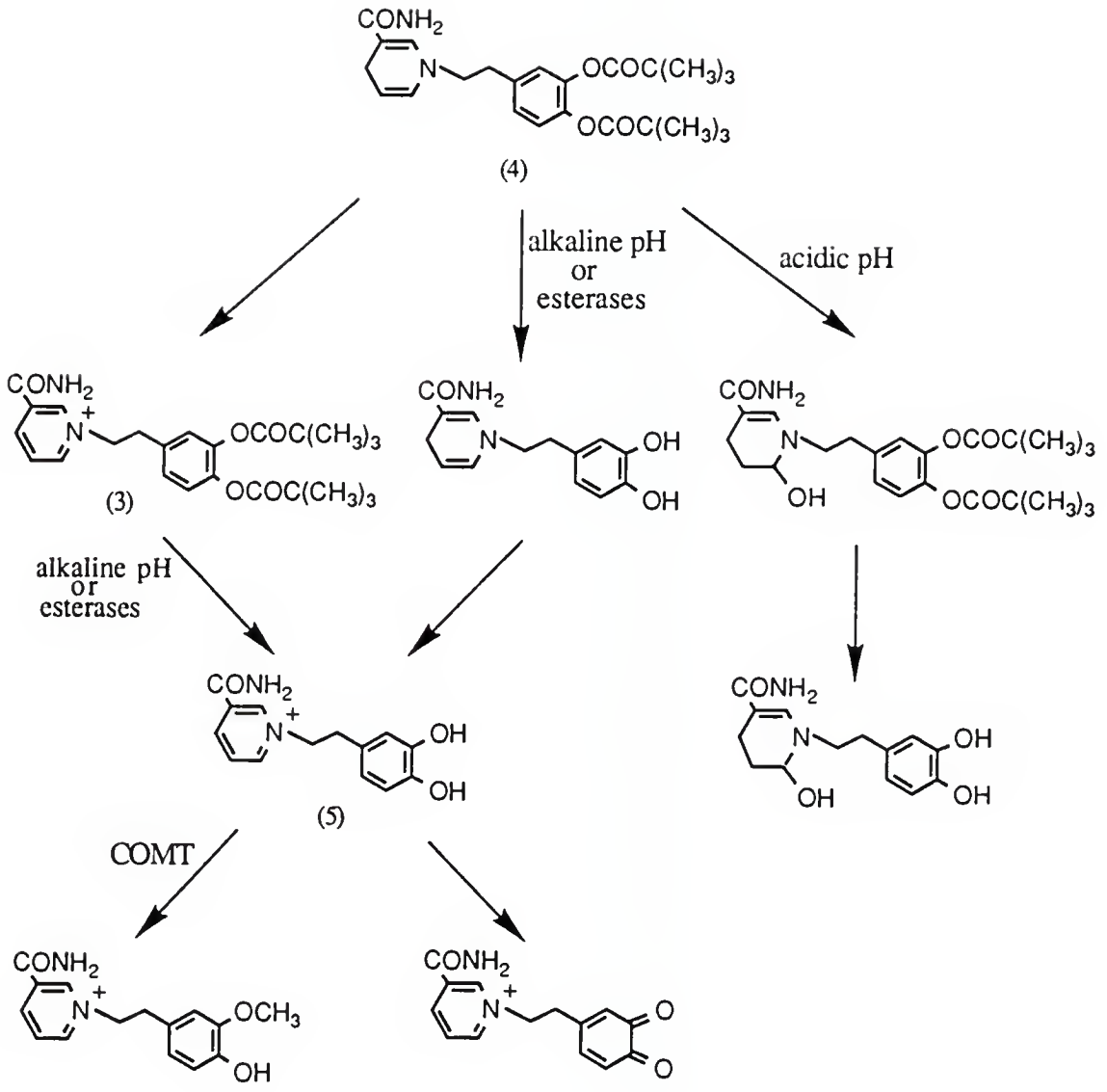

Figure 39. Degradation and metabolic pathways of the redox dopamine analogue (4) and its quaternary metabolite (3) in vitro and/or in vivo.

Stability in the rat brain homogenate

Dihydro compounds E, H, and J exhibited half lives ranging from 2 to 50 min in the rat brain homogenate. Degradation pathways, as shown in Figure 38, consisted in oxidation to the quaternary and sequential hydrolysis of the two ester bonds.

The corresponding quaternary compounds (with the exception of I) showed even lower half lives suggesting that the oxidation of the dihydro (or else the trigonelline group) facilitates ester bond cleavage. In other words, the rate limiting step for the hydrolysis of the dihydro group is the oxidation to the corresponding pyridinium. The surprisingly long half life of the quaternary I is probably due to the fact that access to esterases may be prohibited by steric and electrostatic interference (both ester groups are bulky and charged).

From the dihydro/quaternary pair 4 and 3, the quaternary showed a much higher half life than the dihydro, demonstrating that the charged side chain stabilizes the molecule relatively to the dihydro which is more vulnerable to degradation.

Stability in whole rat blood

Shorter half lives, as expected due to the abundance of esterases in the blood compared to the brain, were obtained in whole rat blood for all dihydro compounds and their quaternary metabolites, and a similar stability profile as in the brain homogenate: charged pyridinium groups hydrolyse faster than the dihydro groups, the exception being the half life of D which is considerably higher than anticipated with no apparent explanation.

Stability in rat liver homogenate

Half life values of 4 and 3 in the rat liver homogenate were somewhere between the values in the blood and brain homogenate (Figure 19), with the dihydro retaining its faster degradation compared to the quaternary. Although obviously metabolic enzymes are found primarily in the liver homogenate, the basic metabolic pathways of 4 and 3 are ester hydrolyses which require mostly unspecific esterases found in abundance in the blood.

In Vivo Distribution Studies

The CDS of 4-methylcatechol (J) rapidly enters the rat brain, after i.v. administration, and is therein converted rapidly to the quaternary metabolite I which is sustained for long releasing 4-methylcatechol (Figure 20 A). Initial high levels of 4MC may be attributed to direct release of 4MC from the CDS which evidently occurs to some extent, while the decrease of 4MC levels with time is due to the extensive metabolism of the catechol moiety. Nevertheless, a small amount of 4MC, provided by the slow but constant hydrolysis of the quaternary in the brain, is maintained for a long period of time. The concentration, therefore, of 4MC within the rat brain ranges from 0.2 mM to 0.02 mM and is comparable with the concentration of 4MC that is effective in the in vitro NGF-stimulatory studies.

Neither the dihydro nor the catechol were detected in the blood even at early times. The dihydro that remained in the circulation was rapidly converted

to the quaternary that was eliminated eventually or gave small amounts of 4MC that were however rapidly eliminated before detection. Ratio of the quaternary metabolite in blood/brain is represented in Figure 20 B.

It should be noted that after peripheral administration (i.v. injection) of equimolar amounts (to the CDS J) of 4MC and in the same drug vehicle, small amount of 4MC was detected in the brain that rapidly disappeared within the first few minutes (results not shown).

The redox dopamine CDS 4 readily crossed the BBB yielding high levels of the quaternary metabolite ("lock-in" form) in the rat brain even at early times, concentrations of which were sustained for long. The quaternary metabolite (3) released the final metabolite (5) that was maintained at higher levels than the quaternary (3) for at least 2 hours (Figures 21 A and 39).

Blood levels of the CDS 4 were undetectable even at early times and only the quaternary metabolites (3 and 5), that were in turn rapidly eliminated, were observed as shown in Figure 22. While these metabolites are rapidly disappearing from the periphery, they are sustained in much higher levels and for longer in the brain (Figures 21A and 23).

The presence and metabolism of CDS 4 and its metabolites was also investigated in the liver. As expected, the dihydro was rapidly converted to the quaternary 3 and that in turn to the pyridinium catechol derivative 5 (Figure 21 B).

In Vivo (CNS) NGF-Stimulatory Activity

The in vivo (CNS) NGF-stimulatory study of the brain-targeted CDS of 4MC (J) showed, after i.v. administration, a 1.76 fold increase in NGF mRNA compared to control in the rat hippocampus (1.3 fold increase compared to the 4MC-control). Administration of 4MC itself demonstrated a small increase (1.3 fold) in NGF mRNA compared to control. In the frontal cortex a 1.32 fold increase was observed by the CDS (1.22 fold increase compared to 4MC-control), while 4MC minimally increased (1.1 fold) the NGF mRNA content in this region compared to control.

The small induction of 4MC itself (4MC-control) on brain NGF mRNA levels (1.3 fold increase in the hippocampus and 1.1 fold in the frontal cortex) may be attributed to its peripheral effects that perhaps may indirectly influence CNS levels, or due to the minimal amounts capable of crossing the BBB in order to induce NGF locally (in the CNS).

The difference of induction in the hippocampus and cortex (NGF seems more inducible in the hippocampus than in the cortex by 4MC or its CDS) could be attributed to different mechanisms of NGF-induction by the compound under investigation in these two regions. Although basal NGF mRNA levels are higher in the frontal cortex than in the hippocampus, higher levels may be induced/produced in the hippocampus from the glia present in this region. Since apart from neuronal cells, glial cells have also been shown in vitro and in vivo (Bakhit et al., 1991) not only capable of producing basal NGF levels but also

being stimulated by agents to induce their production (literature data but also observations from the in vitro experiments conducted herein), and since they are absent from the cortex region of the brain, it would be convincing to assume local hippocampal production of NGF mRNA by those cells as an additional source of NGF in that region. Furthermore, it would be interesting to investigate the relative β-adrenergic receptor distribution in these two brain regions, since one of the mechanisms proposed for NGF induction through which catechol possibly acts to produce an effect, as elaborated in other chapters, is BAR stimulation.

In Vitro NGF-Stimulatory Activity

First, 4MC was evaluated in the C6 glioma cell culture. Highest activity was at a concentration of 0.1 mM (highest dose that was not cytotoxic) upon which NGF content in the culture medium increased almost 3 fold (Figure 27 A, Table 3). This value is higher but comparable with the 1.4-1.9 fold NGF increase in the C6 medium content after treatment with 0.01 mM isoproterenol, (although isoproterenol is orders of magnitude more potent than 4MC), the β-adrenergic agonist that has been used extensively in previous assays in order to demonstrate the β-adrenergic receptor mediated NGF induction. The 4MC isosters, 5MHP and 2HC (at concentrations from 0.1 to 0.2 mM) showed lower activity in the C6 cells. Statistical significant difference in NGF content compared to the control was shown by 5MHP (0.15mM) with a 1.55 fold increase in NGF while 2HC (0.1mM) demonstrated no significant activity (Table 3). The NGF-induction in

the C6 cell line by 5MHP was comparable to other catechol or catecholamine NGF-inducing compounds. Isosteric substitution of the catechol with the N-hydroxy-pyridone seems to retain significant activity complying with the suggested receptor mediation, in this case, for NGF induction.

A different biological profile was observed for the isosters in the L-M cells (Figure 27 B, Table 4): 5MHP (0.1-0.2mM) increased (1.5-1.7 fold) NGF content in the culture medium while 2HC was relatively inactive. However in this cell line, 4MC at a concentration of 0.05 mM increased NGF approximately 14 fold (confirming earlier reports). The two isosters therefore can be considered inactive in the L-M cells.

In contrast, the pyridinium catechol derivative 5 demonstrated the reverse effect compared to the isosters, in the two cell lines (Figures 28 A and B). Being inactive in the C6 glioma, it showed significant activity in the L-M cells, increasing the NGF content more than two-fold over the control.

The inactivity (Figure 29) of the protected at the catechol moiety compounds (esterified catechol derivatives 4 and 3) in the L-M cell line serves as a conformation of the previous observations that the catechol function is required for activity. These derivatives (the structure of 3 is identical to 5 except that the catechol function is protected) show minimal activity since the catechol moiety needs to be liberated first (hydrolysis of the esters) which does not readily proceed in the culture medium of these cells (presence of esterases or alkaline pHs facilitate this conversion).

Intracellular levels of NGF protein of the C6 glioma cells after incubation with 4MC, isosters, and derivative 5, were determined in order to verify that the levels of NGF measured in the cell culture medium are from de novo intracellular synthesis and subsequent extracellular secretion. Intracellular levels of treated cultures were close to those of the controls confirming the previous hypothesis. The slight decrease of intracellular NGF protein levels detected after treatment with 2HC (0.2 mM) and 5 (0.15 mM) may be due to minimal cytotoxicity of these compounds that stimulate secretion of NGF from the cells before the de novo synthesis can compensate the loss and maintain intracellular levels.

The de novo synthesis of NGF protein was also attempted to be established by measuring the intracellular NGF mRNA levels of the cell cultures after the respective treatments. The total RNA from the C6 cells was extracted and blotted in order to measure the induction in NGF mRNA, but no significant levels of NGF mRNA were detected after hybridisation with the NGF probe. As confirmed in a subsequent assay, starting the treatments after the cell cultures had reached the stage of confluency (the cultures were left to grow to that stage in order to obtain an appropriate and sufficient amount/number of cells for optimizing the RNA extraction and subsequent detection of message RNA) proved detrimental to this assay since cell functions (such as mRNA synthesis) are diminished at that stage of the cell life-cycle. This hypothesis/observation was confirmed by treating confluent cells with 4MC and measuring NGF protein levels: As anticipated, levels of NGF induction by 4MC decreased (relative to cell numbers) as cells became more confluent (1 and 2 days) while at the

confluency stage (4 days) no NGF protein could be detected neither by controls (untreated confluent cultures) nor by treated cultures (Figure 31).

QSAR

The best correlations between activity of the catechol derivatives as NGF-inducers in L-M cells derived from the quantum mechanical calculations, are those that are related directly or indirectly to the oxidation potential of the catechols (R=0.72 to 0.83 as shown in equations 1-3 or Table 6).

The values of the adiabatic ionization potential (IPa) and of the parameter Q can be considered to describe respectively a transition state and the final product of the oxidation of a catechol (A) to the corresponding quinone (E), (Figure 40 A). A probable mechanism describing this oxidation is shown in Figure 40 B.

From the IPa and Q values (Table 5) we can deduce that the energy (expressed as heat of formation) of the radical cation of the catechol (B) is the highest followed by the energy of the quinone (E) and then by the catechol (A). The hypothetical energetic diagram for the oxidation of the catechol via the transition state to the ortho quinone is depicted in the diagram of Figure 41.

These observations/hypotheses indicated the significance of relating the sum of the absolute values of IPa and parameter Q, expressed as SAQ, with activity. This relation gave the best simple correlation (R=0.84, equation 6) compared to all other parameters (Table 6). In addition, from equation 6 it is

deduced that the lower the SAQ values of a catechol derivative the higher its activity (since activity is expressed as mM concentration). Therefore the lower the sum of the IPa and Q, or else the lower the energetic barrier (Figure 41) for the oxidation of a catechol to the quinone via the transitional radical cation (the lower the IPa) and the more stable the quinone derivative (the lower the Q), the more active apparently the catechol is. By adding one more geometrical parameter (the ovality of the molecules) the best correlation with activity was achieved (R=0.90, equation 7) that is capable of predicting the activity of a catechol as an NGF inducer in L-M cells in a significant way, as shown in Figures 33 and 34.

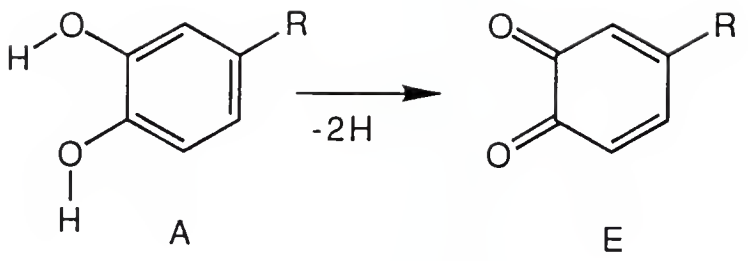

A.

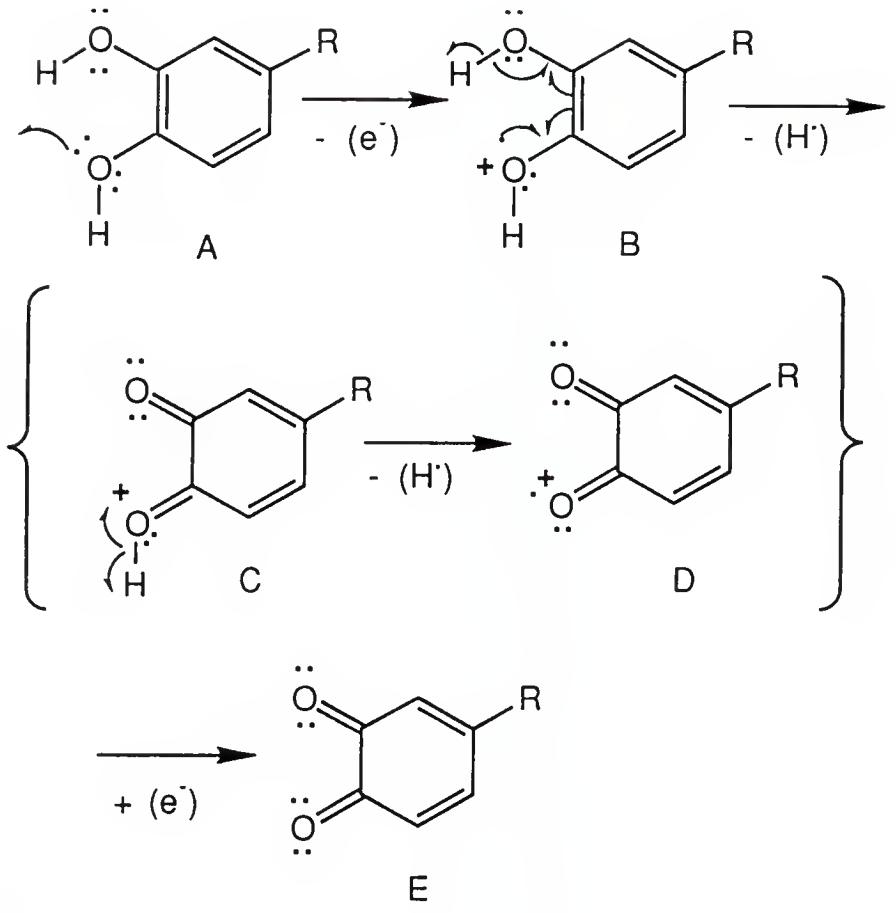

B

Figure 40. A) Oxidation of a catechol derivative to the quinone.
B) A probable mechanism of oxidation of a catechol derivative to the corresponding quinone.

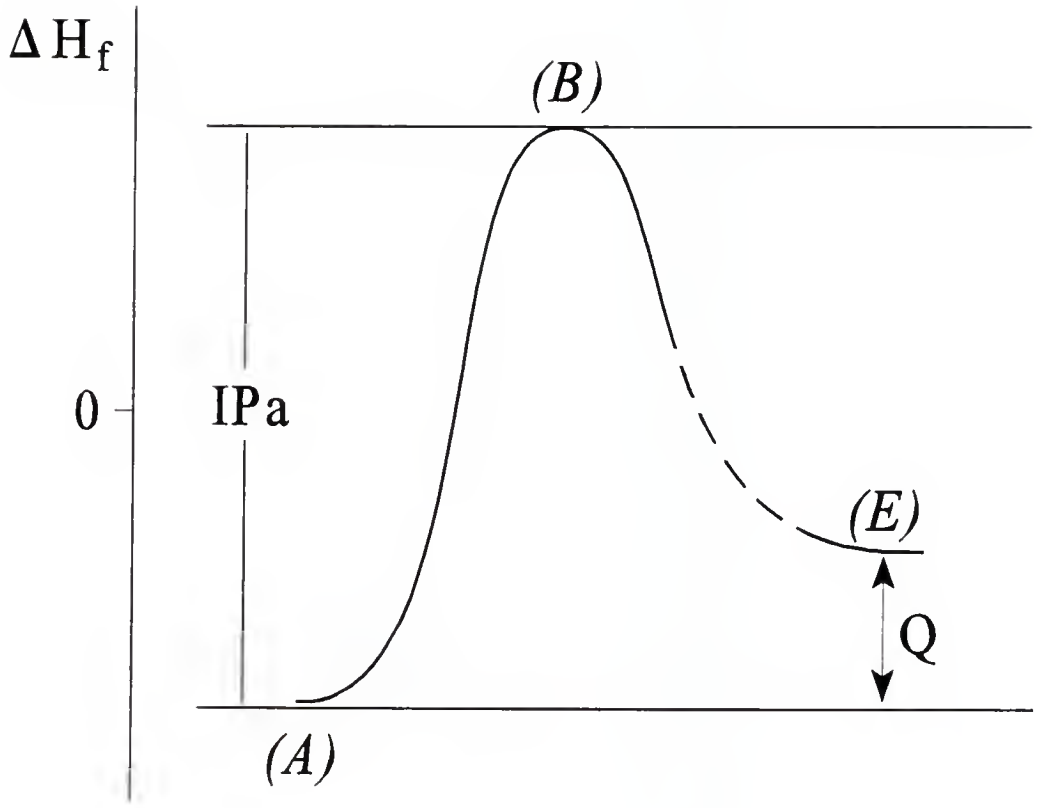

Figure 41. Hypothetical energetic diagram for the oxidation of the catechol (A) via the transition state (B) to the ortho quinone (E).

CHAPTER 5
CONCLUSIONS

Overall, significant levels of 4MC, the compound of interest, as well as the pyridinium catechol derivative (5) were attained within the rat brain with the corresponding CDSs, while levels of these compounds in the periphery were not only very low but rapidly disappeared. Thus, selective and sustained delivery of the compounds of interest to the brain was achieved. Furthermore, the in vivo increase in NGF mRNA in the hippocampal and cortical region of the rat brain by the 4MC CDS, demonstrates the feasibility of NGF-induction within the CNS by peripheral administration of a 4MC brain targeted CDS, and lends credit towards the development of dihydropyridine CDS derivatives for other established NGF inducers. Apart from the therapeutic application of such derivatives, this peripheral (non-invasive nor damaging to the CNS) administration of efficient NGF-inducers would provide perhaps a better means to study the in vivo mechanism of NGF stimulation, as well as consequent effects of NGF, with a controlled dosage and treatment schedule of administration of NGF-stimulating compounds. Moreover, site specific brain-targeting provides possibly the only means for peripheral administration of NGF-stimulating agents for CNS application since the well documented peripheral NGF-induction (in the peripheral

nervous system) would be a serious, indiscriminate, and consistent undesired side-effect.

The results of the in vitro assays for NGF stimulation, when taken together, indicate the necessity for the actual catechol moiety for NGF induction in the L-M cell line since isosteric substitution of that moiety (5MHP or 2HC) or its protection (3, 4) renders the molecule relatively inactive, while retention of the catechol moiety (in compound 5) retains significant activity. The lower activity of 5 compared to other active catechol derivatives can be attributed to its charged pyridinium side chain that could interfere with cellular uptake.

In contrast, the catechol moiety does not seem essential for activity in the C6 glioma cells and its isosteric/isoelectronic replacement retains significant activity (5MHP), confirming that different mechanisms are in effect in the two cell lines under investigation for NGF stimulation. (β-adrenergic receptor mediation in the case of C6 cells is most probable.)

Interestingly, the findings/observations in the L-M cells support recent suggestion (Murakami et al., 1993) that the stimulatory effects of catechol derivatives on NGF production and secretion in L-M cells are predominantly mediated by the quinones formed by autoxidation in the culture medium of these cells, a hypothesis/mechanism of action that is further supported by the extended theoretical studies conducted herein. The isosters, although retaining steric and electronic similarity with 4MC, lack the specific "oxidizable" catechol structure. Consequently, this can account for their inactivity in this cell line and furthermore can shed some light to the interesting question about why the specific catechol

function is necessary for activity in the L-M cell line while at the same time it is relatively dispensable in the C6-glioma cell line.

Elucidation of mechanisms(s) involved for the induction of NGF biosynthesis would be very important for the development of an NGF-inducing therapeutic, by eliminating compounds that act via non-specific ways, and by developing a drug with the appropriate specificity and efficacy by rational (mechanism-based) design.

The attempt to correlate activity of catechol derivatives with few molecular or electronic descriptors was successful: good correlation was found between NGF stimulatory activity in L-M cells and the IPa or SAQ descriptors. This strongly suggests that activity is related to the oxidative capacity of the catechol moiety since NGF stimulation increases along with the increase in the oxidative potential of the catechol (equations 1, 6, and 7). The easier the catechol can be oxidised, the more active it is. Thus, using descriptors of oxidation, such as IPa or SAQ, an estimate of activity or inactivity of novel catechol derivatives may be obtained.

Furthermore, since the mechanism responsible for the stimulation of NGF by catechol derivatives is still under investigation, our results support recent findings that suggest an oxidation process involved in this stimulatory effect. Since it was reported that antioxidants prevented the stimulatory effect of the catechol derivative DOPS, while several quinone derivatives increased NGF content (Murakami et al., 1993, Takeuchi et al., 1990), it was strongly suggested that the stimulatory effect of catechol derivatives on NGF secretion in L-M cells is predominantly mediated by the quinones formed by autoxidation in the culture of

these cells. Thus, NGF may be induced by oxidative stress as a protective response of cells. Interestingly enough, the large induction of NGF by oxidizable agents (catechols) in the fibroblastic L-M cells (a mouse connective tissue derived cell line) compared to that in the glioma cells, could also be interpreted in terms of the different physiological functions of these two cell types: glial cells have a supportive and trophic role in the nervous system while the fibroblast-like connective tissue derived cells pertain in addition a protective role to the surrounding tissues and thus probably have increased antioxidant or detoxifying mechanisms.

These findings are of particular interest when taking under consideration the fact that catechol derivatives also stimulate NGF in vivo (in rat brain), and that quinones are most probably formed also in vivo. Thus, not only the mechanism of NGF stimulation but also the protective role of NGF itself on neurons becomes an intriguing question to resolve, especially when considering that the cause of degeneration of NGF-responsive neurons in diseases such as Alzheimer's is yet to be determined.

It is well known that catechols readily oxidize upon exposure to air and that the rate of this "autoxidation" depends on the amount of metal ions present. Of the various oxidising agents in living systems, the ubiquitous and present in high concentrations oxygen is probably the most important (Graham et al., 1978, Bindoli et al., 1992). Furthermore, the oxidation of catechols in living systems is a complex process that can lead not only to the corresponding quinones but also to various oxygen derived species, that are detoxified by various pathways as

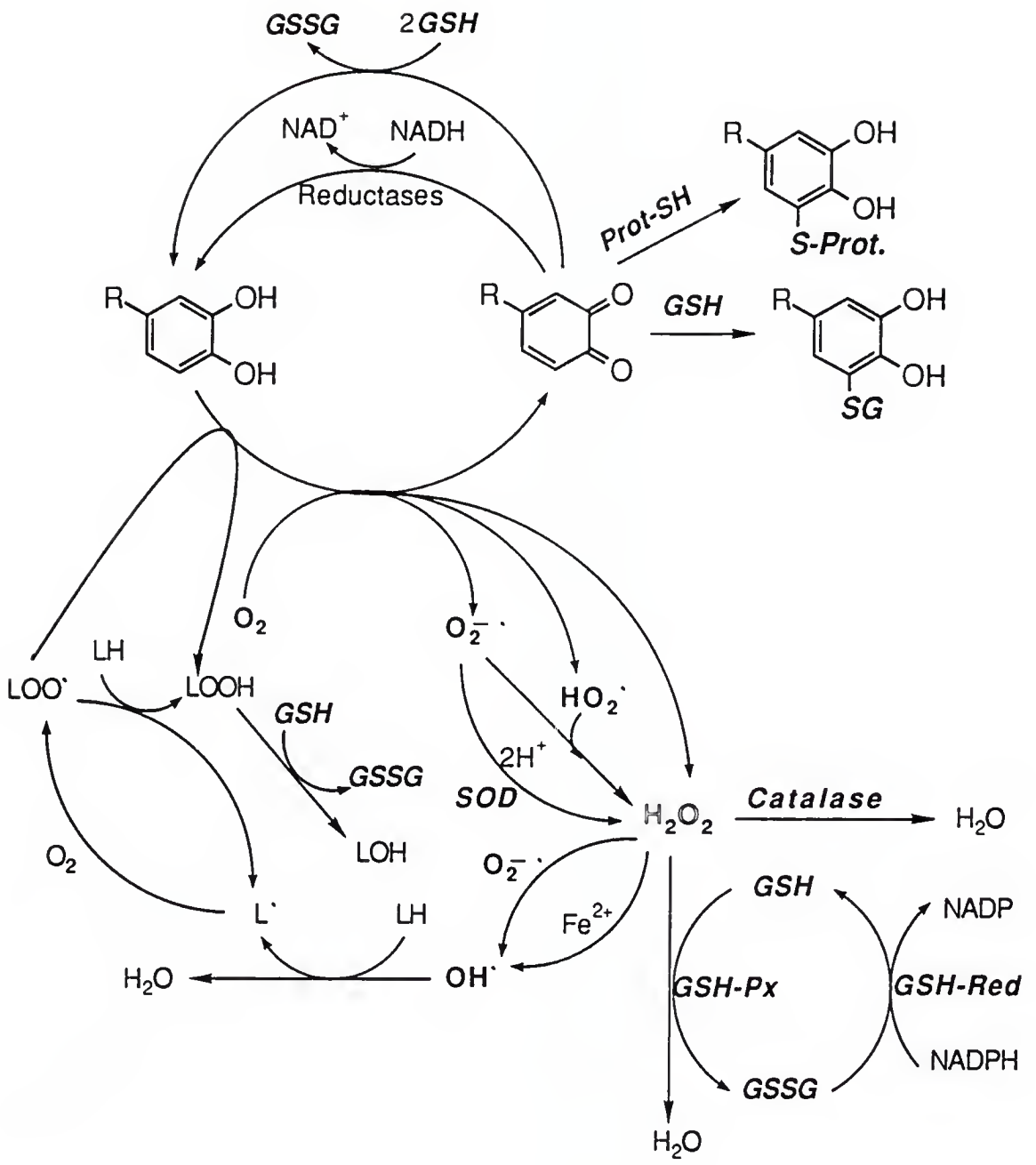

Figure 42. Oxidants and antioxidants believed and proposed to play a role in the redox reactions of catechol derivatives in cells. Autoxidation of catechols proceeds via 1-electron transfer reaction producing radical intermediates. Potential antioxidative or radical scavenging properties are also depicted. Possible pathways of glutathione depletion.

proposed in Figure 42 . Redox cycling of the catechol may cause continuous generation of H_2O_2 and other intermediates and lead thus to a decrease in intracellular GSH level. The rate of oxidation therefore of a catechol derivative can be determinant of the depletion of cellular GSH concentrations.

In normal conditions there is a steady state balance between the production of oxygen-derived free radicals and their destruction by cellular antioxidant systems. This balance, however, can be broken naturally or experimentally either by increasing the free radical production or by decreasing the defence systems. It is also understood that antioxidant enzymes seem to act cooperatively and thus each has a specific irreplaceable role in cell defence and all of them have to be present to ensure total protection. The inhibition of only one of the antioxidant enzymes could lead to deleterious effects (Michiels et al., 1994).

It is possible that temporary depletion of GSH and related enzymes, that are rapidly consumed for the detoxification of reactive products generated from the autoxidation of the catechol, **may initiate a mechanism which leads to NGF biosynthesis.** It is therefore herein proposed that **this disturbance in cellular homeostasis of antioxidant enzymes serves as a triggering event for cellular NGF biosynthesis and release.** NGF's well documented cytoprotective effects would consequently give further support and justify this hypothesis providing a rational "cause-and-effect" purpose for this induction. As described in the literature, NGF can act to elevate GSH levels and thus restore the homeostasis of the cell. Thus, **such a feedback regulating mechanism for NGF production is conceivable as an early and initial response of cells to oxidative stress.** This

hypothesis is very well supported by the in vitro induction of NGF gene expression (Pechan et al., 1992) by H_2O_2, since cellular detoxification of H_2O_2 may involve consumption of GSH and related enzymes as also shown in Figure 42.

The mechanisms of neuroprotective actions of NGF are unknown. Increased cell survival of NGF-treated PC12 cells after oxidant injury (Jackson et al., 1990) suggested that neurotrophic factors may play a role in the detoxification of free radicals generated by oxidative stress. Mechanisms responsible for the increased cell survival of NGF-treated neurons when challenged with oxidant stress (Davies et al., 1990) may be an increased cellular defence system that would include antioxidant enzymes and antioxidants (e.g. SOD, GSH) and/or a stimulated cellular repair system (that would involve protein, lipid, and DNA repair enzymes).

NGF has been reported to restore decrease in catalase activity while increasing SOD and glutathione peroxidase activity in the brain of aged rats (Nistico et al.,1991 and 1992). The protection of NGF of PC12 cells from peroxidation (Jackson et al., 1990) gas been shown to be attributed to NGF mediated increase in γ-glutamylcysteine synthetase (GCS) activity (the rate limiting enzyme for GSH synthesis), increase in GSH levels, and stimulation of GSH peroxidase, as well as effects on the metabolism of pyridine nucleotides (NAD, NADP) (Jackson et al., 1992).

Numerous hypotheses about the role of NGF in oxidant homeostasis in neurons can be derived from the abundant experimental data surrounding the

diverse fields of neurotrophins and oxidative stress, fields that only very recently have shown to share some common ground. For example, one such hypothesis can provide an additional role for the, activated by NGF, 2nd messenger protein kinase C, since it is documented that protein kinase C inhibits lipid peroxidation in brain membranes, an effect that is further postulated not to be turned on unless concentrations of vitamin E decreases due to its consumption in free radical reactions! (Kagan et al., 1992) An other example could be the perturbation in intracellular calcium homeostasis as a consequence of free radical mediated neuronal structural damage that can be attenuated by NGF through its ability to prevent the excessive elevation of Ca^{2+} (Mattson et al., 1993).

In conclusion, the decrease of concentrations of NGF and of its mRNA which occurs in the brain during senescence (Whittemore et al., 1987) could be responsible not only for the degeneration of cholinergic pathways as suggested in AD but also for the imbalance in the enzymes responsible for the degradation of free radicals formed in specific areas of the brain. Since the pathology of many chronic neurological diseases has been postulated to involve oxidant homeostasis, broader and more pervasive beneficial effects of NGF treatment can be anticipated, while NGF-induction in the brain may further be useful in arresting chronic degeneration in the CNS by multiple mechanisms. However, given the complexity of systems involved in AD, it is unlikely that any single drug will be completely efficacious in treating this disorder. Future research on neuroprotection is therefore both challenging and promising.

Those who refuse to go beyond fact rarely get as far as fact.

T. H. Huxley

(Levi-Montalcini, R., in "Developmental Neurobiology and the Natural History of Nerve Growth Factor", 1982)

REFERENCES

Adams, J.D., & Odunze, I.N., Oxygen Free Radicals and Parkinson's Disease, Free Radic. Biol. Med., 10, 161-169 (1991)

Altar, A., Efficacy of Neurotrophc Factors Against CNS Degeneration, (Abstract) 3rd Suncoast Workshop on the Neurobiology of Aging, Amelia Island, Florida (1995)

Ariens, E.J.,Chapter 1 in *Drug Design*, v. 1, Ed. Ariens, E.J., Academic Press (1971)

Atkinson, M.R., Morton, R.K., & Naylor, R., Synthesis of Glycosylpyridinium Compounds from Glycosylamines and from Glycosyl Halides, J. Chem. Soc., 610-615 (1965)

Awatsuji, H., Furukawa, Y., Hirota, M., Murakami, Y., Nii, S., Furukawa, S., & Hayashi, K., Interleukin-4 and -5 as Modulators of Nerve Growth Factor Synthesis/Secretion in Astrocytes, J. Neurosc. Res., 34, 539-5454 (1993)

Bakhit, C., Armanini, M., Bennett, G.L., Wong, W.L.T., Hansen, S.E., & Taylor, R., Increase in Glia-Derived NGF Following Destruction of Hippocampal Neurons, Brain Res., 56, 76-83, (1991)

Ballarin, M., Ernofrs, P., Lindefors, N., & Persson, H., Hippocampal Damage and Kainic Acid Injection Induce a Rapid Increase in mRNA for BDNF and NGF in the Rat Brain, Exp. Neurol., 114, 35-43, (1991)

Barnaby, G., & Persson, H., Regulation of Neurotrophin mRNA Expression in the Rat Brain by Glucocorticoids, Eur. J. Neurosci., 4, 396-403, (1992)

Bigge, C.F., & Boxer, P.A., Neuronal Cell Death and Strategies for Neuroprotection, Chapter 2 in Annual Reports in Medicinal Chemistry, 29, (1994)

Binderup, E., & Hansen, E.T., Chlorosulfates as Reagents in the Synthesis of Carboxylic Esters Under Phase-Transfer Conditions, Synthetic Communications, 14, (9), 857-864 (1984)

Bindoli, A., Rigobello, M.P., & Deeble, D.J., Biochemical and Toxicological Properties of the Oxidation Products of Catecholamines, Free Radic. Biol. Med., 13, 391-405 (1992)

Bodor, N., & Brewster, M., Problems of Delivery of Drugs to the Brain, Pharmacol. Ther., 19, 337-386 (1983)

Bodor, N., Brewster, M., & Farag, H., Site-Specific Sustained Release of Drugs to the Brain, Science, 214, 1370-1372, (1981)

Bodor, N., & Farag, H., Improved Delivery Through Biological Membranes. XI. A Redox Chemical Drug Delivery System and its use for Brain Specific Delivery of Phenethylamine, J. Med. Chem., 26, 313-318 (1983 a)

Bodor, N., & Farag, H., Improved Delivery Through Biological Membranes. 13. Brain-Specific Delivery of Dopamine with a Dihydropyridine-Pyridinium Salt Type Redox Delivery system, J. Med. Chem., 26, (4), 528 (1983 b)

Bodor, N., Gabanyi, Z. & Wong,C.-K., A New Method for the Estimation of Partition Coefficient. J. Am. Chem. Soc., 111, 3783-3786 (1989).

Bodor, N., & Huang, M.-J. An Extended Version of a Novel Method for the Estimation of Partition Coefficients, J. Pharm. Sci., 81, 272-281 (1992)

Bodor, N., & Simpkins, J., Brain-Specific, Sustained Release of Dopamine with a Redox Delivery System, Science, 221, 65-67, (1983)

Bowman, W.C., & Rand, M.J., *Texbook of Pharmacology*, Second edition, Blackwell Scientific Publications, (1980)

Brewster, M., Robledo-Luiggi, C., Miyakeb, A., Pop, E., & Bodor, N., Brain-Enhanced Delivery of Anti-Dementia Drugs, Chapter in *Novel Approaches to the Treatment of Alzheimer's Disease*. E. MEYER, J. SIMPKINS, and J.YAMAMOTO, (Advances in Behavioral Biology, v.36). ,PLENUM EDS. N.Y., 173-183 (1989)

Brewster, M., Venkatraghavan, V., Shek, E., & Bodor, N., Facile, One-Step Preparation of Trigonellinate Esters, Synthetic Communication, 17, (4), 451-455 (1987)

Burger, A., *Burger's Medicinal Chemistry*, 3rd ed. New York, Wiley-Interscience (1970)

Burger, A., Comprehensive Medicinal Chemistry: the Rational Design, Mechanistic Study & Therapeutic Application of Chemical Compounds, v.1 General principles, ed. N.Y. Pergamon Press (1990)

Butler, J., & Hoey, B.M., Reactions of Glutathione and Glutathione Radicals with Benzoquinones, Free Radic. Biol. Med., 12, 337-345 (1992)

Carman-Krzan, M., Vige, X., & Wise, B. C ., Regulation by Interleukin-1 of NGF Secretion and NGF mRNA Expression in Rat Primary Astroglial Cultures, J. Neurochem., 56, 636-643, (1991)

Carman-Krzan, M., & Wise, B. C ., Arachidonic Acid Lipoxygenation May Mediate Interleukin-1 Stimulation of Nerve Growth Factor Secretion in Astroglial Cultures, J. Neurosc. Res., 34, 225-232 (1993)

Carswell, S., The Potential for Treating Neurodegenerative Disorders with NGF-Inducing Compounds, Exp. Neurol., 124, 36-42 (1993)

Carswell, S., Hoffman, E. K., Clopton-Hartpence, K., Wilcox, H. M., & Lewis, M. E., Induction of NGF by Isoproterenol, 4-Methylcatechol and Serum Occurs by Three Distinct Mechanisms. Mol. Brain Res., 15, 145-150 (1992).

Casiraghi, G., Casnati, G., Pochini, A., Puglia, G., Ungaro, R., & Sartori, G., Uncatalyzed Phenol-Formaldehyde Reactions. A convenient Synthesis of Substituted 2,2'-Dihydroxy-Diphenylmethanes, Synthesis, Communications, 143-146 (1981)

Casiraghi, G., Casnati, G., Puglia, G., & Sartori, G., Selective Reactions Between Phenols and Formaldehyde. A superior Synthesis of Salicyl Alcohols, Synthesis, Communications, 124-125 (1980)

Cassidy, F., Orlek, B.S., & Hadley, M.S., Chemical Approaches to the Enhancement of Cholinergic Function for the Treatment of Senile Dementia, Chapter 3, in *Anti-dementia Agents. Research and Prospects for Therapy*. Edited by Nicholson, D., Academic Press, (1994)

Cheng, B., & Mattson, M.P., NGF and bFGF Protect Rat Hippocampal and Human Cortical Neurons Against Hypoglycemic Damage by Stabilizing Calcium Homeostasis, Neuron, 7, 1031-1041 (1991)

Chomczynski, P., & Sacchi, N., Single-Step Method of RNA Isolation by Acid Guanidinium Thiocyanate-Phenol-Chloroform Extraction, Anal. Biochem., 162, 156-159 (1987)

Cohen, G., Oxidative Stress in the Nervous System, Chapter 16 in *Oxidative Stress* Edited by Sies, H., Academic Press (1985)

Cohen, N.C., Blaney, J.M., Humblet, C., Gund, P., & Barry, D.C., Molecular Modeling Software and Methods for Medicinal Chemistry, J. Med. Chem., 33, (3), 883-894 (1990)

Cordell, B., β-Amyloid Formation as a Potential Therapeutic Target for Alzheimer's Disease, Ann. Rev. Pharmacol. Toxicol., 34, 69-89, (1994)

Dal Toso, R., De Bernardi, M. A., Costa, E., & Mocchetti, I., Beta-Adrenergic Receptor Regulation of NGF-mRNA Content in Rat C6-2B Glioma Cells, Neuropharm., 26, (12), 1783-1786, (1987)

Dal Toso, R., De Bernardi, M. A., Brooker, G., Costa, E., & Mocchetti, I., Beta-Adrenergic and Prostaglandin Receptor Activation Increases Nerve Growth Factor mRNA Content in C6-2B Rat Astrocytoma cells, J. Pharm. Exp. Ther., 246, (3), 1190-1193, (1988)

Davies, K.J.A., Wiese, A.G., Sevanian, A., & Kim, E.H., Repair Systems in Oxidative Stress, in *Molecular Biology of Aging*, Edited by Finch, C.E., Johnson, T.E., Wiley-Liss, 123-141 (1990)

De Bernardi, M.A., Fabrazzo, M., & Mocchetti, I., Transcriptional Regulation of Nerve Growth Factor Gene, in "*Neurotransmitter Regulation of Gene Transcription*" ed. Costa, E., Joh, T., p. 37-46, N.Y.: Thieme (1991)

Dewar, M. J. S., Zoebisch, E. G., Healy, E. F., & Stewart, J. J. P., AM1: A New General Purpose Quantum Mechanical Molecular Model. J. Am. Chem. Soc., 107, 3902-3909 (1985).

D'Mello, S., & Heinrich, G., Induction of Nerve Growth Factor Gene Expression by 12-O-Tetradecanoyl Phorbol 13-Acetate, J. Neurochem., 55, 718-721, (1990)

D'Mello, S., & Heinrich, G., Multiple Signalling Parthways in the Regulation of Nerve Growth Factor Production in L929 Fibroblasts, J. Neurochem., 57, 1570-1576, (1991)

Eisner, U., & Kuthan, J., The Chemistry of Dihydropyridines, Chemical Reviews, 72, (1), 1 (1972)

Fabrazzo, M., Costa, E., & Mocchetti, I., Stimulation Of Nerve Growth Factor Biosynthesis In Developing Rat Brain By Reserpine: Steroids As Potential Mediators, Mol. Pharmacol., 39, 144-149 (1990)

Fisher, W., Wictorin, K., Bjorklund, A., Williams, L.R., Varon, S., & Gage, F.H., Amelioration of Cholinergic Neuron atrophy and Spatial Memory Impairment in Aged Rats by NGF, Nature, 329, 65-68 (1987)

Follesa, P., & Mocchetti, I., Regulation of Basic Fibroblast Growth Factor and Nerve Growth Factor mRNA by b-Adrenergic Receptor Activation and Adrenal Steroids in Rat Central Nervous System, Mol. Pharmacol., 43, 132-138 (1992)

Fraser, D.A., Hall, R.W. & Raum, A.L., Preparation of 'High-Ortho' Novolak Resins I. Metal Ion Catalysis and Orientation Effect, J. Appl. Chem., 676-688 (1957)

Friedman, H. L., Influence of Isosteric Replacements Upon Biological Activity, Symposium on Chemical-Biological Correlation, *National Academy of Science-National Research Council*, Publication no 206, Washington, D.C., p. 295, (1951).

Friedman, W.J., Altiok, N., Fredholm, B.B., & Persson, H., Mechanisms of Nerve Growth Factor mRNA Regulation by Interleukin-1b in Hippocampal Cultures: Role of Second Messengers, J. Neurosc. Res., 33, 37-46 (1992)

Friedman, W.J., Larkfors, L., Ayer-Lelievre, C., Ebendal, T., Olson, L.,& Persson, H., Regulation of b-NGF Expression by Inflammatory Mediators in Hippocampal Cultures, J. Neurosci. Res., 27, 374-382,(1990)

Fujita, T., Iwassa, J., & Hansch, C., Progress in Physical Organic Chemistry, 12, 91, (1976)

Furukawa, S., Kamo, I., Furukawa, Y., Akazawa, S., Satoyoshi, E., Itoh, K., & Hayashi, K., A Highly Sensitive Enzyme Immunoassay for Mouse b-Nerve Growth Factor, J. Neurochem., 40, 734-744 (1983)

Furukawa, Y., Fukazawa, N., Miyama, Y., Hayashi, K., & Furukawa, S., Stimulatory Effect of 4-Alkylcatechols and their Diacetylated Derivatives on the Synthesis of Nerve Growth Factor, Bioch. Pharmacol., 40, (10), 2337-2342, (1990)

Furukawa, Y., Furukawa,S., Ikeda, F., Satoyoushi, E., & Hayashi, K., Aliphatic Side Chain of Catecholamine Potentiates the Stimulatory Effect of the Catechol Part on the Synthesis of Nerve Growth Factor. FEBS Lett, 208, 258-262 (1986 a).

Furukawa,Y., Furukawa, S., Satoyoshi, E., & Hayashi, K., Catecholamines Induce an Increase in Nerve Growth Factor Content in the Medium of Mouse L-M Cells, J. Biol. Chem., 261, (13), 6039-6047, (1986 b)

Furukawa,Y., Furukawa, S., Satoyoshi, E., & Hayashi, K., Regulation of Nerve Growth Factor Synthesis/Secretion by Catecholamine in Cultured Mouse Astroglial Cells, Biochem. and Biophys. Res. Commun., 147, (3), (1987)

Furukawa, Y., Tomioka, N., Satoyoushi, E., Hayashi K., & Furukawa, S. Catecholamines Increase Nerve Growth Factor mRNA Content in Both Mouse Astroglial Cells and Fibroblast Cells. FEBS Lett., 247, 463-467 (1989)

Gardner, J.N., & Katritzky, A.R., N-oxides and Related Compounds. Part V. The Tautomerism of 2- and 4-Amino- and -Hydroxy-Pyridine 1-Oxide, J. Chem. Soc., 4375 (1957)

Graham, D.G., Tiffany, S.M., Bell, W.R., & Gutknecht, W.F., Autoxidation Versus Covalent Binding of Quinones as the Mechanism of Toxicity of Dopamine, 6-Hydroxydopamine, and Related Compounds Toward C1300 Neuroblastoma Cells in Vitro, Mol. Pharmacol., 14, 644-653 (1978)

Guldberg, H.C. & Marsden, C.A., Catechol-O-Methyl Transferase: Pharmacological Aspects and Physiological Role, Pharmacol. Rev., 27, 135-206, (1975)

Hagg, T., Manthorpe, M., Vahlsing, H.L., & Varon, S., Delayed Treatment with Nerve Growth Factor Reverses the Apparent Loss of Cholinergic Neurons after Acute Brain Damage, Exp. Neurol., 101,303-312 (1988)

Halliwell, B., Reactive Oxygen Species and the Central Nervous System, *Free Radicals in the Brain. Aging, Neurological and Mental Disorders*, Edited by Packer, L., Prilipko, L., & Christen, Y., ed. Springer-Verlag, (1992)

Halliwell, B., & Gutteridge, J.M.C., Free Radicals and Toxicology, Chapter 6 in Free Radicals in Biology and Medicine, Second Edition, Clarendon Press (1989)

Hammett, L.P., Physical Organic Chemistry, 2nd Ed. McGraw-Hill, N.Y., (1970)

Hanaoka, Y., Ohi, T., Furukawa, S., Furukawa, Y., Hayashi, K., & Matwukura, S., The Therapeutic Effects of 4-Methylcatechol, a Stimulator of Endogenous Nerve Growth Factor Synthesis, on Experimental Diabetic Neuropathy in Rats, J. of the Neurological Sciences, 122, 28-32 (1994)

Hanasaki, Y., Ogawa, S., & Fukui, S., The Correlation Between Active Oxygens Scavenging and Antioxidative Effects of Flavonoids, Free Radic. Biol. Med., 16, (6), 845-850 (1994)

Hansch, C., Lipophilic Character and Biological Activity of Drugs II: The Parabolic Case, J. Pharm. Sciences, 62 (1), 1(1973)

Hansch, C., Chapter 2 in *Drug Design*,v. 1, Ed. Ariens, E.J., Academic Press (1971)

Harbaugh, R.E., Nerve Growth Factor as a Potential Treatment in Alzheimer's Disease, Biomed. & Pharmacother., 43, 483-485 (1989)

Hashimoto, Y., Omae, F., & Furukawa, S., Reduction of NGF Protein Level in Rat Dorsal Hippocampus Following Administration of Kainic Acid. Neurosc. Lett., 140, 203-205 (1992)

Hefti, F., Potential Pharmacological Use of Neurotrophic Factors in the Treatment of Neurodegenerative Diseases, in Meyer, E.M., Simpkins, JW., Yamamoto J., (eds): *Novel Approaches to the treatment of Alzheimer's Disease*, Plenum Press, New York, 63-70, (1989)

Hefti, F., & Mash, D.C., Localization of Nerve Growth Factor Receptors in the Normal Human Brain and in Alzheimer's Disease, Neurobiol. Aging, 10, (1), 75-87, (1989)

Hengerer, B., Lindholm, D., Heumann, R., Ruther, U., Wagner, E.F., & Thoenen, H., Lesion-Induced Increase in Nerve Growth Factor mRNA is Mediated by c-fos, Proc. Natl. Acad. Sci., 87, (10), 3899-3903 (1990)

Heumann, R., Hengerer, B., Brown, M., & Perry, H., Molecular Mechanisms Leading to Lesion-Induced Increases in Nerve Growth Factor Synthesis, Annals New York Academy of Sciences, 633, 581-582, (1991)

Houlgatte, R., Wion, D., & Brachet, P., Serum Contain a Macromolecular Effector Promoting the Synthesis of Nerve Growth Factor (NGF) in L Cells, Biochem. and Biophys. Res. Commun., 150, (2), 723-730 (1988)

Iversen,L.L., & Hargreaves, R., After Tacrine - Summing up Current Drug Research Lines, (Abstract) Current Research into Therapies for Alzheimer's Disease, pre-satellite symposium to the 2nd European Congress of Pharmaceutical Sciences, Berlin (1994)

Jackson, G.R., Apffel, L.,Werrbach-Perez, K., & Perez-Polo, J.R., Role of Nerve Growth Factor in Oxidant-Antioxodant Balance and Neuronal Injury. I. Stimulation of Hydrogen Peroxide Resistance, J. Neurosc. Res., 25, 360-368 (1990 a)

Jackson, G.R. ,Werrbach-Perez, K., & Perez-Polo, J.R., Role of Nerve Growth Factor in Oxidant-Antioxidant Balance and Neuronal Injury. II. A Conditioning Lesion Paradigm, J. Neurosc. Res., 25, 369-374 (1990 b)

Jackson, G.R., Werrbach-Perez, K., Ezell, E.L., Post, J.F.M., & Perez-Polo, J.R., Nerve Growth Factor Effects on Pyridine Nucleotides after Oxidant Injury of Rat Pheochromocytoma Cells, Brain Res., 59, 239-248 (1992)

Jenner, P., Dexter, D.T., Sian, J., Schapira, A.H.V., & Marsden, C.D., Oxidative Stress as a Cause of Nigral Cell Death in Parkinson's Disease and Incidental Lewy Body Disease, Ann. Neurol., 3, S82-S87 (1992)

Jovanovic, S.V., Steenken, S., Tosic, M., Marjanovic, B., & Simic, M.G., Flavonoids as Antioxidants, J. Am. Chem. Soc., 116, 4846-4851 (1994)

Kaechi, K., Nippon-Seik.-Gak.-Zasshi, 66, (10), 1051-1058 (1992)

Kaechi, K., Furukawa, Y., Ikegami, R., Nakamura, N., Omae, F., Hashimoto, Y., Hayashi, K., & Furukawa, S., Pharmacological Induction of Physiologically Active Nerve Growth Factor in Rat Peripheral Nervous System. J. Pharmacol. Exp. Ther. 264, 1, 321-326 (1993)

Kagan, V.E., Bakalova, R.A., Koynova, G.M., Tyurin, V.A., Serbinova, E.A., Petkov, V.V., Petkov, V.D., Staneva, D.S., & Packer, L., Antioxidant Protection of the Brain Against Oxidative Stress, *Free Radicals in the Brain. Aging, Neurological and Mental Disorders*, Edited by Packer, L., Prilipko, L., & Christen, Y., ed. Springer-Verlag, (1992)

Katritzky, A.R., The Structure and Reactivity of 2-Aminopyridine 1-Oxide. J. Chem. Soc., 191(1957)

Kehrer, J.P., & Lund, L.G., Cellular Reducing Equivalents and Oxidative Stress, Free Radic. Biol. Med., 17, (1), 65-75 (1994)

Kitagawa, K., Matsumoto, M., Oda, T., Niinobe, M., Hata, R., Handa, N., Fukunaga, R., Isaka, Y., Kimura, K., Maeda, H., Mikoshiba, K., & Kamada, T., Free Radical Generation During Brief Period of Cerebral Ischemia May Trigger Delayed Neuronal Death, Neurosc., 35, (3), 551-558 (1990)

Knusel, B. J., Neurotrophins and Alzheimer's Disease, (Abstract) 3rd Suncoast Workshop on the Neurobiology of Aging, Amelia Island, Florida (1995)

Korolkovas, A., Essentials of Medicinal Chemistry, 2nd Ed., Willey Interscience (1988)

Kost, A., Gromov, S.P., & Sagitullin, R.S., Pyridine Ring Nucleophilic Recyclizations, Tetrahedron, .37, 3427-3454 (1981)

Krogsgaard-Larsen, P., Neurotransmitter Receptors as Pharmacological Targets in Alzheimer's Disease: Design of Drugs on a Rational Basis, Chapter 1 in *Drug Design for Neuroscience*, Edited by Kozikowski, A.P., Raven Press (1993)

Krogsgaard-Larsen, P., Amino acid Neurotransmitters in Alzheimer's Disease : Focus on AMPA and GABA-(A) Receptors, (Abstract) Current Research into Therapies for Alzheimer's Disease, Pre-satellite symposium to the 2nd European Congress of Pharmaceutical Sciences, Berlin (1994)

Langmuir, I., The Arrangement of Electrons in Atoms and Molecules, J. Am. Chem. Soc., 41, 868 (1919)

Langmuir, I., Isomorphism, Isosterism and Covalence, J. Am. Chem. Soc., 41 1543 (1919)

Lapchak, P. A., Nerve Growth Factor Pharmacology: Application to the Treatment of Cholinergic Neurodegeneration in Alzheimer's Disease, Exp. Neurol. 124, 16-20 (1993)

Lapchak, P. A., & Hefti, F., Recombinant Human Nerve Growth Factor Increases Presynaptic Cholinergic Function in the Hippocampal Formation

Following partial Fimbrial Transections: Measures of Newly Synthesized and endogenous Acetylcholine, (Abstract) 2nd Suncoast Workshop on the Neurobiology of Aging, Amelia Island, Florida (1992)

Larsen, A.A., Catecholamine Chemical Species at the Adrenergic Receptors. Nature, 224, 25-27 (1969).

Lettre, V.H., Haede, W., & Ruhbaum, E., Zur Darstellung von Derivaten des Nicotinsaureamids, Annalen Der Chemie, 579, 122-132 (1953)

Levi-Montalcini, R., Developmental Neurobiology and the Natural History of Nerve Growth Factor, Ann.. Rev. Neurosci., 5, 341-62 (1982)

Litster, J.E., & Tieckelmann, H., The Thermal Rearrangements of 2-Alkenyloxypyridine 1-Oxides, J.Amer.Chem.Soc., 90, 4361 (1968)

Longo, A.M., Synthesis of Nerve Growth Factor in Rat Glioma Cells, Develop. Biol., 65, 260-270 (1978)

Longo, A.M., & Penhoet, E.E., Nerve Growth Factor in Rat Glioma Cells, Proc. Nat. Acad. Sci., 71, (6), 2347-2349 (1974)

Lott, W.A., & Shaw, E., Analogs of Aspergillic Acid. II. Various Antibacterial Heterocyclic Hydroxamic Acids, J. Amer. Chem. Soc., 71, 70-73 (1949)

Mattson, M.P., & Cheng, B., Growth Factors Protect Neurons Against Excitotoxic/Ischemic Damage by Stabilizing Calcium Homeostasis, Stroke, v. 24, no. 12 (1993 a)

Mattson, M.P., Cheng, B., & Smith-Swintosky, V.L., Mechanisms of Neurotrophic Factor Protection against Calcium- and Free Radical-Mediated Excitotoxic Injury: Implications for Treating Neurodegenerative Disorders, Exp. Neurol., 124, 89-95 (1993 b)

Matsuoka, I., Meyer, M., & Thoenen, H., Cell-Type-specific Regulation of Nerve Growth Factor (NGF) Synthesis in Non-neuronal Cell: Comparison of Schwann Cells with Other Cell Types, The Journal of Neuroscience, 11 (10), 3165-3177 (1991)

McCall, J.M., & Panetta, J.A., Traumatic and Ischemia/Reperfusion Injury to the CNS, Chapter 4 in Annual Reports in Medicinal Chemistry, 27, (1992)

Michiels, C., Raes, M., Toussaint, O., & Remacle, J., Importance of Se-Glutathione Peroxidase, Catalase, and Cu/Zn-sod for Cell Survival Against Oxidative Stress, Free Radic. Biol. Med., 17, (3), 235-248 (1994)

Mobley, W.C., Nerve Growth Factor in Alzheimer's Disease: To Treat of not to Treat?, Neurobiol. of Aging, 10, 578-580 (1989)

Montero, C.N., & Hefti, F., Neurob. Aging , 10, 739-743 (1989)

Mocchetti, I., Theoretical Basis for a Pharmacology of Nerve Growth Factor Biosynthesis, Annu.Rev.Pharmacol.Toxicol. 32, 303-328 (1991)

Mocchetti, I., Pharmacological Regulation of Nerve Growth Factor Biosynthesis: In Vitro and In Vivo Studies, (Abstract) 2nd Suncoast Workshop on the Neurobiology of Aging,, Amelia Island, Florida (1992)

Mocchetti, I., De Bernardi, M. A., Szekely, A. M., Alho, H., Brooker, G., & Costa, E., Regulation of Nerve Growth Factor Biolynthesis by b-Adrenergic Receptor Activation in Astrocytoma Cells: A Potential Role of c-Fos Protein, Proc. Natl. Acad. Sci., 86, 3891-3895, (1989)

Mohs, R.C., & Davis, K.L., The Experimental Pharmacology of Alzheimer's Disease and Related Dementias, Chapter 91 in *Psychopharmacology* Ed. Meltzer, H.Y., Raven Press, N.Y., (1987)

Munns, P.L., & Leach, K.L., Two Novel Antioxidants, U74006F and U78517F, Inhibit Oxidant-Stimulated Calcium Influx, Free Radic. Biol. Med., 18, (3), 467-478 (1995)

Murakami, A., Tatsuno, T., Kimura,T., Noguchi, H., & Nakamura, M., Regulation of Nerve Growth Factor Secretion in L-M Cells by Catechol Derivatives, Neurosci. Res., 17, 71-75 (1993)

Murase, K., Hattori, A., Kohno, M., & Hayashi, K., Stimulation of Nerve Growth Factor Synthesis/Secretion in Mouse Astroglial Cells by Coenzymes, Biochem. and Mol. Biol. Intern., 30, (4), 615-621 (1993)

Murphy, R.A., Oger, J., Saide, J.D., Blanchard, M.H., Arnason, B.G.W., Hogan, C., Pantazis, N.J., & Young, M., Secretion of Nerve Growth factor by Central Nervous System Glioma Cells in Culture, The Journal of Cell Biology, 72, 769-773 (1977)

Nagata, W., Okada, K., & Aoki, T., Ortho-Specific a-Hydroxyalkylation of Phenols with Aldehydes. An Efficient Synthesis of Saligenol Derivatives, Synthesis, Communications, 365, (1979)

Nistico, G., Ciriolo, M.R., Fiskin, K., Iannone, M., De Martino, A., & Rotilio, G., NGF Restores Decrease in Catalase and Increases Glutathione Peroxidase Activity in the Brain of Aged Rats, Neurosc. Lett., 130, 117-119 (1991)

Nistico, G., Ciriolo, M.,R., Fiskin, K., Iannone, M., De Martino, A., & Rotilio, G., NGF Restores Decrease in Catalase Activity and Increases Superoxide Dismutase and Glutathione Peroxidase Activity in the Brain of Aged Rats, Free Radic. Biol. Med., 12, 177-181 (1992)

Nitta, A., Hasegawa, T., & Nabeshima, T., Oral Administration of Idebenone, a Stimulator of NGF Synthesis, Recovers Reduced NGF Content in Aged Rat Brain, Neurosc. Lett., 163, 219-222 (1993)

Olson, L., Nerve Growth Factor: Therapeutic Aspects, (Abstract) Current Research into Therapies for Alzheimer's Disease, pre-satellite symposium to the 2nd European Congress of Pharmaceutical Sciences, Berlin (1994)

Olson, L., NGF and the Treatment of Alzheimer's Disease, Exp. Neurol., 124, 5-15 (1993)

Packer, L., Free Radical Scavengers and Antioxidants in Prophylaxy and Treatment of Brain Diseases, *Free Radicals in the Brain. Aging Neurological and Mental Disorders*, Edited by Packer, L., Prilipko, L., & Christen, Y., ed. Springer-Verlag, (1992)

Pan, Z., & Perez-Polo, R., Role of Nerve Growth Factor in Oxidant Homeostasis: Gluatathione Metabolism, J. Neurochem., 61, 1713-1721 (1993)

Pearson, R.G., Absolute Electronegativity and Hardness Correlated with Molecular Orbital Theory. Proc. Natl. Acad. Sci., 83, 8440-8441 (1986)

Pechan, P.A., Chowdhury, K., & Seifert, W., Free Radicals Induce Gene Expression of NGF and bFGF in Rat Astrocyte Culture. NeuroReport, 3, 469-472 (1992)

Perez-Polo, J.R., Hall, K., Livingston, K., & Westlund, K., Steroid Induction of NGF Synthesis in Cell Culture, Life Sciences, 21, 1535-1543 (1977)

Perez-Polo, J.R., Foreman, P.J., Jackson, G.R., Shan, D., Taglialatela, G., Thorpe, L.W., & Werrbach-Perez, K., Nerve Growth Factor and Neuronal Cell Death, Mol. Neurobiol,. 4, 57-91 (1990)

Phelps, C.H., Trophic Factors and Alzheimer's Disease, Neurob. of Aging, 10, 584-586 (1989)

Phelps, C.H., Gage, F.H., Growdon, J.H., Hefti, F., Harbaugh, R., Johnston, M.V., Khachaturian, Z.S., Mobley, W.C., Price, D.L., Raskind, M., Simpkins, J., Thal, L.J., & Woodcock, J., Potential Use of Nerve Growth Factor to Treat Alzheimer's Disease, Neurob. Aging, 10, 205-207 (1989)

Piovesan, P., Pacifici, L., Taglialatela, G., Ramacci, M.T., & Angelucci, L., Acetyl-L-Carnitine Treatment Increases Choline Acetyltransferase Activity and NGF Levels in the CNS of Adult Rats Following Total Fimbria-Fornix Transection, Brain Res., 633, 77-82 (1994)\

Pop, E., Anderson, W., Prokai-Tatrai, K., Brewster, M., & Bodor, N., Redox Analogs of Centrally Acting Amines: Design, Synthesis and Properties of

a Tranycypromine Derivative with a Potentially Enhaced Terapeutic Index, J. Biopharm. Sci., 2, (1), 11023 (1991)

Rekker, R.F., The Hydrophobic Fragmental Constant, Its Derivation and Application; a Means of Characterizing Membrane Systems, Pharmacochemistry Library, 1, Ed. Nauta, W.T., & Rekker, R.F., Elsevier Publishing Company, (1977)

Riva, M.A., Gale, K. & Mocchetti, I., Basic Fibroblast Growth Factor mRNA Increases in Specific Brain Regions Following Convulsive Seizures, Mol. Brain Res., 00, 1, (1992)

Rogers, J., Clinical Trial of Indomethacin in Alzheimer's Disease, Neurology, 43, 1609-1611, (1993)

Sambrook, J., Fritsch, E.F., & Maniatis, T., Molecular Cloning : a Laboratory Manual, Cold Spring Harbor, N.Y. (1989)

Saporito, M.S., Brown, E., Hartpence, K.C., Wilcox, H.M., Robbins, E., Vaught, J.L., & Carswell, S., Systemic Dexamethasone Administration Increases Septal Trk Autophosphorylation in Adult Rats via an Induction of Nerve Growth Factor, Mol. Pharmacol., 45, 395-401 (1993 a)

Saporito,M. S., Brown, E., Hartpence, K.C., Wilcox, H.M., Vaught, J.L., & Carswell, S., Chronic 1,25-Dihydroxyvitamin D3-Mediated Induction of Nerve Growth Factor mRNA and Protein in L929 Fibroblasts and in Adult Rat Brain, Brain Res., 633, 189-196 (1993 b)

Saporito,M. S., Wilcox, H.M., Hartpence, K. C., Lewis,M.E., Vaught, J. L., & Carswell, S., Pharmacological Induction of Nerve Growth Factor mRNA in Adult Rat Brain. Exp. Neurol., 12, 295-302 (1993 c).

Schwartz, J.P., Stimulation of Nerve Growth Factor mRNA Content in C6 Glioma Cells by a b-Adrenergic Receptor and by Cyclic AMP, Glia, 1, 282-285 (1988)

Schwartz,J.P., Chuang, D-M., & Costa, E., Increase in Nerve Growth Factor Content of C6 Glioma Cells by the Activation of a b-Adrenergic Receptor, Brain Res., 137, 369-375 (1977)

Schwartz, J.P., & Costa, E., Regulation of Nerve Growth Factor Content in C6 Glioma Cells by b-Adrenergic Receptor Stimulation, Naunyn-Schmiedeberg's Arch. Pharmacol., 300, 123-139, (1977)

Schwartz, J.P., & Costa, E., Regulation of Nerve Growth Factor Content in a Neuroblastoma Cell Line, Neuroscience, 3, 473-480 (1978)

Schwartz, J.P., & Mishler, K., b-Adrenergic Receptor Regulation, Through Cyclic AMP, of Nerve Growth Factor Expression in Rat Cortical and Cerebellar Astrocytes, Cell.and Mol. Neurob., 10, (3), 447-457(1990)

Schindler, U., The Utility of Nootropics in Primary Senile Dementia, Chapter 6 in *Anti-dementia Agents. Research and Prospects for Therapy.* Edited by Nicholson, D., Academic Press, (1994)

Selkoe, D.J., Aging Brain, Aging Mind, Scientific American, Sept. issue (1992)

Shi, M., Gozal, E., Choy, H.A., & Forman, H.J., Extracellular Glutathione and γ–Glutamyl Transpeptidase Prevent H_2O_2-Induced Injury by 2,3-Dimethoxy-1,4-Naphthoquinone, Free Radic. Biol. Med., 15, 57-67 (1993)

Shinoda, I., Furukawa, Y., & Furukawa, S., Stimulation of Nerve Growth Factor Synthesis/Secretion by Propentofylline in Culture Mouse Astroglial Cells, Biochem. Pharmacol., 39 (11), 1813-1816, (1990)

Simpkins, J., & Bodor, N., Brain-Enhanced Drug Delivery Systems for the Treatment of Dementia, Chapter 4 in *"Alzheimer's Disease,New Treatment strategies"*, Ed. Khachaturian, Z.S., Blass, J.P., Marcel Dekker , Inc. (1992)

Sinet, P.M., & Ceballos-Picot, I., Role of Free Radicals in Alzheimer's Disease and Down's Syndrome, Free Radicals in the Brain. Aging, Neurological and Mental Disorders, Edited by Packer, L., Prilipko, L., & Christen, Y., ed. Springer-Verlag, (1992)

Springer, J.E., Experimental Evidence for Growth Factor Treatment and Function in Certain Neurological Disorders, Exp. Neurol., 124, 2-4, (1993)

Stadtman, E.R., Protein Oxidation and Aging, Science, 257, 1220 (1992)

Steiner, P., Pfeilschifter, J., Boeckh, C., Radeke, H., & Otten, U., Interleukin-1β and Tumor Necrosis Factor-α Synergistically Stimulate Nerve Growth Factor Synthesis in Rat Mesangial Cells, Am. J. Physiol., 261, F792-F798 (1991)

Stone, E.A., Manavalan, J.S., Basham, D.A., & Bing, G., Effect of Yohimbine on Nerve Growth Factor mRNA and Protein Levels in Rat Hippocampus, Neuroscience Lett., 167, 11-13, (1994)

Stone, T.W., Excitatory Amino Acids and Dementia, Chapter 8 in *Anti-dementia Agents. Research and Prospects for Therapy.* Edited by Nicholson, D., Academic Press, (1994)

Szabo, L., & Kretzshemar, R., Therapeutic Potential of Calcium Antagonists in the Treatment of Dementia, Chapter 10, in *Anti-dementia Agents.*

Research and Prospects for Therapy. Edited by Nicholson, D., Academic Press, (1994)

Takeda, M., Kanayama, G., Taniguchi, N., & Nishimura, T., The Present Status and Problems in Development of Drugs for Alzheimer's Disease in Japan, (Abstract) 3rd Suncoast Workshop on the Neurobiology of Aging, Amelia Island, Florida (1995)

Takeuchi,R., Murase, K., Furukawa, Y., Furukawa, S. & Hayashi, K., Stimulation of Nerve Growth Factor Synthesis/Secretion by 1,4-Benzoquinone and its Derivatives in Cultured Mouse Astroglial Cells. FEBS, 261, 63-66 (1990)

Tamura, Y., Miki, Y., Honda, T., & Ikeda, M., Synthesis of 3-Substitued N-Aminopyridinium Salts, J. Heterocycl. Chem., 9, 865-868 (1972)

Thoenen, H., Zafra, F., Hengerer, B., & Lindholm, D., The Synthesis Of Nerve Growth Factor And Brain-Derived Neurotrophic Factor In Hippocampal And Cortical Neurons Is Regulated By Specific Transmitter Systems, . Ann. N.Y. Acad. Of Sciences, 86-90 (1991)

Thoenen, H., The Changing Scene of Neurotrophic Factors, TINS,. 14, (5), (1991)

Thornton, D.E., Jones, K.H., Jiang, Z., Zhang, H., Liu, G., & Cornwell, D.G., Antioxidant and Cytotoxic Tocopheryl Quinones in Normal and Cancer Cells, Free Radic. Biol. Med., 18, (6), 963-976 (1995)

Tonnaer, J.A.D.M., & Dekker, A.J.A.M., Nerve Growth Factor, Neurotrophic Agents and Dementia, Chapter 5 in *Anti-dementia Agents. Research and Prospects for Therapy*. Edited by Nicholson, D., Academic Press, (1994)

Turner, J.D., GABAergic Systems and Dementia, Chapter 9 in *Anti-dementia Agents. Research and Prospects for Therapy*. Edited by Nicholson, D., Academic Press, (1994)

Unger, S.H., Chapter 1 in *Drug Design*,v. 9, Ed. Ariens, E.J., Academic Press (1980)

Vige, X., Costa, E., & Wise, B.C., Mechanism of Nerve Growth Factor mRNA Regulation by Interleukin-1 and Basic Fibroblast Growth Factor in Primary Cultures of Rat Astrocytes, Mol. Pharmacol., 40, 186-192 (1991)

Walsh, T.J., Site-Specific Pharmacology for the Treatment of Alzheimer's Disease, Exp. Neurol., 124, 43-46, (1993)

Weskamp, G., Gasser, U.E., Dravid, A.R., & Otten, U., Fimbria-Fornix Lesion Increases Nerve Growth Factor Content in Adult Rat Septum and Hippocampus, Neurosci. Lett.., 70, 121-126, (1986)

Whittemore, S.R., & Seiger, A., The Expression, Localization and Functional Significancer of β-Nerve Growth Factor in the Central Nervous System, Brain Res. Rev., 12, 439-464 (1987)

Wiche, G., In Vitro Synthesis of Nerve Growth Factor Related Glioma C6 cell Polypeptides, Biochem. Biophys. Res. Commun., 89, (2), 620-626 (1979)

Wion, D., Macgrogan, D., Neveu, I., Jehan, Houlgatte, R., & Brachet, P., 1, 25-Dihydroxyvitamin D3 is a Potent Inducer of NGF Synthesis, J. Neurosci. Res., 28, 110-114, (1991)

Wion, D., Houlgatte, R.,Barbot, N., Barrand, P., Dicou, E., & Brachet, P., Retinoic Acid Increases the Expression of NGF Gene in Mouse L Cells, Biochem. Biophys. Res. Commun., 149, (2), 510-514 (1987)

Wion, D., Mac Grogan, D., Houlgatte, R., & Brachet, P., Phorbol 12-Myristate 13-Acetate (PMA) Increases the Expression of the NGF Gene in Mouse L-929 Fibroblasts, FEBS, 262, (1), 42-44 (1990)

Wolff, M.E., *Burger's Medicinal Chemistry and Drug Discovery* v.1 Principles and Practice, 5th Ed. (1995)

Woodard, P., Winwood, D., Brewster, M., Estes, K., & Bodor, N., Improved Delivery Through Biological Membranes XXI. Design, Synthesis and Antiseizure Activity of Brain-Specific Anticonvulsive agents, Drug Des. & Del., 6, 15-28 (1990)

Yamaguchi, K., Tsuji, T., Wakuri, S., Yazawa, K., Kondo, K., Shigemori, H., & Kobayashi, J., Stimulation of Nerve Growth Factor Synthesis and Secretion by Fellutamide A in Vitro, Biosci. Biotech. Biochem., 57, (2), 195-199 (1993)

Yoon, S.-H., Bodor, N., & Simpkins, J.W., Synthesis and In Vitro Dopaminergic Activity of (2-Aminoethyl)-1-Hydroxy-2-Pyridone Type Dopamine Analogs, Drug Design and Discovery, 10, 35-44 (1993)

Yoshida, K., & Gage, F.H., Fibroblast Growth Factors Stimulate NGF Synthesis and Secretion by Astrocytes, Brain Res., 538, 118-126 (1991)

Yoshida, K., & Gage, F.H., Cooperative Regulation of Nerve Growth Factor Synthesis and Secretion in Fibroblasts and Astrocytes by Fibroblast Growth Factor and Other Cytokines, Brain Res., 569, 14-25 (1992)

Zafra, F., Castren, E., Thoenen, H., & Lindholm, D., Interplay Between Glutamate and γ-Aminobutyric Acid Transmitter Systems in the Physiological Regulation of Brain-Derived Neurotrophic Factor and Nerve Growth Factor Synthesis in Hippocampal Neurons, Proc. Natl. Acad. Sci., 88, 10037-10041 (1991)

Zafra, F., Hengerer, B., Leibrock, J., Thoenen, H., & Lindholm, D., Activity Dependent Regulation of BDNF-and NGF-mRNAs in the Rat Hippocampus is Mediated by non-NMDA Glutamate Receptors. EMBO J. 9: 3545-3550, (1990).

Zafra, F.,Lindholm, D., Castren, E., Hartikka, J., & Thoenen, H., Regulation of Brain-Derived Neurotrophic Factor and Nerve Growth Factor mRNA in Primary Cultures of Hippocampal Neurons and Astrocytes, J. Neurosc., 12 (12),4793-4799 (1992)

Zhang, Y., Tatsuno, T., Carney, J.M., & Mattson, M.P., Basic FGF, NGF, and IGFs Protect Hippocampal and Cortical Neurons Against Iron-Induced Degeneration, J. Cerebral Blood Flow and Metabolism, 13, 378-388 (1993)

Zincke, T., Ueber Dinitrophenylpyridiniumclorid und Dessen Umwandlungsproducte, Annalen der Chemie, 33, 361-382 (1903)

BIOGRAPHICAL SKETCH

Angeliki Kourounakis was born on October 10, 1967, in London, England. She went to the first grades of school in Montreal, Canada, after which she moved to Thessaloniki, Greece, where she completed her middle and high school education. In 1986 she entered the College of Pharmacy of the Aristotelian University of Thessaloniki, Greece, and graduated with a B. Pharm. in 1990. In 1991 she joined the graduate program of the Centre for Drug Discovery / Medicinal Chemistry, College of Pharmacy, University of Florida, and completed her Ph.D. in the summer of 1995.

I certify that I have read this study and that in my opinion it conforms to acceptable standards of scholarly presentation and is fully adequate, in scope and quality, as a dissertation for the degree of Doctor of Philosophy.

Nicholas S. Bodor, Chair
Graduate Research Professor of
Pharmaceutics

I certify that I have read this study and that in my opinion it conforms to acceptable standards of scholarly presentation and is fully adequate, in scope and quality, as a dissertation for the degree of Doctor of Philosophy.

James W. Simpkins
Professor of Pharmacodynamics

I certify that I have read this study and that in my opinion it conforms to acceptable standards of scholarly presentation and is fully adequate, in scope and quality, as a dissertation for the degree of Doctor of Philosophy.

Margaret O. James
Professor of Medicinal Chemistry

I certify that I have read this study and that in my opinion it conforms to acceptable standards of scholarly presentation and is fully adequate, in scope and quality, as a dissertation for the degree of Doctor of Philosophy.

Guenther Hochhaus
Associate Professor of Pharmaceutics

I certify that I have read this study and that in my opinion it conforms to acceptable standards of scholarly presentation and is fully adequate, in scope and quality, as a dissertation for the degree of Doctor of Philosophy.

Alan R. Katritzky
Kenan Professor of Chemistry

This dissertation was submitted to the Graduate Faculty of the College of Pharmacy and to the Graduate School and was accepted as partial fulfillment of the requirements for the degree of Doctor of Philosophy.

August, 1995

Dean, College of Pharmacy

Dean, Graduate School